Developing critical coalescence concentration curves using dilution and determining frother-like properties of oil sands process water

Marc Nassif

Department of Mining and Materials Engineering

McGill University

Montréal, Canada

June 2013

A thesis submitted to the office of Graduate Studies and Research in partial fulfillment of the requirements for the degree of Master of Engineering

ABSTRACT

In flotation, the rate with which mineral particles are recovered is governed by the bubbles generated. The smaller the bubbles, the more surface area is available for transport to the froth zone. Surface-active species, known as frothers, are commonly added to help produce small bubbles in flotation. They are believed to act by coalescence prevention and have different characteristics based on their chemical and structural formulas. Many methods have been developed to categorize the classes of frothers, describing different behaviours and material constants. One such method is the critical coalescence concentration (CCC) of a frother which is determined from a plot of Sauter mean bubble size (D_{32}) vs. frother concentration, referred to here as the 'addition' method.

Industrial flotation systems can encounter a number of naturally occurring surfactants and salts that also influence bubble size, such as during oil sands extraction. In effect there is a 'system' CCC. The thesis introduces a new dilution method to identify a system CCC. It is shown that the system CCC can be expressed as an equivalent frother concentration to provide context and a means of comparing water samples. Process water samples from the thickener overflow in Shell Albian Sands were tested. The study showed variability in the frother-equivalence of the process waters reaching at most the equivalent of 60 ppm of DF-250, a value that is much higher than the range of frother concentrations commonly employed in the minerals industry.

The viability of using gas holdup to provide an estimate of process water D_{32} is also explored. A gas holdup to D_{32} correlation was established and used in developing the CCC curve of a sample, the advantage being gas holdup is an easier parameter to measure. It is concluded that the dilution and frother equivalent techniques can be used to help identify system hydrodynamic properties. A longer term ambition is to consider using gas holdup for on-line application to evaluate possible changes in process waters which may impact these hydrodynamic properties.

RESUME

Dans le procédé de flottation, la vitesse avec laquelle les particules minérales sont récupérés est régie par les bulles générées. Le plus les bulles sont petites, le plus d'aire superficielle disponible pour le transport vers la zone de mousse. Les espèces tensio-actifs, connus comme agents moussants, sont ajoutés pour aider à produire de petites bulles. Ils sont soupçonnés d'agir par la prévention de la coalescence et ont des caractéristiques différentes en fonction de leurs formules chimiques et structurales. De nombreuses méthodes ont été mises au point pour classer les catégories d'agents moussants. Une telle méthode est la concentration de coalescence critique (CCC) d'un agent moussant qui est déterminée à partir d'un graphique de diameter Sauter qui represente la taille moyenne des bulles (D_{32}) contre la concentration d'agent moussant, une méthod dénommé «Addition».

Les systèmes de flottation industriels peuvent rencontrer un certain nombre d'agents tensio-actifs d'origine naturelle et les sels qui influencent également la taille des bulles, comme lors de l'extraction des sables bitumineux. En effet, il ya un «système» CCC. La thèse présente une nouvelle méthode de dilution pour identifier un système CCC. Il est démontré que le système CCC peut être exprimée comme une concentration équivalente d'agent moussant, ce qui contribue a fournir un contexte et un moyen de comparer des échantillons d'eau. Les échantillons d'eau de procédé provenant du débordement d'épaississant dans Shell Albian Sands ont été testés. L'étude a révélé une variabilité dans l'équivalence d'agent moussant des eaux de process atteignant tout au plus l'équivalent de 60 ppm de DF-250, une valeur qui est plus élevé que la gamme de concentrations d'agent moussant couramment utilisés dans l'industrie des minéraux.

La viabilité de l'utilisation de la rétention de gaz pour fournir une estimation du D_{32} des échantillons d'eau est aussi explorée. Une corrélation entre la rétention de gaz et D_{32} a été établie et utilisée dans le développement de la courbe CCC d'un échantillon, l'avantage étant la simplicité de mesurer le retenue de gaz. Il est conclu que la technique de dilution peut être utilisé pour aider à identifier les propriétés hydrodynamiques du système. Une ambition à long terme est d'utiliser la rétention de gaz pour des applications en ligne pour évaluer les changements possibles dans les eaux de procédé qui peuvent influencer ces propriétés hydrodynamiques.

CONTRIBUTION OF AUTHORS

This thesis was prepared in accordance with the guidelines for "Manuscript-Based Thesis Preparation" at McGill University. The following manuscripts were written by the author and used in preparation of this thesis. Chapters 5 and 6 consist of Manuscripts 1 and 2 respectively:

-Manuscript 1: Marc Nassif, James A. Finch, Kristian E. Waters, 2013. Developing critical coalescence concentration curves for industrial process waters using dilution (Published in Minerals Engineering Journal, Volume 50 pp.64-68)

-Manuscript 2: Marc Nassif, James A. Finch, Kristian E. Waters, 2013. Exploring frother-like properties of process water in bitumen flotation (submitted to Minerals Engineering Journal)

The manuscripts above are co-authored by Prof. James A. Finch and Prof. Kristian E. Waters in their capacity as research supervisors. Beyond the contributions of the co-authors, the author performed all the work presented in this dissertation.

ACKNOWLEDGMENTS

I would like express my utmost gratitude and appreciation to Professor Jim Finch and Professor Kristian Waters for their guidance and the opportunity to undertake this challenge. The many months spent exploring the new techniques under their supervision have been very enlightening. I would like to thank Gavin Freeman and Jason Schaan from Shell Canada Ltd. for supporting the project and helping meet the objectives of the study. I greatly enjoyed learning about the oil sands industry in depth, touring and meeting everyone in Albian Sands. I hope to have contributed, however small, towards the continuous development of our vast resources here in Canada.

I would like to thank Dr. Cesar Gomez and Dr. Miguel Maldonado from the Mineral Processing Research Group at McGill University for their assistance in getting the required instruments for testing in Edmonton and getting me better acquainted with column operation and flotation fundamentals. I would also like to thank Raymond Langlois at McGill University for his technical guidance and assistance.

Last but certainly not least, I would like to thank Dale Ladoon and Robert Ewing from Coanda R&D in Edmonton for helping me set up the apparatus and get settled in their research facility and in Edmonton for the duration of the experiments.

My heartfelt thanks go out to everyone who contributed to this project.

TABLE OF CONTENTS

LIST OF FIGURES

LIST OF TABLES

CHAPTER 1: INTRODUCTION

1.1. General Background

Mining and mineral processing have long been at the core of the global economy, supplying various base and precious metals to the industry. An example is the processing of minerals that are rich in copper, such as chalcopyrite, extracted from the ores using separation techniques. The copper rich mineral concentrate is then smelted and refined to obtained pure copper.

In general, mineral processing steps are divided between comminution and separation. The objective of comminution is to the reduce particle size and to liberate valuable mineral grains in the ore matrix such that economic extraction is feasible. Some particles however remain locked with unwanted "gangue" material. The comminution step is divided between crushing and grinding. Crushing as the name implies broadly reduces the large ore rocks into smaller rocks which are then screened. Grinding is used for further size reduction and homogenization, and could be either conducted on wet or dry material.

The mineral separation methods currently in use are gravity, flotation and magnetic. The most common separation process is flotation where bubbles are used to carry the mineral grains of interest to the top of the unit thereby forming a rich froth layer. A number of flotation units using different operating principles for generating bubbles are used in industry, including mechanical cells, column cells and pneumatic cells. Mechanical cells are large flotation tanks and by far the most commonly used. They employ impellers at the bottom of the tank to break down the forced air stream introduced through a central shaft into smaller bubbles. Column flotation on the other hand is used when more selectivity is desired (Finch and Dobby, 1990) and makes use of porous spargers located at the bottom of a column to generate small bubbles without the need for intensive mixing devices (Figure 1.1). Pneumatic cells such as the Jameson cell are self-aspirated and, by introducing the slurry as a jet in a downcomer, are capable of entraining tiny bubbles (Clayton et al., 1991). Flotation relies heavily on the differences in the physical and chemical properties of the minerals, on the characteristics of the bubbles generated, and on the complex interactions between the two. The flotation process is divided between the pulp (collection) zone

where all the gas dispersion and collision/collection takes place and the froth zone where mineral-bubble aggregates are collected along with some entrained material.

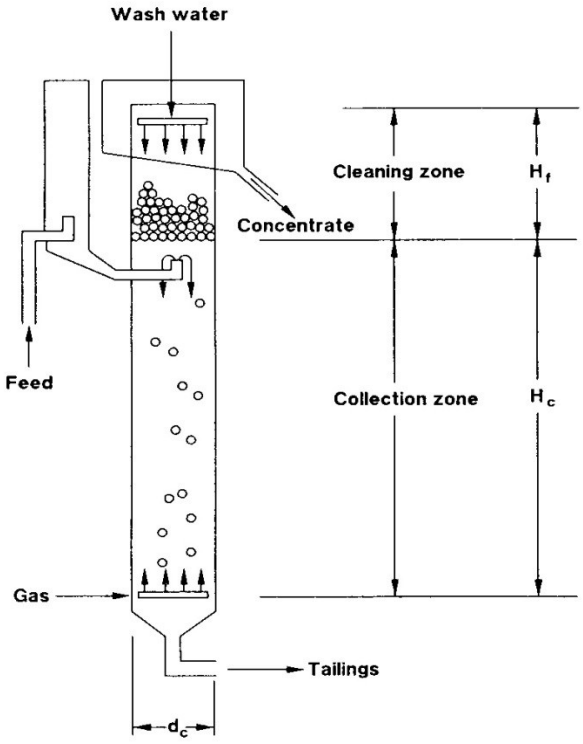

Figure 1.1 - Flotation Column Diagram from Finch and Dobby, 1990

In order to characterize the bubbles generated and their effect on flotation performance, gas dispersion parameters were developed such as gas holdup, bubble size and superficial gas velocity. Many instruments to measure these parameters on-site have been and are continuously being devised to improve plant performances (Gorain et al., 1997; Deglon et al., 2000; Finch et al., 2000; Yianatos et al., 2001; Hernandez-Aguilar, 2004; Nesset et al., 2006). Water chemistry is also known to be crucial in mineral flotation and can either inhibit or assist flotation recovery (Klimpel and Hansen, 1987; Crozier and Klimpel, 1989; Klimpel and Isherwood, 1991; Comley et al., 2002). Reagents such as collectors are added to the slurry to render hydrophilic minerals hydrophobic, depressants to make gangue hydrophilic, and frothers to generate desired hydrodynamics, namely small bubble size and stable froth. Many natural surfactant systems are encountered in the industry (Schramm et al., 2000; Quinn et al., 2007) such that small bubbles and stable froth are generated without the need for commercial frother addition.

A relatively new frontier for the study of natural surfactants in mineral processing can be found in the oil sands of Alberta. The Canadian oil sands are among the largest reserves of hydrocarbons in the world, containing the equivalent of 1.7 trillion barrels of oil, of which 170 billion barrels are recoverable using current technology. The largest deposits are found in the Athabasca region in Alberta where large open-pit mining operations such as Albian Sands (Shell), Syncrude, Suncor, Horizon (CNRL) and Kearl (Imperial Oil) are located (ERCB, 2011). Extracting bitumen from mined oil sands requires mineral processing techniques. The extraction process conditions the oil sands with heated water and caustic soda, and makes use of mechanical agitation and air flotation to separate the sand and bitumen components. Natural surfactants are known to be released into the process upon conditioning the "ore" which facilitates the recovery of bitumen (Schramm et al., 2000; Masliyah et al., 2011). While most of the factors affecting separation and recovery have been relatively well examined, studies of gas dispersion and the hydrodynamics of these natural surfactants in bitumen flotation are still lacking.

1.2. Frothers in Flotation

Frothers are used to improve mineral collection by helping produce smaller bubbles (which offer a larger surface area per unit volume) and a more stable froth. These chemicals are amphiphilic (exhibit both hydrophilic and lipophilic properties), having both a polar group and non-polar group and tend to adsorb on the water/air interface (Leja and Schulman, 1954). They are believed to act on bubbles by retarding and preventing coalescence thereby preserving a bubble's size (Harris, 1982; Hofmeier et al., 1995, Comley et al, 2002). A number of different frother classes are used in the mineral industry each tailored to the need of the ore body being extracted. In addition to inhibiting coalescence, these surface-active agents in general lead to an increase in froth formation, slower rising bubbles and improved gas dispersion in the flotation unit. Together these effects increase the probability of interaction between bubbles and particles and ultimately lead to higher flotation recoveries.

Frothers used in the mineral industry are commonly either aliphatic alcohols which have been used for decades or polyglycol frothers. Alcohol based frothers have low solubility in water but offer fast flotation kinetics at relatively low dosages (Crozier and Klimpel, 1989). The enhanced water drainage gives them better selectivity (due to less entrapment of unwanted minerals) but

the brittle froth layer limits their range of applicability to fine or medium particle flotation. Polyglycol frothers offer more versatility than alcohol frothers having higher water solubility, more persistence throughout the flotation units at lower dosages, more stable froth. They tend to form thicker boundary layers around the bubbles making them good at recovering coarse particles but also have slower flotation kinetics (Cappuccitti and Nesset, 2009).

Many techniques have been established over the years that describe quantifiable frother properties. These characterization methods rely on two essential principles in flotation: bubble size reduction and foam/froth stability. The most commonly used foam index is DFI (Dynamic frothability index) developed by Malysa et al. (1987). While most methods relied on foam properties to differentiate between frothers, Randall et al. (1989), Tucker et al. (1994), and Sweet et al. (1997) studied bubble coalescence and attempted to quantify the effect of frother concentration on bubble size. Cho and Laskowski (2002) showed when bubble collisions occur, the effect of frother addition on decreasing bubble size becomes evident. It was shown that the ability of frother to retard bubbles' coalescence and even prevent these occurrences is responsible for the bubble size decrease in commercial cells (Hofmeier et al., 1995, Comley et al., 2002; Cho and Laskowski, 2002; Finch et al., 2008). It was also observed that beyond a particular concentration all coalescence is ceased rendering the measured bubble diameters constant. Based on their observations, Cho and Laskowski (2002) introduced a new parameter to compare the effect of different frothers on bubble size. This concentration referred to as critical coalescence concentration (CCC) varies between frothers and can therefore be used to compare their strengths. Stronger frothers reach their CCC at a lower concentration. Cho and Laskowski also showed that the type of flotation cell does not affect the unique CCC value for each frother. They also correlated a foam index (DFI) to CCC and showed that it is possible to predict the value of CCC from literature values for DFI. It was shown that strong frothers have a high DFI and a low CCC while weaker and more selective frothers have a high CCC and a low DFI.

Identifying the CCC point of individual frothers is done by developing a critical coalescence concentration (CCC) curve which is plotting bubble diameter versus frother concentration. This method however is unable to tackle natural surfactant systems such as those found in Xstrata Raglan and in the oil sands. It is neither feasible nor practical to isolate the individual surfactants responsible for bubble size reduction to determine the CCC by the addition method.

1.3. Thesis

1.3.1. Research Objective

The objective is to find and explore a viable method for characterizing the hydrodynamics of natural surfactant "systems" in oil sands process waters. A novel dilution method is proposed to tackle the surfactant systems encountered in order to identify system critical coalescence concentration (CCC). The novel method has to give identical results to the addition technique using commercial frothers for assurance. Once established, the technique can be used on any industrial waters, including oil sands process water. Additional methods of comparison to common frothers are also to be explored.

1.3.2. Thesis Organization

The thesis consists of seven chapters organized as follows:

-***Chapter 1*** introduces the reader to the mineral processing industry, oil sands extraction, and to the objective and challenges of the research

-***Chapter 2*** is a literature review on the gas dispersion parameters and the effects of different factors on their behaviour

-***Chapter 3*** is a literature review on frother chemistry, classification and characterization methods

-***Chapter 4*** describes the apparatus used and the experimental procedures

-***Chapter 5*** is presented as Manuscript 1, "Developing critical coalescence concentration curves for industrial process waters using dilution" (Submitted to Minerals Engineering Journal). The paper describes a dilution method that overcomes limitation of the conventional addition method to develop CCC curves

-***Chapter 6*** is presented as Manuscript 2, "Exploring frother-like properties of process water in bitumen flotation" (Submitted to MetSoc conference 2013). The paper utilizes the newly established dilution technique in Manuscript 1 to explore process water of the oil sands industry, namely from the thickener overflow

-***Chapter 7*** presents conclusions and recommendations for future work including the longer term ambition use gas holdup for on-line application to evaluate possible changes in process waters which may impact these hydrodynamic properties

1.4. References

Cappuccitti, F., Nesset, J. E., 2009. Frother and collector effects on flotation cell hydrodynamics and their implication on circuit performance. In Proceedings 7th UBC-McGill-UA International Symposium on Fundamentals of Mineral Processing (Eds. C. Gomez, J. Nesset, S. Rao), CIM, pp. 169-182.

Cho, Y.S., Laskowski, J.S., 2002. Effect of Flotation Frothers on Bubble Size and Foam Stability. International Journal of Mineral Processing, Vol. 64, pp. 69-80

Clayton, R., Jameson, G.L., Manlapig, E.V., 1991. The development and application of the Jameson cell. Minerals Engineering, Vol. 4, pp. 925-933

Comley, B.A., Harris, P.J., Bradshaw, D.J., Harris, M.C., 2002. Frother characterization using dynamic surface tension measurements. International Journal of Mineral Processing, Vol. 64, pp. 81-100

Crozier, R.D., Klimpel, R.R., 1989. Frothers: Plant practice. Gordon and Breach, New York, NY, pp. 257-280

Deglon, D.A., Egya-Mensah, D., Franzidis, J.P., 2000. Review of Hydrodynamics and Gas Dispersion in Flotation Cells on South African Platinum Concentrators. Minerals Engineering, Vol. 13, pp. 235-244

Energy Resources Conservation Board (ERCB), 2011. ST98: Alberta's Energy Reserves 2011 and Supply/Demand Outlook 2012-2021. Calgary

Finch, J.A., Dobby, G.S., 1990. Column Flotation. Pergamon Press, New York, 1990

Finch, J.A., Xiao, J., Hardie, C., Gomez, C.O., 2000. Gas Dispersion Properties: Bubble Surface Area Flux and Gas Holdup. Minerals Engineering, Vol. 13, pp. 365-372

Finch, J.A., Nesset, J.E., Acuna, C., 2008. Role of frother on bubble production and behaviour in flotation, Part 3: Frother and bubble size reduction. Minerals Engineering, Vol. 21, pp. 949-957

Gorain, B.K., Franzidis, J.P., Manlapig, E.V., 1997. Studies on Impeller Type, Impeller Speed and Air Flow Rate in an Industrial Scale Flotation Cell - Part 4: Effect of Bubble Surface Area Flux on Flotation Performance. Minerals Engineering, Vol. 10, pp. 367-379

Grau, R.A., Heiskanen, K., 2003.Gas Dispersion Measurements in a Flotation Cell. Minerals Engineering, Vol. 16, pp. 1081-1089

Harris, P.J., 1982. Frothing phenomena and frothers in Flotation principles. Edited by R.P. King. Chapter 13, pp. 237-250.

Hernandez-Aguilar, J.R., 2004. An imaging technique for sizing bubbles in flotation systems. PhD thesis McGill University

Hofmeier, U., Yaminsky, V.V., Christenson, H.K., 1995. Observations of solute effects on bubble formation. Journal of Colloid and Interface Science, Vol. 174, pp. 199-210

Klimpel, R.R., Hansen, R.D., 1987. Frothers: Reagents in Mineral Technology. Marcel Dekker, New York, NY, pp. 663-681.

Klimpel, R.R., Isherwood, R.D., 1991. Some industrial implications of changing frother chemical structure. International Journal of Mineral Processing, Vol. 33, pp.369-381

Leja, J., Schulman, J.H., 1954. Flotation Theory: Molecular Interactions Between Frothers and Collectors at Solid–Liquid–Air Interfaces. Trans. AIME Vol. 199, pp. 221–228

Malysa, E., Malysa, K., Czarnecki, J., 1987. A method of comparison of the frothing and collecting properties of frothers. Colloids and Surfaces, Vol. 23, pp. 29-39

Masliyah, J.H., Czarnecki, J., Xu, Z., 2011. Handbook on Theory and Practice of Bitumen Recovery from Athabasca Oil Sands - Volume 1: Theoretical Basis. Kingsley Knowledge Publishing, pp. 246-256

Nesset, J.E., Hernandez-Aguilar, J.R., Acuna, C., Gomez, C.O., 2006.Some gas dispersion characteristics of mechanical flotation machines. Minerals Engineering, Vol. 19, pp.807-815

Quinn, J.J., Kracht, W., Gomez, C.O., Gagnon, C., Finch, J.A., 2007. Comparing the effect of salts and frother (MIBC) on gas dispersion and froth properties. Minerals Engineering, Vol. 20, pp. 1296–1302

Randall, E.W., Goodall, C.M., Fairlamb, P.M., Dold, P.L., O'Connor, C.T., 1989. A method for measuring the sizes of bubbles in two- and three-phase systems. Journal of Physics, Section E, Scientific Instrumentation 22, pp. 827–833

Schramm, L.L., 2000. Surfactants: Fundamentals and Applications in the Petroleum Industry. Cambridge University Press, pp. 377-378.

Tucker, J.P., Deglon, D.A., Franzidis, J.P., Harris, M.C., O'Connor, C.T., 1994. An evaluation of a direct method of bubble size distribution measurement in a laboratory batch flotation cell. Minerals Engineering, Vol. 7, pp. 667–680

Yianatos, J.B., Bergh, L.G., Condori P., Aguilera, J., 2001. Hydrodynamic and Metallurgical Characterization of Industrial Flotation Banks for Control Purposes. Minerals Engineering, Vol. 14, pp. 1033-1046

CHAPTER 2: LITERATURE REVIEW

In mineral flotation the rate and efficiency with which particles are recovered from the pulp phase is driven by the characteristics and the dispersion of bubbles. The pulp or collection zone is the focus of many gas control parameters used to optimize mineral recovery such as gas flow rate, gas holdup and bubble size distribution. A surfactant class known as frother is used to improve mineral collection by helping produce smaller bubbles which improve the flotation rate of recovery. Special emphasis on frothers is given since frother type and concentration are key, and at times the foremost, factors governing gas dispersion.

2.1. Gas Dispersion Parameters

Three main dispersion parameters are used to monitor unit performance in air flotation: superficial gas velocity (J_g), gas holdup (E_g), and bubble size (D_b). An additional parameter, bubble surface area flux (S_b), was derived by combining J_g and D_b to compare the solids' carrying rate and is largely used today to optimize unit performance (Finch and Dobby, 1990; Gorain et al., 1997; Hernandez et al., 2003; Nesset et al., 2005). Various instruments have also been developed to measure the gas dispersion parameters on-line in flotation units (Gorain et al., 1995a, 1995b, 1996; Gomez and Finch, 2007).

2.1.1. Superficial Gas Velocity (J_g)

Superficial gas velocity, J_g (cm/s), is calculated by dividing the gas flow rate Q_g (cm^3/s) by the cross sectional area of the flotation unit, A (cm^2):

$$J_g = \frac{Q_g}{A} \tag{2.1}$$

Superficial gas velocity is convenient since it allows comparison between flotation units of various dimensions and under different operating conditions. Operation range is usually between 0.5-2.5 cm/s in industrial cells governed by optimal recovery/grade conditions such as desired bubble size, froth height and overflow rate (Finch and Dobby, 1990).

2.1.2. Bubble Size (D_b)

In flotation the size of the bubbles affect the collection efficiency and rate of transport of the solids to the froth phase. The smaller the bubbles generated the more collisions with particles and the greater the bubble surface area for transport of the collected particles. Numerous methods to measure bubble size in flotation units have been developed. A common optical method is the UCT (University of Cape Town) Bubble Size Analyzer which uses optical detectors to determine the velocity and length of the equivalent volume of bubbles drawn into a capillary of known inside diameter, along with total gas volume collected in a cylinder to calculate bubble size distribution (Randall et al., 1989; Tucker et al., 1994). A common photographic method is the McGill Bubble Size Analyzer which is based on the analyses of a large series of images of bubbles in a transparent chamber drawn off from the flotation cell and analyzed off-line using software to calculate bubble size distribution (Chen et al., 2001; Hernandez-Aguilar, 2004). Other methods to calculate bubble size are by estimation form gas holdup, gas and liquid flow rates using drift flux analysis (Yianatos et al., 1988; Dobby et al., 1988; Finch and Dobby, 1990).

One method commonly used to characterize bubble size distributions is the Sauter mean bubble diameter (D_{32}). The D_{32} (mm) represents the size of a bubble having the same total bubble volume to surface area ratio as the bubble size distribution and is defined as:

$$D_{32} = \Sigma_1^n \frac{D_i^3}{D_i^2} \tag{2.2}$$

where a D_i is bubble diameter. Given that flotation is driven by bubble surface area, the D_{32} is the mean size commonly used in flotation studies. In practice, bubble sizes measured in flotation units range between 0.5 - 2.0 mm (Gorain et al., 1995a). The differences in bubble size is believed to be a result of the frequency of bubble coalescence and possibly air stream breakup (Grau and Laskowski, 2006; Finch et al., 2008). Bubble size has been shown to be mostly affected by frother concentration, but is also a function of generation method (impeller, sparger or downcomer) and of gas flow rate (superficial gas velocity).

2.1.2.1. Effect of Frother Addition on Bubble Size

In most mineral flotation systems, surfactants known as frothers are added to help produce bubbles of about 1 mm (Nesset et al., 2006). The reduced bubble size and larger surface area to volume ratio can increase flotation rate more than 10-fold (Ahmed and Jameson, 1985). Frothers are hetero-polar compounds that adsorb at the air/water interface (Leja and Schulman, 1954) thereby lowering the surface tension of water. They are commonly held to act on bubbles through coalescence prevention (Harris, 1976). The ability of frother to decrease bubble size by decreasing surface tension alone does not affect bubble size to a large degree at the frother concentrations ranges commonly employed, such as 10-15 ppm of DF-250 (Sweet et al., 1997; Aldrich and Feng, 1999). Case in point is the addition of salt which in effect increases surface tension but decreases bubble size (Finch et al., 2008). Cho and Laskowski (2002) showed that bubble size depended on bubble collision and subsequently on their ability to coalesce. It is hypothesized that a frother is generally acting to preserve a bubble's size through coalescence prevention, which is believed to mainly occur at creation sites (Harris, 1982; Espinosa-Gomez et al., 1988; Hofmeier et al., 1995, Comely et al., 2002; Cho and Laskowski, 2002; Finch et al., 2008). The addition of frother decreases D_{32} to a minimum that occurs at a specific concentration beyond which frother addition has minimal effect on D_{32}. The function of frothers in flotation and its effect on bubble size is explained in details in Section *2.2*.

This concentration referred to as critical coalescence concentration (CCC) varies between frothers and can therefore be used to compare their strengths, with stronger frothers reaching their CCC at a lower concentration.

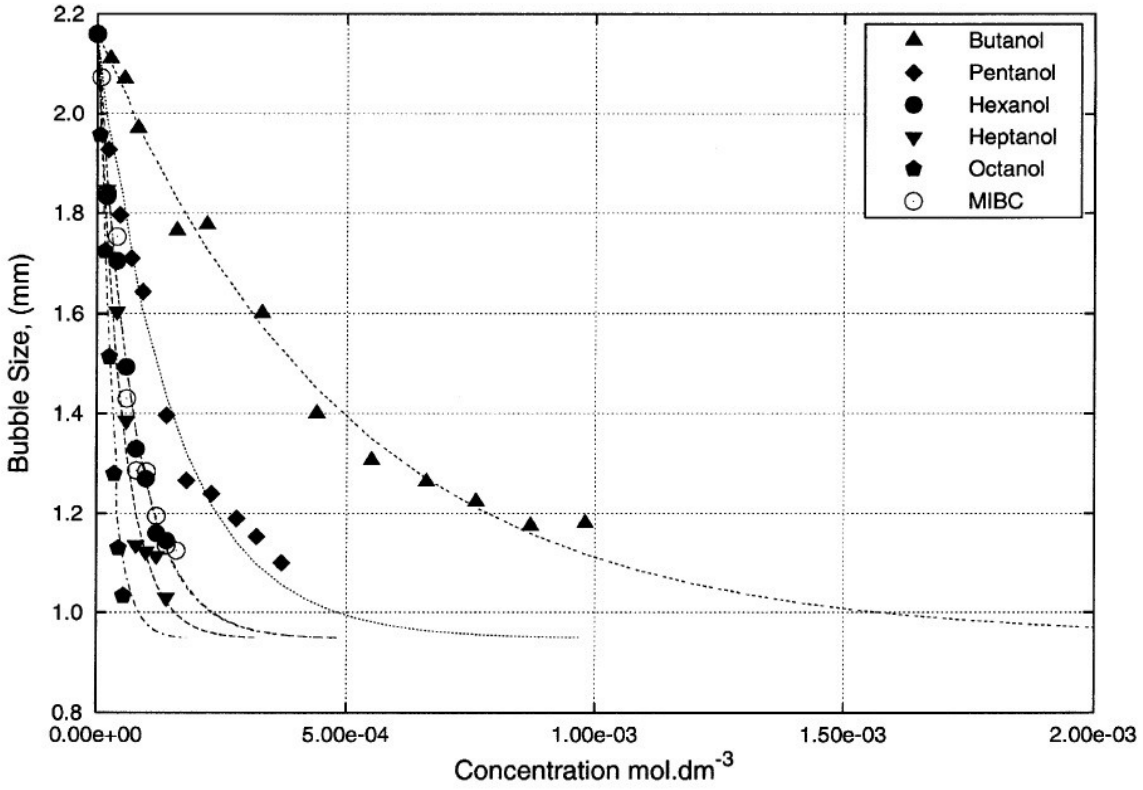

Figure 2.1 - D_{32} as a function of bulk frother concentration (Sweet et al., 1997)

2.1.2.2. Effect of Superficial Gas Velocity on Bubble Size

Gas flow rate, or superficial gas velocity, has been shown to have a pronounced effect on the bubble size generated in flotation units. It was shown that as the superficial gas velocity increased so did the bubble size (Finch and Dobby, 1990). Dobby and Finch (1986) proposed the following correlation between gas velocity and bubble size:

$$d_b = c\upsilon_g^n \tag{2.3}$$

Where d_b is bubble size, υ_g is superficial gas velocity and "c" and "n" are constants related to the bubble generation material and slurry chemistry. Nesset et al. (2006) proposed a modification to Equation 2.3 which takes into account the bubble size D_0 generated at near zero gas velocities, believed to be the notional creation size of the bubbles prior to coalescence. The modification is as follows:

$$D_{32} = D_0 + CJ_g^n \tag{2.4}$$

The inherent bubble size D_0 was shown to be around the 0.5-0.6 mm for the mechanical shear device. The effect of the shearing mechanism is also highlighted in Figure 2.2 whereby different impeller/stator designs lead to different bubble size measurements (Gorain et al., 1995a; Nesset et al., 2006). However an increase in the speed of the impeller, which in effect is an increase in energy input, was shown to have no observable effect on bubble size measurements. The use of sparging mechanism and various sparging materials is also shown to result in different bubble size measurements (Finch and Dobby, 1990).

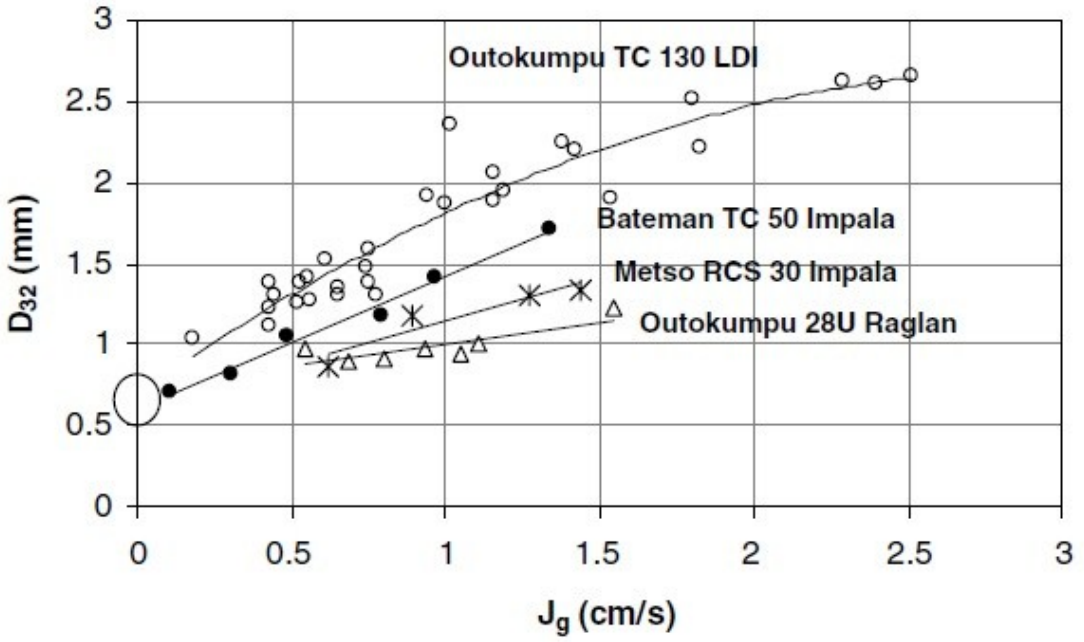

Figure 2.2 - Effect of superficial gas velocity on bubble size using different generation devices (Nesset et al., 2006)

2.1.3. Gas Holdup (E_g)

Gas holdup refers to the ratio of gas volume per total unit volume commonly quoted as a percentage. It is prominently used across many industries to measure the amount of gas in slurry. The formula for gas holdup (%) is given by:

$$E_g = \frac{V_g}{V_{total}} \times 100 \tag{2.5}$$

where V_g is the volume of gas and V_{total} is the total unit volume. Gas holdup is one of the dispersion parameters used to characterize flotation performance. It is the easiest parameter to measure and as such many studies are targeted at understanding the factors influencing its

behaviour in the hope of unlocking valuable correlations to flotation performance (Finch and Dobby, 1990; Zhou et al., 1993; Azgomi et al., 2007). A number of variables influence gas holdup, most important of which are superficial gas velocity, bubble size, slurry flow rate and solids content.

The operation of a flotation cell largely depends on the effect of superficial gas velocity, where increasing superficial gas velocity leads to an increase in gas holdup. The increase in gas flow rate (superficial gas velocity) leads to a transition in flow regimes from what is termed "Bubble Flow Regime" (Finch and Dobby, 1990) to "Turbulent Flow Regime". Flotation is best undertaken under bubbly flow regimes (Gorain et al., 1995b; Dahlke et al., 2005).

Bubble size is also known to greatly affect gas holdup, where small bubbles (which rise slower) lead to larger gas holdup measurements. It was also found that different frothers could present different bubble sizes (D_{32}) at identical gas holdup values, traced to an effect of frother type on bubble rise velocity, independent of its effect on bubble size (Tan et al., 2013).

The effect of solid particles on gas holdup was also studied. It was shown that as the solid concentration increased there was a general decrease in gas holdup (Kara et al., 1982; Koide et al., 1984; De Swart et al., 1995; Banisi et al., 1995). This was attributed to bubble break-up prevention and an increase in bubble rise velocity. However, much debate still surrounds the bubble formation mechanism and as such the conclusions remain controversial (Finch et al., 2008).

Gas holdup can be measured using many devices most common of which are level rise, differential pressure and conductivity change measurements. On-line measurement devices for gas holdup in commercial flotation cells have been developed based on these operating principles (Gorain et al., 1995b; Gomez and Finch, 2007). Other instruments for gas holdup measurements rely on X-ray, γ-ray, optical or sound signal analyses. One such example is the relatively new SONARtrac® gas holdup measurement device which makes use of sonar technology developed by CiDRA (CiDRA model GH-100).

2.1.4. Bubble Surface Area Flux (S_b)

Bubble surface area flux is a derived dispersion parameter incorporating superficial gas velocity and bubble size. It was shown to be very useful in predicting flotation unit hydrodynamics and performance in industry (Gorain et al., 1997; Gomez and Finch, 2007; Nesset, 2011)

$$S_b = 6\frac{J_g}{D_b} \tag{2.6}$$

where S_b is bubble surface area flux (s^{-1}), J_g is superficial gas velocity (cm/s) and D_b is bubble diameter (cm). It is related to the rate of particles flotation through the flotation rate constant (k) as follows:

$$k = P \times S_b \tag{2.7}$$

where P is a probability constant of the particle related to collection efficiency. Bubble surface area flux was also shown to relate to gas holdup (E_g in %) according to the following equation (Finch et al., 2000) :

$$S_b = 5.5E_g \tag{2.8}$$

2.2. Frothers

Frothers are used to improve mineral collection by helping produce smaller bubbles through coalescence prevention (Finch et al., 2008) (which offer a larger surface area per unit volume, SA:V in Figure 2.3) and by producing a more stable froth. These chemicals are amphiphilic (exhibit both hydrophilic and lipophilic properties), having both a polar group and non-polar group. The non-polar group is usually a hydrocarbon that can be straight, branched, cyclic or aromatic whereas the polar group usually is a hydroxyl (─OH), carboxyl (─COOH), carbonyl (─C═O─), ester (─COOR), amine (─NH_2), phosphate (═PO_4), sulphate (═SO_4) or nitrile (─CN) (Wrobel, 1953; Laskowski, 1998). This amphiphilic characteristic of frothers makes them prone to adsorption at the water/air interface at the moment of bubble generation.

Gibbs' adsorption isotherm is commonly used to describe the excess frother concentration on the surface of a bubble as a function of bulk concentration and changes in surface tension (Wrobel, 1953; Masliyah et al., 2011):

$$\Gamma_i = -\frac{C_i}{RT}\frac{\partial \sigma}{\partial C_i} \tag{2.9}$$

where Γ: Surface excess concentration (mol/m^2)

C: Concentration in the bulk of the solution (mol)

R: Gas constant (8.314 m^3 Pa / K·mol)

T: Absolute temperature (K)

σ: Surface tension (N/m)

In Equation 2.9, the variables on the right hand side can be determined experimentally and the surface excess concentration of the frother that is adsorbed at the interface can subsequently be evaluated showing the dependence of surface tension on frother concentration. The term $\frac{\partial \sigma}{\partial C_i}$ is also referred to as surface activity of the frother and is affected by its chemistry.

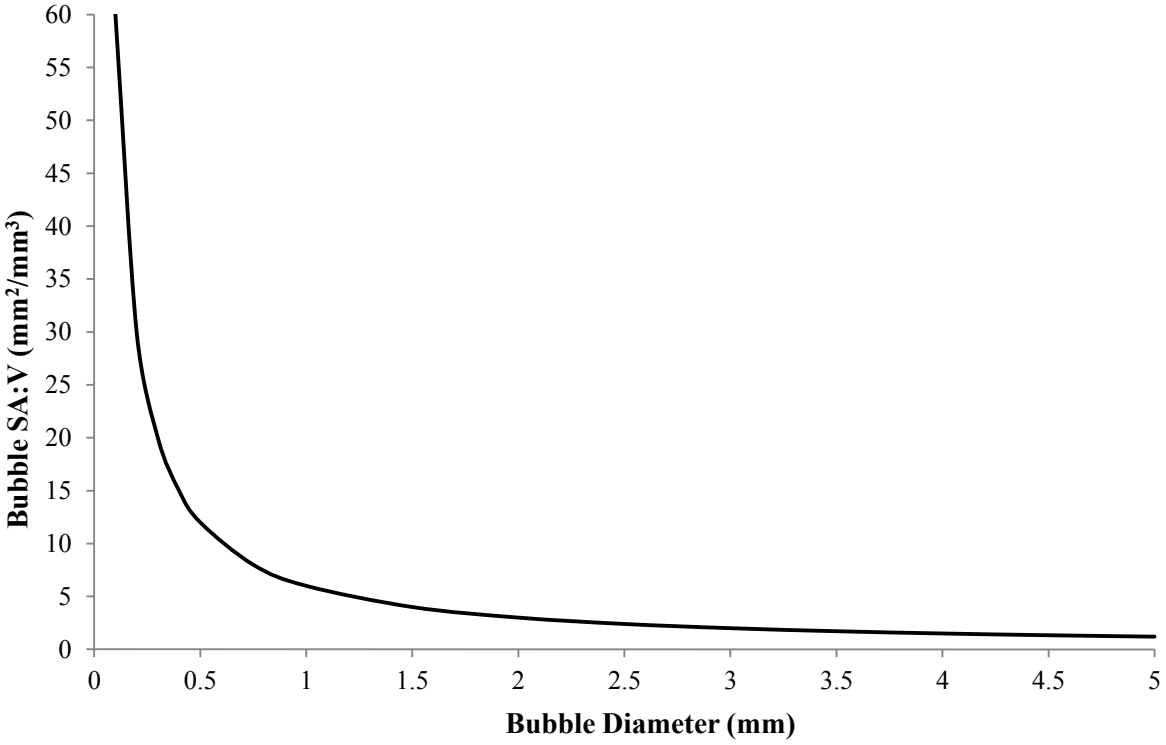

Figure 2.3 - Bubble surface area to volume ratio (SA:V) as a function of bubble diameter

2.2.1. The effect of frother addition on bubble coalescence

Once adsorbed, the frothers tend to form a tight liquid film around the bubble as seen in Figures 2.4 and 2.5 with varying thicknesses depending on frother chemistry (Gelinas et al., 2005). The liquid film is attributed to hydrogen bonding between the hydrophilic group of the frothers and water molecules. Frothers are believed to act on bubbles by retarding and preventing coalescence thereby preserving a bubble's size, which mostly occurs at creation sites (Harris, 1982; Espinosa-Gomez et al, 1988; Hofmeier et al., 1995, Comley et al, 2002).

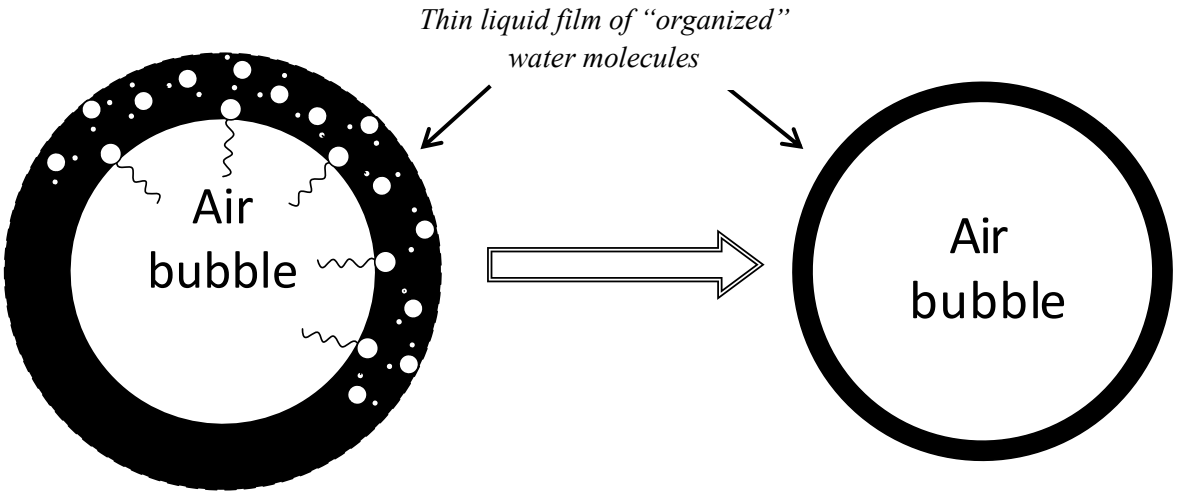

Figure 2.4 - Simplified representation of hydrogen bonding and formation of thin liquid film around bubble

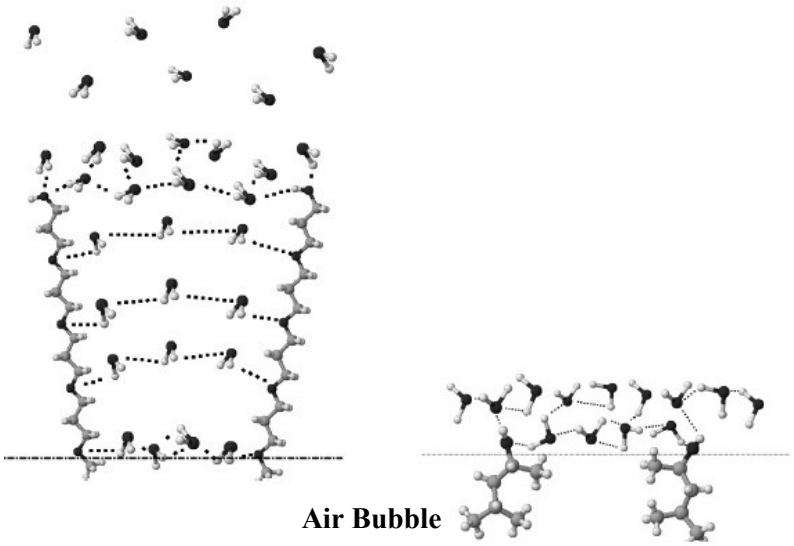

Figure 2.5 - Thin liquid film structure of DF-250 frother (left) and MIBC frother (right) (Gelinas et al., 2005)

Coalescence is the process through which multiple bubbles join up to form a single large bubble, and usually takes place over three stages: *Collision, film thinning* and *rupture* (Oolman and Blanch, 1986; Prince and Blanch, 1990). Collision is dependent on the hydrodynamics of the bulk liquid phase (mainly on gas and liquid flow conditions). As collision occurs, thinning begins and is dependent on the hydrodynamics of the liquid film surrounding the bubble. In effect it is dependent on forces associated with surface tension gradients and surface visco-elastic effects due to the presence of surface active agents. If contact time is sufficiently long and under favorable conditions, a flattening of contact area is observed followed by a gradual expansion as the thin liquid film drains out (Figure 2.6). If the film reaches a critical minimum thickness, rupture occurs due to the instability of the bubble's shape. This is a rapid step when compared to collision and thinning. For coalescence between bubbles to occur, the time it takes for the film to thin and rupture (coalescence time) must be shorter than the contact time. Coalescence time is usually at the order of hundreds of milliseconds (Marrucci, 1969). Initial film thickness in air-water systems typically range between 10^{-2} to 10^{-4} cm and must thin to approximately 10^{-6} cm to coalesce (Kirkpatrick and Locket, 1974; Kim and Lee 1987; Prince and Blanch, 1990).

Frothers inhibit bubble coalescence by increasing the coalescence time. This is achieved by controlling the hydrodynamics of the liquid film associated with surface tension gradient (film elasticity) and diffusion/adsorption of surfactants to the surface layer (surface viscosity). A frother imparts elasticity to the liquid films surrounding the bubbles, known as Gibbs elasticity, which opposes deformation under external forces by inducing a surface tension gradient. When a liquid film is stretched the local frother concentration at that particular surface decreases which in turn leads to a higher local surface tension. Therefore, there is a net force towards the area of low frother concentration which opposes deformation (Dukhin et al., 1998). Gibbs elasticity is calculated according to the following equation (Hofmeier et al., 1995):

$$E = \frac{\partial \sigma}{\partial lnA} \tag{2.10}$$

where E: Gibbs elasticity (N/m)

σ: Surface tension (N/m)

A: Film surface area (m^2)

Equation 2.10 is usually multiplied by a factor of two when looking at binary bubble coalescence to account for both liquid-air interfaces of the liquid film. The surface tension gradient and low local surface frother concentration also induce a flow in the adjoining liquid layer opposing the frother drainage, known as the Marangoni effect (Probstein, 1989; Hofmeier, 1995). Together, Gibbs elasticity and the Marangoni effect oppose bubble deformation and frother drainage which prevents bubble coalescence.

At slower rates of deformation, diffusion of frother from the bulk solution and adsorption at the bubble surface reduces the surface tension gradients. This intrinsic characteristic of the surface is referred to as dilational viscosity (Fruhner and Wantke, 1996). It is calculated using the following equation:

$$\eta = \frac{\partial \sigma}{\partial lnA / \partial t} \tag{2.11}$$

where η: Surface dilational viscosity (N·s/m)

σ: Surface tension (N/m)

A: Film surface area (m^2)

t: Time (s)

The hydrogen bonding between the polar groups in the frothers and the water molecules, and the formation of an organized layer of water, is also believed to contribute to the surface viscosity in helping prevent coalescence (Finch et al., 2006; Finch et al., 2008).

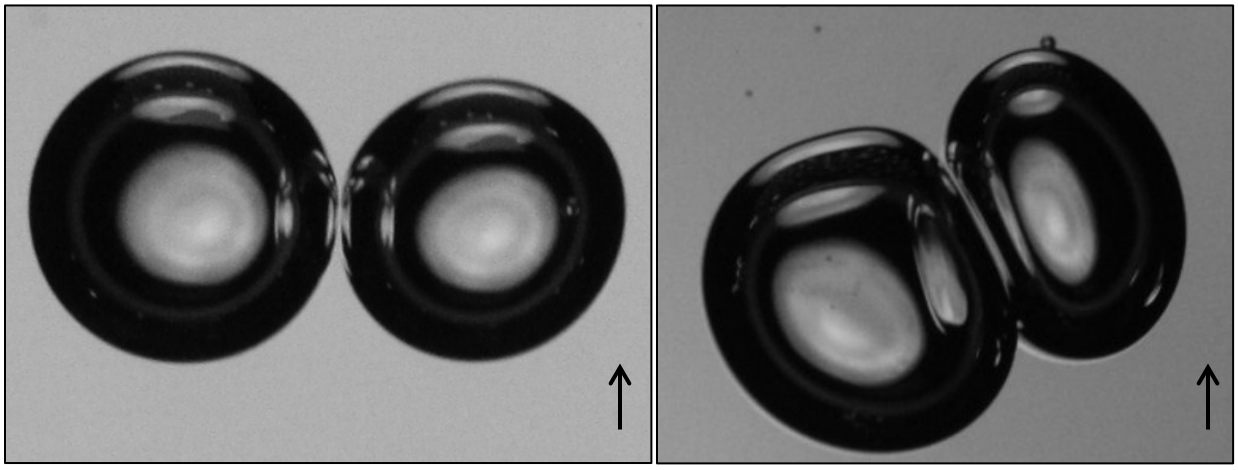

Figure 2.6 - Collision and liquid film thinning prior to rupture during bubble coalescence (Magnified segments of collected images from DF-250 tests – Unpublished results, Marc Nassif 2011)

2.2.2. Frother chemistry and classes

2.2.2.1. Guidelines

A number of different frother classes are used in the mineral industry each tailored to the need of the ore body being extracted. In addition to inhibiting coalescence, these surface-active agents in general lead to an increase in froth formation, slower rising bubbles and improved gas dispersion in the flotation unit. Together these effects increase the probability of interaction between bubbles and particles and ultimately lead to much higher recoveries.

The general guidelines for the use of commercial frothers in mineral flotation can be summarized as follows (Klimpel and Hansen, 1987):

a) The froth layer produced must be stable enough to allow the gangue in the water collected in the bubble's wake to drain out of the froth
b) The froth layer should be of sufficient height to act as an additional layer of separation mainly at low concentrations
c) The froth should break readily once removed to the launder and allow for further treatment outside the cell
d) A neutral frother should have no collecting properties which would jeopardize proper process control and potentially lead to uneconomic operation
e) Must have low sensitivity to moderate pH changes and dissolved salt concentrations
f) Must readily disperse in an aqueous medium, but not necessarily be readily soluble
g) Must be relatively cheap and abundant
h) Must be environmentally safe taking into account downstream process water recycling

2.2.2.2. Chemistry and classes

Frothers used in the mineral industry can be divided into three main classes: alcohols, alkoxy paraffins and polyglycols.

a) Alcohols

Alcohol frothers (R-OH) are divided into three main categories based on the variation in the non-polar organic component. The categories are aliphatic, aromatic and cyclic alcohols consisting of 4 to 10 carbon atoms.

Aliphatic alcohols are the most common alcohol frothers where the R-group is either a linear or branched carbon chain. These aliphatic alcohols have been used for decades in the industry. They have low solubility in water, are sensitive to pH changes and form froth layers that do not retain a lot of water and are brittle. In return, they offer fast flotation kinetics at relatively low dosages but are not very persistent and require stage addition (Crozier and Klimpel, 1989). The enhanced water drainage gives them better selectivity but the brittle froth layer limits their range of applicability to fine or medium particle flotation. Recovering coarse particles using aliphatic alcohol frothers is a difficult task that requires higher dosages and involves trade-offs between selectivity and overall recovery. An increase in aliphatic alcohol frother dosage improves the recovery of coarser particles at the expense of selectivity such that the overall process recovery reaches a maximum and decreases with further increase in concentration. Hence, these frothers are generally used to recover fine to medium sized particles using low to moderate dosages at high pH values (Klimpel and Hansen, 1987, 1988). It was found that the lower the carbon content the higher the recovery capability but the lower the selectivity and vice versa. It was also established that aliphatic alcohol frothers containing six carbon chains (C_6) offer the maximum production of froth while still providing selectivity, such as methyl isobutyl carbinol – MIBC (Crozier and Klimpel, 1989; Cappuccitti, 2011).

Pine oil and cresylic acid have also been used in the industry for decades as frothers (Crozier and Klimpel, 1989; Cappuccitti, 2011; Khoshdast and Sam, 2011). The aromatic alcohol α-terpineol is found in pine oil and the cyclic alcohols o-cresol and 2,3-xylenol are found in cresylic acid. These frothers also have a low solubility in water but are used instead of aliphatic alcohols when less pH-sensitivity is needed, while also acting like a collector due to enhanced adsorption onto hydrophobic minerals. Froths generated using pine oil have small bubbles and low water drainage but also break down easily in launder. They do not work well at high dosages and can lead to a froth layer completely collapsing. Froths generated by cresylic acid on the other hand have slightly larger bubbles and marginally better selectivity. The use of cyclical and aromatic frothers is limited and decreasing due to environmental concerns such as high phenol content, which is toxic, and an inherent variability in composition of supplied frothers (Crozier and Klimpel, 1989; Cappuccitti, 2011).

b) Alkoxy Paraffins

The alkoxy-type frothers are similar in characteristics to pine oil but form a froth that is less sensitive to over dosages. TEB (1,1,3-Triethoxybutane: $C_{10}H_{22}O_3$) is the most common alkoxy-type frother and is extensively used in South Africa, Chile and Australia but is banned in the USA due to its low flash point (Crozier and Klimpel, 1989; Cappuccitti, 2011).

c) Polyglycols

Polyglycol frothers offer more versatility than alcohol frothers, having higher water solubility, more persistence throughout the flotation units at lower dosages, generating a more stable froth and being less sensitivity to pH changes (Moyo, 2005). They tend to form thicker boundary layers around the bubbles making them good at recovering coarse particles but also have slower flotation kinetics. These types of frothers are sufficiently persistent that there is no need for stage addition (can be diluted as they move down a bank) but can also pose operational problems downstream (Cappuccitti, 2011). Two types of polyglycol frothers are central in this group: polypropylene glycol ethers (CH_3-$(O$-$C_3H_6)_n$-OH) and polypropylene glycols (H-$(O$-$C_3H_6)_n$-OH).

Polypropylene glycol ethers range from highly soluble in water to partially soluble as the number of carbons in the molecules increases. This characteristic can be used to tailor frothers based on the requirements of the particular ore body being treated (Klimpel and Hansen, 1987, 1988). If bulkier bubbles and a more persistent froth is required such that coarser particles are recovered, a polypropylene glycol ether with a lower molecular weight (less carbon content) is chosen such that it is more hydrophilic. Polypropylene glycols frothers on the other hand offer very similar characteristics as polypropylene glycol ethers but with even more persistence, higher water retention, extremely stable froth and very low sensitivity to pH changes. This makes them the most powerful commercial frothers in the industry capable of recovering heavy and coarse particles; however this comes at the expense of downstream issues.

2.2.2.3. Hydrophilic-Lipophilic Balance (HLB) scale

A common practice is to blend different types of frothers such that all the desired characteristics are used to optimize flotation recovery. The most used blends being alcohol frothers and a smaller portion of glycol based frother such as MIBC with DF-250 (Klimpel and Isherwood, 1991; Cappuccitti, 2011).

A common balance used to describe the amphiphilic properties of a frother is the Hydrophilic-Lipophilic Balance (HLB) number. This empirical (HLB) number introduced by Griffin (1949) is an experimental measure of the difference in strength between the polar and non-polar groups of the surfactants. High HLB numbers indicate a stronger polar group and better hydrophilicity and small numbers indicate a strong hydrophobic non-polar group. The HLB number can be calculated according to the following relation (Davies, 1957):

$$HLB = 7 + \sum(hydrophilic\ group\ numbers) + \sum(lipophilic\ group\ numbers) \qquad (2.12)$$

where for example the hydrophilic hydroxyl group (-OH) has an HLB number of 1.9 and the hydrophobic alkyl (-CH_3) and propylene (-CH_2-CH_2-CH_2-O-) groups have HLB values of -0.475 and -0.15 respectively. This scale provides an additional measure of solubility and a method of differentiation between frothers, with surfactants having an HLB number less than 4 considered insoluble in water. For instance, the water soluble frother DF-250 has an HLB of 7.8 whereas the less soluble MIBC has an HLB of 6.

Table 2.1 - Classification of flotation frothers in the mineral industry (Crozier and Klimpel, 1989; Laskowski 2004; Cappuccitti, 2011; Khoshdast and Sam, 2011)

Group	Example	Structural Formula	Mol. wt (g/mol)	Density (g/ml)	Solub. (g/l)	HLB
Aliphatic Alcohols	**MIBC** $C_6H_{14}O$	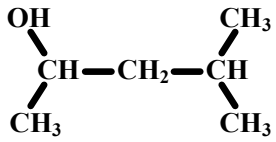	102.17	0.808	17	6
Aromatic Alcohols	**o-Cresol** C_7H_7O	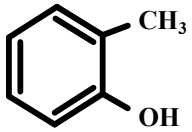	108.14	1.05	25	-
Cyclic Alcohols	**α-Terpineol** $C_{10}H_{18}O$	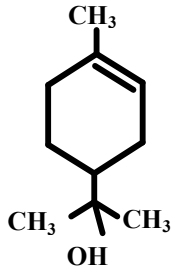	154.25	0.919	2.2	5.4
Alkoxy Paraffins	**TEB** $C_{10}H_{22}O_3$	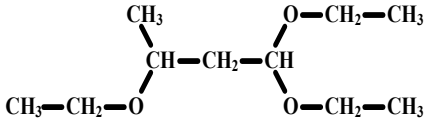	190	0.891	-	6.6
Polyglycol Ethers	**DF-250** $C_{13}H_{28}O_5$	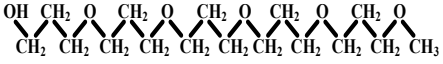	264.36	0.98	Total	7.8
Polyglycols	**DF-1400** $C_{18}H_{38}O_7$	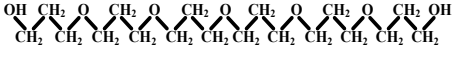	366.49	1.007	Total	10

2.3. Oil Sands

The oil sands of Canada are among the largest reserves of hydrocarbons in the world, containing the equivalent of 1.7 trillion barrels of oil, of which 170 billion barrels are recoverable using current technology, third to Saudi Arabia and Venezuela (ERCB, 2011). The oil sands are found as unconsolidated sandstone deposits consisting of very heavy crude known as bitumen and sand, and are separated by a thin film of water containing mineral rich clays (Clark, 1944; Mossop, 1980; Takamura, 1982; Hall et al., 1983). The largest deposits are found in the Athabasca region of Alberta, namely the Wabiskaw-McMurray deposit which contains the highest bitumen saturation. All large open-pit mining operations such as Albian Sands (Shell), Syncrude, Suncor, Horizon (CNRL) and Kearl (Imperial Oil) are located in this area, with a bitumen ore grade ranging between 9 wt. % - 13 wt. % and a total established mineable bitumen reserve of 27 billion barrels (ERCB, 2011; Masliyah et al., 2011). Another oil sands recovery method is the in-situ operations pioneered by Cenovus Energy and Imperial Oil, which has been used to extract oil where the deposit is too deep for economic mining. The most common commercially used in-situ method is steam-assisted gravity drainage (SAGD) in which two parallel horizontal wells are drilled into the formation at different depths. Steam is introduced from the upper well to heat the formation and reduce the viscosity such that the bitumen, along with condensed steam, flow to the lower well and is pumped to the surface. This operation requires a minimum overburden thickness of 75 m (ERCB 2011). It is estimated that 80% of the oil sands reserves are recoverable using in-situ methods compared to 20% using mining. Total production from the oil sands for the year 2011 was 277,200 m^3/d of bitumen divided equally between mining and in-situ operations for the year.

The focus of this study is the processing of oil sands for the extraction of bitumen. The commercial method used for extracting bitumen from mined oil sands is called Clark hot-water extraction. In this process, the mined oil sands are conditioned with caustic soda and hot water (50°C to 80 °C), aerated and transferred using pipeline hydrotransport to a large gravity separation tank, the primary separation cell (PSC) (Clark, 1929; Clark and Pasternak, 1932; Masliyah et al., 1981; Schramm et al., 2000; Masliyah et al., 2011). Most of the bitumen is recovered in a rich froth formed in the PSC. The middlings, a slurry in the middle of the PSC, and tailings are drawn off to conventional mechanical flotation cells in order to recover the

remaining bitumen. This process has been shown to give very high recoveries for bitumen-rich estuarine ores, but poorer recoveries for leaner marine ores (Schramm and Smith, 1985a).

A key characteristic of the Canadian oil sands is the thin water film surrounding the sand grains (Figure 2.7), which renders them easier to separate from hydrophobic bitumen using water-based separation methods such as hot water extraction. The extraction process decreases the viscosity due to the increase in temperature, and the increase in pH releases natural surfactants from the bitumen (Leja and Bowman, 1968; Sanford, 1983). This facilitates the ablation and liberation of bitumen from sand lumps through mechanical agitation (Takamura and Chow, 1985; Schramm and Smith, 1985a; Hupka and Miller, 1991). Depending on the ore grade and the amount of fine particles, different levels of NaOH are needed to release sufficient surfactants to reach what is termed as the critical free surfactant concentration. This is the concentration at which maximum recovery is achieved (Schramm and Smith, 1985b, 1990a, 1990b). Rich ores have a low fines content and therefore need less process aid to reach the critical surfactant concentration. The surfactants released following caustic addition are predominantly aliphatic carboxylates - $CH_3(CH_2)_{x>4}COONa$ - having typically carbon chains ranging from C_{15} to C_{17} (Schramm et al., 1987; Schramm et al., 2000).

The main solid gangue is quartz (90% by mass) which once washed resembles fine beach sand (130-150 μm), with minor amounts of feldspar, muscovite, chert and clay minerals (Schramm et al., 2000). Clays are mainly aluminosilicate minerals: kaolinite, illite, and montmorillonite. The bitumen occupies the interstitial space. The crude bitumen also contains relatively high levels of nitrogen, oxygen, sulfur and metals. It is however deficient in hydrogen relative to carbon. Such characteristics mean the bitumen ore requires a series of upgrading steps prior to becoming a viable synthetic crude similar to light crude oil.

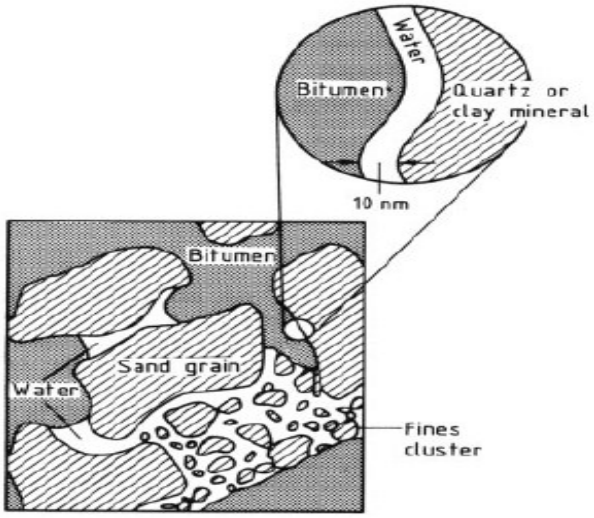

Figure 2.7 - Oil Sands Structure (Takamura et al., 1982)

2.3.1. Bitumen extraction

Removing almost all of the bitumen from the sand is a relatively challenging task generally summarized in a four-step process:

1. The ore is mixed with hot water, NaOH, and air. Large clusters are broken down and coarse material is removed (tumblers, hydrostransport)
2. The resultant slurry is fed into a primary separation cell (PSC) where the sand settles at the bottom. A mixture of sand, water and bitumen (called middlings) remains suspended in the middle and bitumen froth floats to the top and is removed for further processing
3. The sand at the bottom of the tank and the middlings go through secondary and tertiary flotation units. The Froth is recycled back to the PSC
4. The PSC froth is diluted with paraffinic solvents to decrease its viscosity and precipitate asphaltenes. Water and solids remaining in the bitumen froth are removed using centrifuges and settling units. The bitumen is then sent to the upgrader to be converted to synthetic crude oil

Once diluted, the product stream (dilbit, mixture of bitumen and paraffinic solvent) is sent to an upgrader, often offsite. Prior to any upgrading, the remaining diluent (paraffinic solvent, mainly hexane) must be removed through a process of distillation. After the paraffinic solvent has been removed, the remaining bitumen is upgraded by applying heat, pressure and hydrogen addition (Masliyah et al., 2004; Shell performance report, 2009).

2.3.2. Surfactants and interfacial tension

If the bitumen droplet and gas bubble collide, attachment is thermodynamically favourable (spontaneous) and the attachment coefficient, A, given as:

$$A=\gamma^{\circ}_{(aq)}+\gamma_{(Bit/aq)}-\gamma^{\circ}_{(Bit)} \quad (2.13)$$

is positive, where $\gamma^{\circ}_{(aq)}$ is the surface tension of the aqueous solution, $\gamma^{\circ}_{(Bit)}$ is the surface tension of the bitumen, and $\gamma_{(Bit/aq)}$ is the interfacial tension between the aqueous solution and bitumen (in N/m or dynes/cm) (Harkins, 1941; Schramm et al., 2000). Spreading will occur if the spreading coefficient, S, given as:

$$S=\gamma^{\circ}_{(aq)}-\gamma_{(Bit/aq)}-\gamma^{\circ}_{(Bit)} \quad (2.14)$$

is positive. A can be written as:

$$A=S+2\,\gamma_{(Bit/aq)} \quad (2.15)$$

thus A is always greater than or equal to S and three combinations can occur:

1-A<0: flotation doesn't occur
2-A>0, S<0: flotation might occur, depending on sufficient quiescent medium so that bit doesn't shear away from bubble
3-A>0, S>0: (encapsulation) flotation occurs and only high mechanical shear can cause it to strip away. Best configuration for PSC

The surfactants required are those which decrease $\gamma_{Bit/aq}$ with minimal lowering of γ°_{aq}. This action is consistent with that of ionic surfactants that have long hydrocarbon tails such that they tend to partition mostly into the bitumen and slightly into the water. $C_{15\text{-}17}$ surfactants match this criterion.

It was found that carboxylate surfactants have greater impact on process efficiency than sulfonate surfactants in many cases. Correlations for optimal recovery versus concentration (during slurry conditioning) work best with this type of surfactants. This optimum concentration has been termed a "slurry-stage critical carboxylate surfactant concentration" (ζ^{0}_{CS}); subscript specifies the carboxylate surfactant (Schramm and Smith, 1987).

$$\zeta^{0}_{CS} = 7.5 \times 10^{-4} N \text{ and } C^{0}_{CS} = 1.2 \times 10^{-4} N \quad (2.16)$$

where N (normality concentration) is the gram equivalent weight of solute per liter of solution. Measuring the concentration requires accounting for flood water which is easy and comes to C^{0}_{CS} which is determined from an assay of process streams such as secondary tailings (batch

extraction test) or PSC middlings (continuous). Reasons for decreased efficiency at higher concentrations include formation of alternate adsorption layer orientation or multiple adsorption layers at interfaces. Sulfonate surfactants come into play in conditions where carboxylate concentration is close to zero (otherwise preferential adsorption of carboxylate surfactant occurs). Should carboxylate concentration be near zero, the correlation for optimum recovery holds for sulfonate surfactants concentration in aqueous phases. This optimum concentration has been termed a "slurry-stage critical carboxylate surfactant concentration" (ζ_{SS}^{0}); similarly, measuring the concentration requires accounting for flood water which is easy and comes to C_{SS}^{0} which is measured in assay of process streams such as secondary tailings (batch extraction test) or PSC middlings (continuous).

$$\zeta_{SS}^{0} = 9.5 \times 10^{-4} N \text{ and } C_{SS}^{0} = 1.5 \times 10^{-4} N \tag{2.17}$$

There are different types of ores requiring varying NaOH input which leads to various C_{SS} and C_{CS} concentrations, also known as free surfactant concentration (close to C_{SS}^{0} and C_{CS}^{0} led to optimum recovery). Different ores have differing reactions to the addition of NaOH which leads to surfactant production, thus at a certain NaOH concentration when some ores have no production of sulfonate, others may have no production of carboxylate.

Oil sand feed composition is an important variable, since compounds react with either NaOH or directly with natural surfactant. The richer ore grade produces more surfactant upon NaOH addition compared to the leaner ore grades, which contains a greater fines content. These fines inhibit the formation of the surfactant either by adsorbing the surfactant as they are produced or by reacting with NaOH itself. Thus a concomitant process is occurring with production of surfactant, decreasing bitumen recovery.

2.3.3. Bitumen flotation

The general PSC froth composition is 60 wt.% bitumen, 10 wt.% solids, 30 wt.% water and contains air, making it more viscous and requiring de-aeration prior to pumping. Secondary froth collected in the mechanical flotation units is of lower grade containing 15 wt.% bitumen, 20 wt.% solids, and 65 wt.% water. It is cleaned in thickeners to remove water and solids then de-aerated. Studies on the temperature effect on flotation were conducted (Schramm et al., 2002; Zhou et al., 2004) which determined that temperatures higher than 50°C have little impact on

improving flotation. These results suggest that for good processing ores, warm water is sufficient to have similar recovery efficiency as the 80°C used in the Clark Hot Water Extraction Process. However, lower operating temperatures decrease the flexibility of a commercial plant to handle different types of ores. Ores containing a high amount of fines do not respond to adjusting parameters such as temperature, aeration, agitation, etc. and the most common way of extracting these ores is by increasing the pH (adding caustic). This in turn increases liberation and de-coagulation between oil sand/clay, but also releases of surfactants which lead to a number of issues such as emulsification (Schramm et al., 2000; Masliyah et al., 2011).

While the bitumen recovery has been correlated to the amount of added process aid, namely NaOH, correlations to bubble hydrodynamic properties, namely bubble size, have rarely been studied. It was shown that smaller bubbles in general led to better bitumen-bubble attachment due to shorter induction time and are subsequently beneficial for bitumen flotation (Yoon and Luttrell, 1989; Gu et al., 2004). Zhou et al. (2000) studied the effect of process water chemistry on gas dispersion in bitumen flotation by measuring the gas holdup in a water column and estimating the bubble size using a drift-flux approach (Finch and Dobby, 1990). They showed that the bubble size decreased with increasing NaOH concentration. They also highlighted the direct relationship between smaller bubble size and higher bitumen recovery, and the detrimental effect of fines in lower grade ores. However, the effects of these surfactant systems on the bubble sizes generated in bitumen flotation, and consequently on the bitumen recovery, have yet to be characterized and their effect on flotation quantified.

2.4. References

Ahmed, N., Jameson, G.J., 1985. The effect of bubble size on the rate of flotation of fine particles. International Journal of Mineral Processing, Vol. 14, pp. 195–215

Aldrich, C., Feng, D., 1999. Effect of Fluid Properties on Two-Phase Froth Characteristics. Industrial and Engineering Chemistry Research, Vol.

Azgomi, F., Gomez, C. O., Finch, J. A., 2007. Characterizing Frothers Using Gas Hold-Up. Canadian Metallurgical Quarterly, Vol. 46, pp. 237-242

Banisi, S., Finch, J. A., Laplante, A.R., 1995. Effect of Solid particles on Gas Hold-up in Flotation Columns: 1 – Measurement. Chemical Engineering Science, Vol. 50, pp. 2329-2334

Cappuccitti, F., 2011. Collector and Frother Chemistry Overview. In: Proceedings of the Mineral Processing Short Course, McGill University, 2011

Chen F., Gomez , C.O., Finch J.A., 2001. Technical Note Bubble Size Measurement in Flotation Machines. Minerals Engineering, Vol. 14, pp. 427-432

Cho, Y.S., Laskowski, J.S., 2002. Effect of Flotation Frothers on Bubble Size and Foam Stability. International Journal of Mineral Processing, Vol. 64, pp. 69-80

CiDRA SONARtrac® Gas Holdup Monitoring System - Model GH-100 Data Sheet. www.cidra.com [online]

Clark, K.A., 1929. Bituminous Sand Processing. Canadian Patent 289058, issued on April 4, 1929

Clark, K.A., Pasternak, D.S.,1932. Hot Water Separation of Bitumen from Alberta Bituminous Sand. Industrial and Engineering Chemistry, Vol. 24, pp. 1410-1416

Clark, K.A., 1944. Hot-Water Separation of Alberta Bituminous Sand. Transcript of Canadian institute of Mining and Metallurgy. Vol. 47, pp. 257-274

Comley, B.A., Harris, P.J., Bradshaw, D.J., Harris, M.C., 2002. Frother characterization using dynamic surface tension measurements. International Journal of Mineral Processing, Vol. 64, pp. 81-100.

Crozier, R.D., Klimpel, R.R., 1989. Mineral Processing and Extractive Metallurgy Review 5, pp. 257-279.

Czarnecki, J., Radoev, B., Schramm, L.L., Slavchev, R., 2005. On the nature of Athabasca oil sands. Advances in Colloid Interface Science. Vol. 114-115, pp. 53-60

Dahlke, R., Gomez, C.O., Finch, J.A., 2005. Technical Note: Operating Range of a Flotation Cell Determined from Gas Holdup vs. Gas Rate. Minerais Engineering, Vol. 18, pp. 977-980

Davies, J.T., 1957. A quantitative kinetic theory of emulsion type, I. Physical chemistry of the emulsifying agent, Gas/Liquid and Liquid/Liquid Interface. Proceedings of the International Congress of Surface Activity, pp. 426-438

De Swart, J.W.A., Krishna, R., 1995. Influence of Particles Concentration on the Hydrodynamic of Bubble Column Slurry Reactors. Chemical Engineering Research and Design, Vol. 73, pp. 308-313

Ding, X., Repka, C., Xu, Z., Masliyah, J., 2006. Effect of illite clay and divalent cations on bitumen recovery. Canadian Journal of Chemical Engineering. Vol. 84, pp. 643-650

Dobby G.S., Yianatos J.B., Finch J.A., 1988. Estimation of Bubble Diameter in Flotation Columns from Drift Flux Analysis. Canadian Metallurgical Quarterly, Vol. 27, pp. 85-90

Dobby, G.S., Finch, J.A., 1986. Partic1e collection in columns - Gas rate and bubble size effects. Canadian Metallurgical Quarterly, Vol. 25, pp. 9-13

Dukhin, S.S., Miller, R., Loglio, G., 1998. Physico-chemical hydrodynamics of rising bubbles. In: Mubius, D., Miller, R. (Eds.), Studies in Interfacial Science, Drops and Bubbles in Interfacial Research, Vol. 6, pp. 367-432

Energy Resources Conservation Board (ERCB), 2011. ST98: Alberta's Energy Reserves 2011 and Supply/Demand Outlook 2012-2021. Calgary

Espinosa-Gomez, R., Finch, J.A., Bernert, W., 1988. Coalescence and froth collapse in the presence of fatty acids. Colloids and Surfaces, Vol. 32, pp. 197-209

Finch, J.A., Dobby, G.S., 1990. Column Flotation. Pergamon Press, New York, 1990

Finch, J.A., Xiao, J., Hardie, C., Gomez, C.Q., 2000.Gas Dispersion Properties: Bubble Surface Area Flux and Gas Holdup. MineraIs Engineering, Vol. 13, pp. 365-372

Finch, J. A., Gelinas, S., Moyo, P., 2006. Frother-Related Research at McGill University, Minerals Engineering, Vol. 19, pp. 726-733

Finch, J.A., Nesset, J.E., Acuna, C., 2008. Role of frother on bubble production and behaviour in flotation. Minerals Engineering, Vol. 21, pp. 949-957

Fruhner, H., Wantke, k.-D., 1996. A new oscillating bubble technique for measuring surface dilational properties. Colloids and Surfaces, A Physiochemical and Engineering Aspects, Vol. 114, pp. 53-59

Gelinas, S., Finch, J.A., Gouet-Kaplan, M., 2005. Comparative reaI-time characterization of frother bubble thin films. Journal of Colloids and Interface Science: In press, corrected proof

Gomez, C. O., Finch, J. A., 2007. Gas Dispersion Measurements in Flotation Cells. International Journal of Mineral Processing, Vol. 84, pp. 51-58. (Special issue honoring Professor Peter King).

Gorain, B.K., Franzidis, J.-P., Manlapig, E.V., 1995a. Studies on impeller type, impeller speed and air flow rate in an industrial scale flotation cell-Part 1: Effect on bubble size distribution. Minerals Engineering, Vol. 8, pp. 615-635

Gorain B.K., Franzidis J.-P., Manlapig E.V., 1995b. Studies on Impeller Type, Impeller Speed and Air Flow Rate in an Industrial Scale Flotation Cell - Part 2: Effect Gas Holdup. Minerals Engineering, Vol. 8, pp. 1557-1570

Gorain B.K., Franzidis J.-P., Manlapig E.V., 1996. Studies on Impeller Type, Impeller Speed and Air Flow Rate in an Industrial Scale Flotation Cell - Part 3: Effect on Superficial Gas Velocity. Minerals Engineering, Vol. 9, pp. 639-654

Gorain, B.K., Franzidis, J.P., Manlapig, E.V., 1997. Studies on Impeller Type, Impeller Speed and Air Flow Rate in an Industrial Scale Flotation Cell - Part 4: Effect of Bubble Surface Area Flux on Flotation Performance. Minerals Engineering, Vol. 10, pp. 367-379

Grau, R.A., Laskowski, J.S., 2006. Role of frothers in bubble generation and coalescence in a mechanical flotation cell. Canadian Journal of Chemical Engineering, Vol. 84, pp. 170-182

Gu, G., Sanders, R.S., Nandakumar, K., Xu, Z., Masliyah, J.H., 2004. A Novel Experimental Technique to Study Single Subble Bitumen Attachment in Flotation. International Journal of Mineral Processing. Vol. 74, pp. 15-29

Harkins, W.D., 1941. A General Thermodynamic Theory of the Spreading of Liquids to Form Duplex Films and of Liquids or Solids to Form Monolayers. The Journal of Chemical Physics, Vol. 9, pp. 552-568

Harris, C.C., 1976. Flotation Machines in Flotation. A.MGaudin Memorial Volume, Vol. 2, Chapter 27, pp.753-815

Harris, P.J., 1982. Frothing phenomena and frothers in Flotation principles. Edited by R.P. King. Chapter 13, pp. 237-250

Hernandez, H., Gomez, C.O., Finch, J.A., 2003. Gas dispersion and de-inking in a flotation column. Minerals Engineering, Vol. 16, pp. 739-744

Hernandez-Aguilar, J.R., Coleman, R.G., Gomez, C.O., Finch, J.A., 2004. A comparison between capillary and imaging techniques for sizing bubbles in flotation systems. Minerals Engineering, Vol. 17, pp. 53–61

Hofmeier, U., Yaminsky, V.V., Christenson, H.K., 1995. Observations of solute effects on bubble formation. Journal of Colloid and Interface Science, Vol. 174. 199-210

Hupka, J., Miller, J.D., 1991. Electrophoretic characterization and processing of Asphalt Ride and Sunnyside tar sand. International Journal of Mineral Processing. Vol. 31, pp. 217-231

Kara, S., Balmohan, G., Shah Y.T., Carr, N.L., 1982. Hydrodynamics and Axial Mixing in a Three-Phase Bubble Column. Industrial Engineering Chemistry Process Design and Development, Vol. 21, pp. 584-594

Kasongo, T., Zhou, Z., Xu, Z., Masliyah, J.H., 2000. Effect of clays and calcium ions on bitumen extraction from Athabasca oil sands using flotation. Canadian Journal of Chemical Engineering. Vol. 78, pp. 674-681

Kim, W. K., Lee, K. L., 1987. Coalescence Behavior of Two Bubbles in Stagnant Liquids. Journal of Chemical Engineering of Japan, Vol. 20, pp. 448-453

Khoshdast, H., Sam, A., 2011. Flotation Frothers: Review of Their Classifications, Properties and Preparation. The Open Mineral Processing Journal, Vol. 4, pp. 25-44

Kirkpatrick, R. D., Lockett, M. J., 1974. The Influence of Approach Velocity on Bubble Coalescence. Chemical Engineering Science Journal, Vol. 29, pp. 2363-2373

Klimpel, R.R., Hansen, R.D., 1987. Frothers. In: P. Somasundaran and B.M. Moudgil (Editors), Reagents in Mineral Technology. Marcel Dekker, New York, NY, pp. 663-681

Klimpel, R.R., Hansen, R.D., 1988. The interaction of flotation chemistry and size reduction in the recovery of a porphyry copper ore. International Journal of Mineral Processing, Vol. 22, pp. 169-181

Klimpel, R.R., Isherwood, S., 1991. Some industrial implications of changing frother chemical structure. International Journal of Mineral Processing, Vol. 33, pp. 369-381

Koide, K., Takazawa, A., Komura, M., Matsunaga H., 1984.Gas Holdup and Volumetrie Liquid-Phase Mass Transfer Coefficient in Solid-Suspended Bubble Columns. Journal of Chemical Engineering of Japan, Vol. 17, pp. 459-466

Laskowski, J. S., 1998. Frothing in Flotation II, Edited by Laskowski J. S. and Woodbum E.T., Chapter 1.

Laskowski, J. S., 2004. Testing Flotation Frothers. In: Physiochemical Problems of Mineral Processing, Vol. 38, pp.13-22.

Leja, J., Schulman, J.H., 1954. Flotation Theory: Molecular Interactions Between Frothers and Collectors at Solid–Liquid–Air Interfaces. Trans. AIME, Vol. 199, pp. 221–228

Leja, J., Bowman, C.W., 1968. Application of Thermodynamics to the Athabasca Tar Sands. Canadian Journal of Chemical Engineering. Vol. 49, pp. 479-481

Marrucci, G., 1969. A Theory of Coalescence. Chemical Engineering Science Journal, Vol. 24, pp. 975-985

Masliyah, J.H., Kwong, T., Seyer, F.A, 1981. Theoretical and experimental studies of gravity separation vessel. Industrial and Engineering chemistry process design and development. Vol. 20, pp. 154-160

Masliyah, J.H., Zhou, Z., Xu, Z., Czarnecki, J., Hamza, H., 2004. Understanding Water-Based Bitumen Extraction from Athabasca Oil Sands. Canadian Journal of Chemical Engineering, Vol. 82, pp. 268-654

Masliyah, J.H., Czarnecki, J., Xu, Z., 2011. Handbook on Theory and Practice of Bitumen Recovery from Athabasca Oil Sands - Volume 1: Theoretical Basis. Kingsley Knowledge Publishing, pp. 115-116

Moyo, P., 2005. Characterization of Frothers by Water Carrying Rate. M.Eng. Thesis, McGill University, pp.36-44

Nesset, J.E., Hernandez-Aguilar, J.R, Acuna, C., Gomez C.O., Finch, J.A., 2005. Some Gas Dispersion Characteristics of Mechanical Flotation Machines. *Proceedings of International Conference SME-IMM,* Centenary of Flotation, Edited by Jameson G., Yoon R.-H. Brisbane, Australia, June 6-9, 2005, pp. 243-250

Nesset, J. E., Hernandez-Aguilar, J. R., Acuna, C., Gomez, C. O., J. A. Finch, 2006. Some Gas Dispersion Characteristics of Mechanical Flotation Machines. Minerals Engineering, Vol. 19, pp. 807-815.

Nesset, J.E., 2011. Flotation Machine Diagnostics. In: Proceedings of the Mineral Processing Short Course, McGill University, 2011

Oolman, T.O., Blanch, H.W., 1986. Bubble coalescence in stagnant liquid. Chemical Engineering Communications, Vol. 43. pp. 237-261

Prince, M.J., Blanch, H.W., 1990. Bubble Coalescence and Break-Up in Air-Sparged Bubble Columns. American Institute of Chemical Engineers (AIChE Journal) 36, pp. 1485-1499

Probstein, R.F., 1989. Physicochemical Hydrodynamics: An Introduction, Butterworths, pp. 300–314

Randall, E.W., Goodall, C.M., Fairlamb, P.M., Dold, P.L., O'Connor, C.T., 1989. A method for measuring the sizes of bubbles in two- and three-phase systems. Journal of Physics, Section E, Scientific Instrumentation, Vol. 22, pp. 827–833

Sanford, E.C., 1983. Processibility of Athabasca oil sand: Interrelationship between oil sand fine solids, process aids, mechanical energy and oil sand age after mining. The Canadian Journal of Chemical Engineering. Vol. 61, pp. 554-567

Shell Oil Sands Performance Report, 2009. Muskeg River Mine &Scotford Upgrader. Found at: http://www.shell.ca/en/aboutshell/our-business-tpkg/business-in-canada/upstream/oil-sands/performance-report.html

Schramm, L.L., Smith, R.G., 1985a. The Influence of Natural Surfactants on Interfacial Charges in the Hot-Water Process for Recovering Bitumen from the Athabasca Oil Sands. Colloids and Surfaces. Vol. 14, pp. 67-85

Schramm, L.L., Smith, R.G., 1985b. Control of Process Aid Used in Hot Water Process for Extraction of Bitumen from Tar Sand. Canadian Patent 1,188,644

Schramm, L.L., Smith, R.G., 1987. Two Classes of Hot Anionic Surfactants and their Significance in Water Processing of Oil Sands. The Canadian Journal of Chemical Engineering. Vol. 65, pp. 799-811

Schramm, L.L., Smith, R.G., 1990a. Monitoring Electrophoretic Mobility of Bitumen in Hot Water Extraction Process Plant Water to Maximize Primary Froth Recovery. Canadian Patent 1265463, issued on February 6, 1990

Schramm, L.L., Smith, R.G., 1990b. Monitoring Surfactant Content to Control Hot Water Process for Tar Sand. Canadian Patent 1270220, issued on June 12, 1990

Schramm, L.L., 2000. Surfactants: Fundamentals and Applications in the Petroleum Industry. Cambridge University Press, pp. 377-378.

Schramm, L.L., Stasiuk, E.N., Yarranton, H., Maini, B.B., Shelfantook, B., 2002.Temperature Effects in the Conditioning and Flotation of Bitumen From Oil Sands in Terms of Oil Recovery and Physical Properties. In: Proceedings of the Canadian International Petroleum Conference, Calgary, Alberta.

Sweet, C., Van Hoogstraten, J., Harris, M., Laskowski, J.S., 1997. The Effect of Frothers on Bubble Size and Frothability of Aqueous Solutions, Proceedings of the second UBC-McGill Bi-annual international symposium of fundamentals of mineral processing, Edited by Finch, J.A., Rao S.R. and Holubec, L, Sudbury, Ontario, August 17-19, pp. 235-245

Takamura, 1982. Microscopic structure of Athabasca Oil Sand. Canadian Journal of Chemical Engineering. Vol. 60, pp. 538-545

Takamura, K., Chow, R.S., 1985. The Electric Properties of the Bitumen/Water Interface, Part II: Application of the ionisable Surface-Group Model. Colloids and Surfaces. Vol.15, pp. 35-48

Tan, Y.H., Rafiei, A.A., Elmahdy, E., Finch, J.A., 2013. Bubble Size, Gas Holdup and Bubble Velocity Profile of Some Alcohols and Commercial Frothers. International Journal of Mineral Processing, Vol. 119, pp. 1-5

Tucker, J.P., Deglon, D.A., Franzidis, J.P., Harris, M.C., O'Connor, C.T., 1994. An evaluation of a direct method of bubble size distribution measurement in a laboratory batch flotation cell. Minerals Engineering, Vol. 7, pp. 667–680

Wrobel, S.A., 1953. Flotation Frothers, Their Action, Composition, Properties and Structure, Recent development in mineral processing, IMM symposium, September 23-25, pp. 431-454

Yianatos, J.B., Finch J.A., Dobby, G.S., 1988. Bubble Size Estimation in a Bubble Swarm. Journal of Colloid and Interface Science, Vol. 126, pp. 37-44

Yoon, R.H., Luttrell, G.H., 1989. The Effect of Bubble Size on Fine Particle Flotation. Mineral Processing and Extractive Metallurgical Review. Vol. 5, pp. 101-122

Zhao, H., Dang-Vu, T., Long, J., Xu, Z., Masliyah, J., 2009. Role of bicarbonate ions in oil sands extraction systems with a poor processing ore. Journal of Dispersion Science and Technology. Vol. 30, pp. 809-822

Zhou, Z.A., Egiebor, N.O., Plitt, L.R., 1993. Frother Effects on Bubble Motion in Swarm. Canadian Metallurgical Quarterly, Vol. 32, pp. 89-96

Zhou, Z., Xu, Z., Masliyah, J., 2000. Effect of Natural Surfactants released from Athabasca Oil Sands on Air Holdup in a Water Column. The Canadian Journal of Chemical Engineering. Vol. 78, pp. 617-624

Zhou, Z.A., Kasongo, T., Xu, Z., Masliyah, J.H., 2004. Assessment of Bitumen Recovery from the Athabasca Oil Sands Using a Laboratory Denver Flotation Cell. Canadian Journal of Chemical Engineering, Vol. 82, pp. 696-703

CHAPTER 3: FROTHER CHARACTERIZATION TECHNIQUES

Over the years, many studies on frothers have investigated new techniques capable of measuring their potential in improving flotation hydrodynamics and determining a material constant for comparison. The various characterization methods rely on two essential principles in flotation: bubble size reduction and foam/froth stability.

3.1. Foam characterization techniques

Foam tests were among the first proposed as new methods to compare frother behaviour, the difference between foam and froth being the absence and presence of solids respectively. These tests are divided into dynamic, where air is constantly supplied to maintain a foam layer, and static, where the air flow is interrupted and the foam layer allowed to collapse.

3.1.1. Dynamic foam tests

3.1.1.1. Foaminess (∑)

The first to propose the use of foam techniques to differentiate frothers was J.J. Bikerman (1938). His work was aimed at establishing foaminess as a unique physical property of a liquid independent of the apparatus and of the amount of material employed in the measurement. A number of methods to tackle the foaming property of a liquid were already proposed prior to this study such as: (1) time required for complete collapse of a lather produced by shaking; (2) dilution of solution till no more foam is formed when shaken; (3) height of foam column generated; (4) inverse rate of drainage. However, none of these methods were independent of the apparatus and materials used (Bikerman, 1938).

Bikerman's method entailed the injection of 1 L of air into a calibrated tube through a porous glass membrane and a frother solution thereby forming a lather (Bikerman, 1938). The majority of experiments were conducted using 1 % w/w commercial n-butyl alcohol (concentration determined from earlier tests to ensure maximum foaming capacity) and 1 % w/w purified commercial n-butyl alcohol.

In order to determine the foaminess of the liquid, the average foam volume (υ) was defined as the difference between the volume occupied by both liquid + foam and the volume occupied by the liquid at rest. The average foam volume is proportional to the air flow rate therefore if the foam volume (υ) is divided by the volume of air streamed (V) in a given time (t) we get:

$$\sum = \frac{\upsilon t}{V} \tag{3.1}$$

where ∑ (s) is the physical property referred to as foaminess that is independent of air flow rate, volume of apparatus, glass porosity and solution volume. A couple of assumptions made about the foam layer were that no bubble coalescence is occurring and no amount of liquid is entrained. These assumptions however rarely hold especially with wet foams.

It was shown that the value of ∑ remains more or less constant (at a given solution volume) whereas the maximum height fluctuates at different flow rates. It was also noted that flow rates that were too slow or too fast caused errors hence a discrepancy in the ∑ values obtained at these conditions.

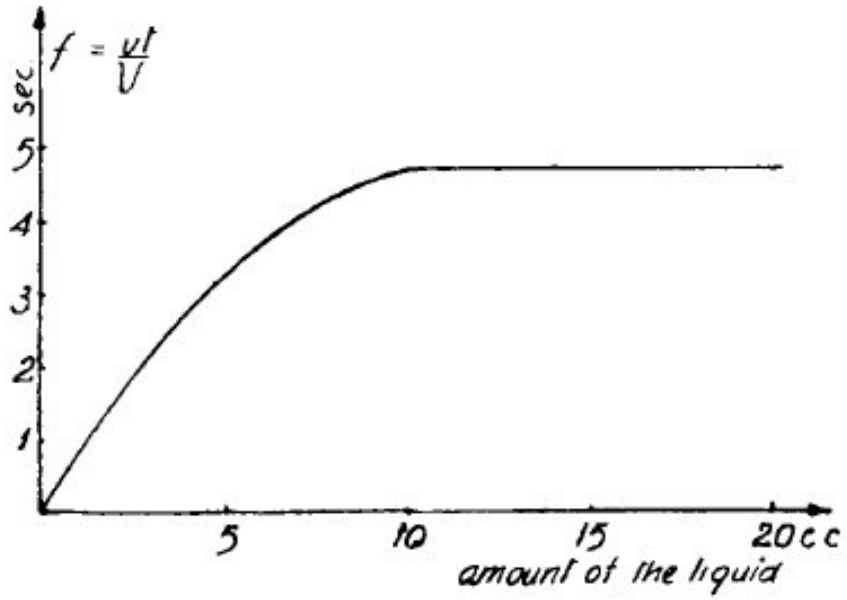

Figure 3.1 - Foaminess of 1% w/w n-butyl alcohol as a function of concentration (Bikerman - 1938)

The size of the septum was shown to not have an effect on ∑ and that the value tends to reach a limit as the amount of liquid increases. It was shown that for 1% w/w n-butyl alcohol at room

temperature $\sum$ = 4.7 s (Figure 3.1) whereas for 1 % w/w commercial n-butyl alcohol "purified" $\sum$ = 7.3 s. The physical interpretation of foaminess is that it represents the lifetime of a bubble in the foam assuming the velocity profile to be constant in both the solution and the foam layer. It was proven by derivation that the time a bubble spends in the foam, $t = \frac{h}{u}$ (where h is foam height in cm and u is the air velocity in cm/s), is none other than $\frac{vt}{V}$.

3.1.1.2. Foamability Index (FI)

An index describing different degrees of foamability was defined by Sun et al. (1952) as the ratio of foam volume produced from a frother solution to the foam volume produced from a standard solution of n-hexyl alcohol. This paved way to create a frother-meter that uses the foaming method in order to grade the frothing capability of a solution based on the standard solution. They also described a stability index (SI) to describe the persistence of a foam layer as the ratio of time it takes for the foam layer to collapse to time it takes the standard solution's foam layer to collapse.

3.1.1.3. Frothability (rt) and dynamic frothability index (DFI)

Malysa et al. (1978) took a closer look at the frothability of frothers and the relationship between the foam persistence and the surface elasticity of bubbles. Frothability was characterized by the retention time (*rt*) of the bubbles in the entire system from generation to rupture. It was calculated from the slope of the linear part of the curves of total gas volume (both in the foam and the solution) as a function of gas flow rate:

$$rt = \frac{\Delta V_g}{\Delta Q_g} \tag{3.2}$$

The gas volume in the system was calculated through the change in total column height. It was found that the retention time increases with frother concentration in an exponential fashion but then transitions to reach a plateau (Figure 3.2). For n-Octanoic acid and n-Octanol in HCl, it was found that n-Octanoic acid has longer retention times (Malysa et al., 1981).

The non-equilibrium surface elasticity of the bubbles were also measured (Marangoni elasticity due to the presence of concentration gradient) using the pulsating bubble method which studies the force necessary to pulsate bubbles using an electromechanical system (Malysa, 1981). The

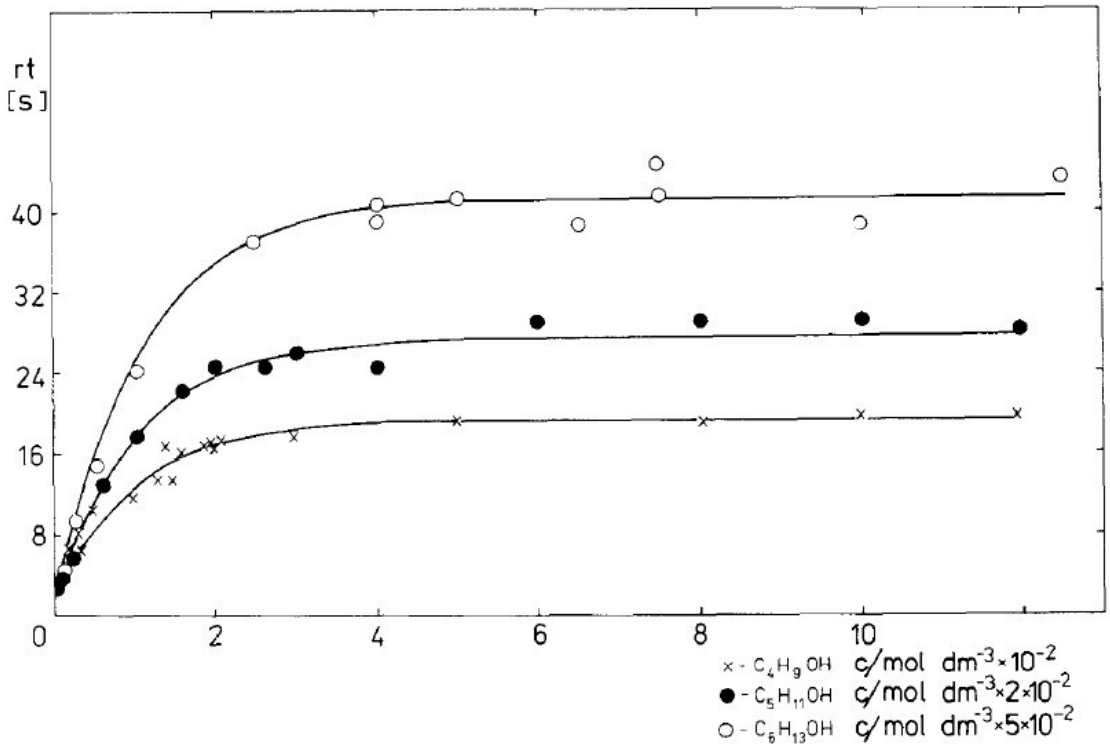

Figure 3.2 - Frothability (rt) as a function of frother concentration (Malysa et al., 1987)

force needed to reach the required bubble pulsation is a function of frother concentration and pulsation frequency (Lukenheimer and Wantke, 1981). The magnitude of the force is therefore a function of the surface elasticity. The accompanying change in surface tension was also measured using the ring tensiometer method. The Marangoni surface dilational modulus is then calculated using an intricate relationship between the changes in frother concentration, change in bubble dimensions and surface tension, adsorption kinetics and the volume of the gas. It was found that changes in elasticity are occurring in the same concentration ranges at which changes in *rt* are observed, and that there exists a positive linear relationship between the Marangoni dilatational modulus (E_m) and frothability but is a function of pulsation frequency. These findings highlighted the role of surface elasticity in foam stability and its effect on frothability.

The relationship between the length of the carbon chain, surface elasticity and retention time was investigated by Malysa et al. (1985). Frothability and oscillating bubble tests were conducted on solutions containing n-butanol, n-hexanol, n-heptanol, n-octanol, n-nonanol and n-decanol in

order to determine the effect of increasing carbon chain length on frother behaviour. It was found that as the carbon chain increased, so did frothability (*rt*) and surface elasticity accordingly reaching a maximum around the C_6-C_8 range. The magnitude of the maxima obtained depended mainly on the concentration of the solute. These observations further confirmed the role of elasticity in stabilizing the foam layer and the importance of solute/frother chemistry and concentration.

Malysa et al. (1987) went on to define a new parameter to describe frothability as a material property of the frother (DFI: dynamic frothability index). This was done to address the limitations of Bikerman's method which assumes an average bubble residence time only in the foam and neglects water entrainment and coalescence, and Sun's limited range of applicability with an arbitrary reference alcohol. Another important issue to address was the effect of frother concentration on frothability (which is observed at different concentration ranges by different frothers). Using frothability values to characterize the frother was only possible at a given concentration and this neglected the difference in surface activity of diverse frothers allowed incorrect conclusions to be reached.

To overcome these dilemmas Malysa et al. (1987) proposed using the tests previously used to develop the frothability (*rt) vs.* concentration *(c)* plots, and defined the new DFI to be the limiting slope at zero concentration as follows:

$$DFI = \left(\frac{\partial rt}{\partial c}\right)_{c=0} \tag{3.3}$$

The following model was used to describe the variation of *rt* with concentration (Figure 3.2):

$$rt - 2.4 = rt_{\infty} \cdot [1 - e^{(-k \cdot c)}] \tag{3.4}$$

where 2.4 is the value of *rt* obtained for distilled water, rt_{∞} is the limiting value as $c \rightarrow \infty$ and *k* is a constant determined experimentally. The fitting was done using the least squares method. Expanding Equation 3.4 into a power series for $c \rightarrow 0$:

$$rt - 2.4 = rt_{\infty} \cdot k \cdot c \tag{3.5}$$

Hence solving for Equation 3.3 we get:

$$DFI = rt_{\infty} \cdot k \tag{3.6}$$

This new parameter allows the comparison of frothers under similar conditions of frothability, taking into account the surface activity of diverse frothers. Furthermore, the product of the newly defined material constant (DFI, in $s.m^3/mol$) and the frother concentration reveals information on the frothing abilities of a particular solution under dynamic conditions. This was confirmed by showing that n-butanol, n-pentanol and n-hexanol solutions all gave similar recoveries of coal if used in amounts that ensure the same frothability, i.e. at the same DFI.c (s) (Figure 3.3).

Sweet et al. (1997) correlated DFI with another new parameter $C_{0.6}$ which represents the concentration at which the sauter mean diameter of the bubbles (D_{32}) is reduced to 0.6 times that of water according to the following empirical formula for alcohols:

$$DFI^{0.64} = \frac{C_{0.6}}{0.059} \textit{ for straight chained alcohols} \tag{3.7}$$

$$DFI^{1.16} = \frac{C_{0.6}}{65.91} \textit{ for branched alcohols} \tag{3.8}$$

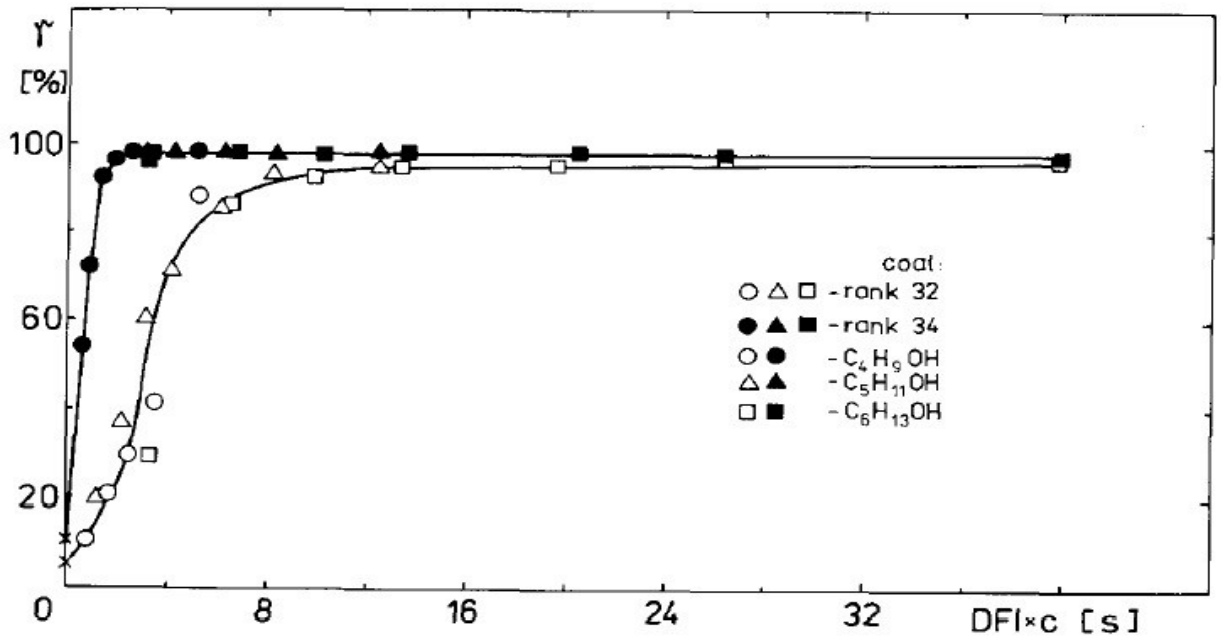

Figure 3.3 - Recovery of coal rank 32 and 34 as a function of DFI.c (Malysa et al., 1986)

3.1.1.4. Dynamic surface tension

Comley et al. (2002) investigated dynamic surface tension measurements in order to compare frothers using the extensively refined maximum bubble pressure technique which makes use of a capillary and a two-wire pressure transmitter as seen in Figure 3.4. They modified the apparatus for high air flow rates by using a capillary facing upwards. Pressure was converted into surface tension using the Laplace equation:

$$\gamma = \alpha \frac{\Delta P}{2} \tag{3.9}$$

where γ is surface tension (N/m), α a characteristic constant of the apparatus (m) and ΔP is P_{max} - $P_{hydrostatic}$ - P_{atm} (N/m^2). N-alcohols, MIBC and DF-200 were tested. The rate limiting step was assumed to be the diffusion of frother molecules to and from the interface while also assuming that adsorption and desorption at the interface is instantaneous. Equilibrium and saturation loading at the surface of a bubble were calculated using a combination of Gibbs' adsorption isotherm and Langmuir's isotherm respectively:

$$\Gamma_m = -\frac{1}{RT}\left(\frac{\partial \gamma}{\partial ln C_b}\right) \tag{3.10}$$

$$\Gamma_m = \Gamma_s \frac{bC_b}{1+bC_b} \tag{3.11}$$

Where Γ_m is the equilibrium surface loading (mol/m^2), Γ_s is the saturation surface loading (mol/m^2), γ is surface tension (N/m), C_b is the bulk frother concentration (mol/m^3) and b is the Langmuir equilibrium constant (m^3/mol).

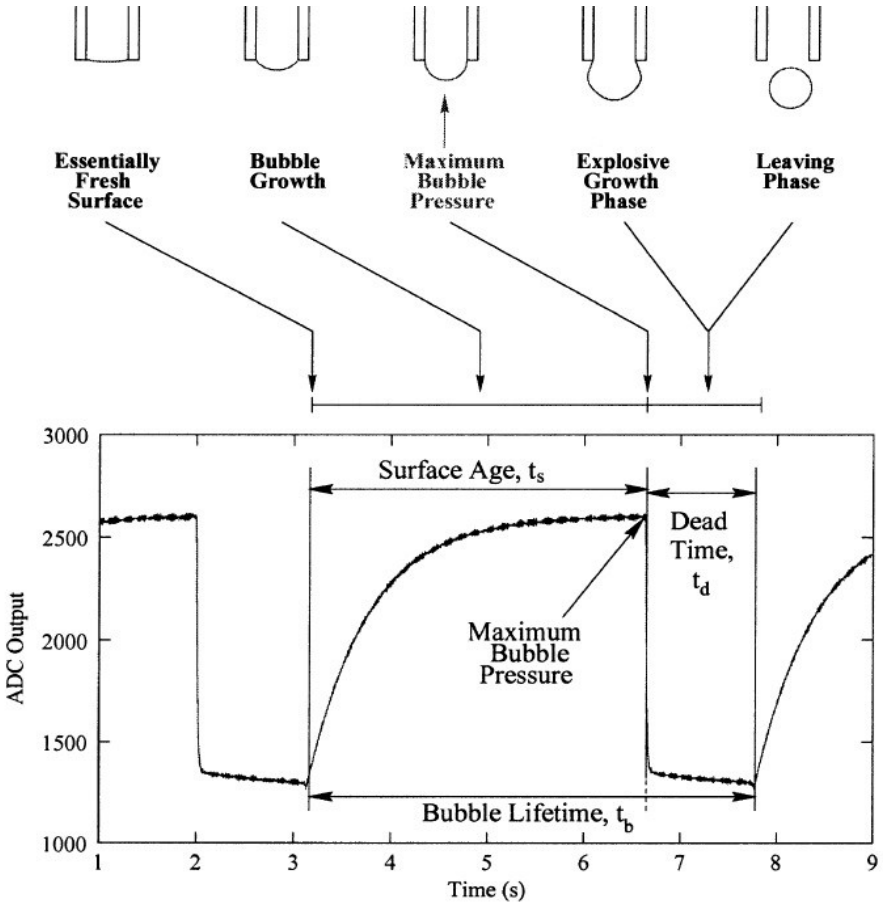

Figure 3.4 - Illustration of progressive bubble pressure phases in the maximum bubble pressure technique (Comley et al., 2002)

By measuring the saturation surface loading, it was shown that the structure of the frother allows for either higher or lower packing. This in turn increases or decreases the time taken to reach equilibrium surface pressure, believed to be due to van der Waals forces between the frother molecules. Octanol for example has the largest packing density at the surface of a bubble (saturation loading Γ_s from Langmuir isotherm) due to its vertical orientation and takes the most time to reach the equilibrium value. DF-200 has the smallest packing density due to alternating occurrence of polar heads and high water solubility (orientations similar to ones in Figure 2.5) which indicates a parallel rather than vertical orientation at the adsorption layer. It was shown that the rate of change in dynamic surface tension typically decreases with increasing chain length for n-alcohols. A comparison between MIBC and hexanol, both having 6 carbons, shows MIBC to have a faster rate of change which is believed to be due to increased solubility (Comley et al., 2002).

3.1.1.5. Froth stability factor and column

Barbian et al. (2003) expanded on the idea of Bikerman's foaminess by relating it to flotation performance. They simulated industrial settings using a modified Denver cell made of a clear front wall to visualize the froth, using platinum ore. They measured foaminess for different surfactant concentrations and at different air flow rates (Figure 3.5). While the higher frother concentrations do give increased foaminess, it was observed that froth stability is very much dependent on operating variables such as air flow rate. By monitoring the change in froth height with time and identifying an equilibrium froth height that is reached, they proposed a model for the variability in froth height as a function of foaminess:

$$H = H_{\max}(1 - e^{t/\tau}) \tag{3.12}$$

where H is the froth height at time t (cm), H_{max} is the equilibrium height (cm) and τ is the foaminess ($\sum$). The equilibrium height depends on the frother concentration and air flow rate.

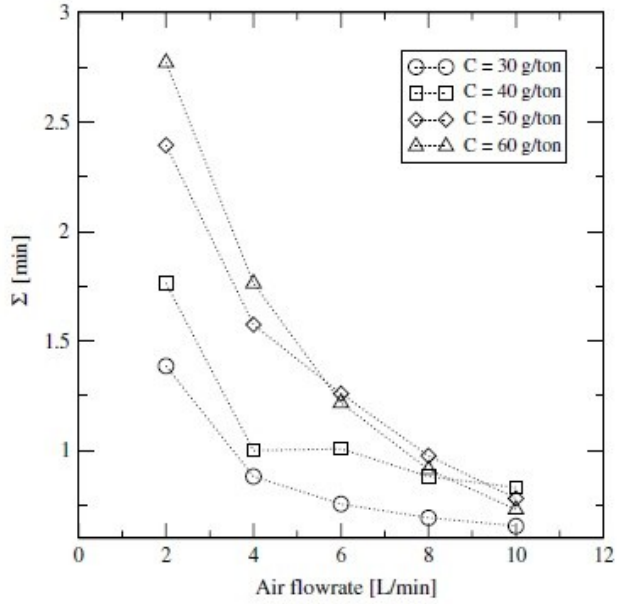

Figure 3.5 - Foaminess as a function of air flow rate at different frother concentrations (Barbian et al., 2003)

Barbian et al. proceeded to correlate the fraction of the height at time t to the equilibrium height with the fraction of the air overflowing as unburst bubbles (α), measured using an imaging technique (Sweet et al., 2000). It was then proposed that is possible to predict the fraction of bubbles that will remain in the overflow using what is defined as a froth stability factor β according to the following equation (Barbain et a., 2003):

$$\beta = 1 - \frac{H}{H_{max}} \tag{3.13}$$

Equation 3.13 was used to predict the fraction of bubbles that will remain in the overflow and proved to be very accurate. This meant that β can be used as an indicator for froth stability in a cell. A vertical column inserted into a flotation cell below the froth-pulp interface was used to collect data in industrial settings. The height is recorded as a function of time (froth velocity) and H_{max} obtained to determine the froth stability factor. It was found that high froth stabilities, which can be detected by β and ∑, occur at lower air flow rates and lead to enhanced flotation performance (Barbian et al., 2004).

3.1.2. Static foam tests

Iglesias et al. (1995) described a modified Bikerman method in which the air flow into a calibrated tube or cylinder is shut off and the foam layer allowed to collapse. The basic concept used was similar to Bikerman's method whereby air is injected into a frother solution in the graduated column. The air flow rate remains constant, and the foam layer allowed to reach Bikerman's equilibrium value after which the flow was shut off and the onset of a drainage stage witnessed. The frothers used were a variety of ethoxylated nonyl phenol solutions (NP+13.5 EO). The foam column height was found to change with time in a logarithmic decay fashion (Figure 3.6).

The decay trends in Figure 3.6 were fitted to a semi-logarithmic scale according to the following equation:

$$H = -a \log t + b \tag{3.14}$$

From which the rate of height change can be calculated:

$$\frac{\partial H}{\partial t} = -\frac{k}{t} \tag{3.15}$$

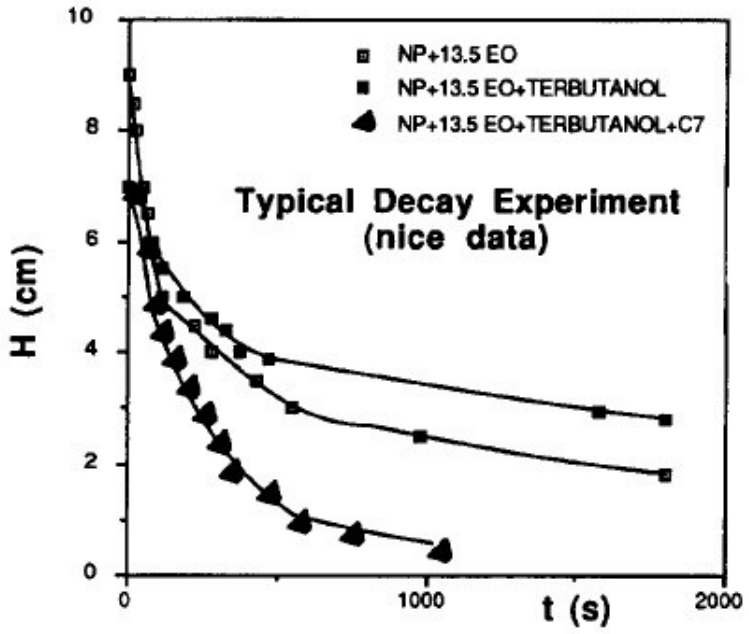

Figure 3.6 - Decay of foam column height with time for different frother solutions (Iglesias et al., 1995)

A new half-time $t_{1/2}$ parameter was defined as the time at which the foam height reaches its half value $H_{1/2}$. By taking the ratio H/H_o where H_0 is the height initially achieved by Bikerman's equilibrium method and re-plotting the data in a dimensionless form a general equation is developed:

$$H/H_o = -\alpha \log(t/t_{1/2}) \tag{3.16}$$

In this dimensionless Equation, the value of α is 0.3-0.4 which is a characteristic parameter that differentiates frother from each other at a given concentration. Another note is that while all frother solutions started at more or less the same equilibrium height, their decay half-time $t_{1/2}$ show a clear difference which is believed to be related to foam stability and drainage. Both $t_{1/2}$ and H_0 allow the extraction of information regarding the foamability of a particular frother solution, and the effect of different reagents.

3.2. Bubble size characterization techniques

Randall et al. (1990), Tucker et al. (1994), and Sweet et al. (1997) studied bubble coalescence and attempted to quantify the effect of frother concentration on bubble size. They used a Leeds flotation cell and a novel method for bubble size measurement known as the UCT Bubble Size Analyzer (BSA) which consisted of a sampler positioned in the cell to collect bubbles. The bubbles pass through a capillary that has a pair of optical detectors 5 mm apart to measure bubble velocity. The bubbles are also collected in a gas burette to measure total gas volume such that it is possible to back-calculate the volume of a single bubble and subsequently calculate bubble diameter, assuming spherical bubbles (Randall et al., 1989).

Sweet et al. (1997) observed that surface tension (γ) does not appear to vary significantly in the concentration ranges tested, despite the fact that bubble size (d_b) and retention time (rt) were very much sensitive to changes (Figure 3.7). Cho and Laskowski (2002) showed that bubble size does not change considerably when increasing frother concentration using a single capillary setup. The moment an additional hole/capillary is introduced and bubble collisions begin to take place, the effect of frother addition on decreasing bubble size is evident below a specific concentration. It is believed that bubbles' coalescence and the ability of frother to retard and even prevent these occurrences is responsible for the bubble size decrease in commercial cells, and that surface tension alone does not affect bubble size to a large degree at these lower concentrations as previously thought. Therefore a frother is generally acting to preserve bubble size through coalescence prevention, which was shown to occur mostly at creation sites (Harris, 1982; Espinosa-Gomez et al., 1988; Hofmeier et al., 1995, Comley et al., 2002; Cho and Laskowski, 2002; Finch et al., 2008).

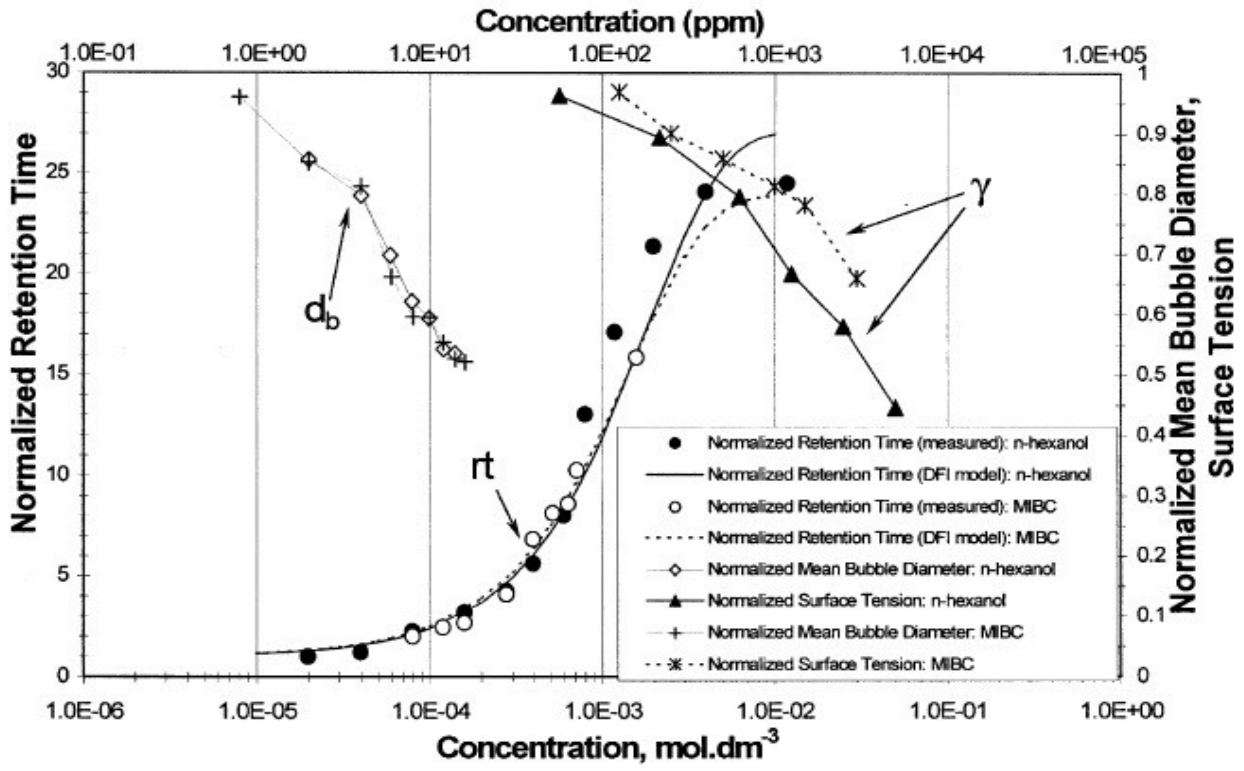

Figure 3.7 - Normalized retention time, sauter mean diameter and surface tension of n-hexanol and MIBC in a modified Leeds cell (Sweet et al., 1997)

It was observed that the addition of frother decreases D_{32}, and that above a certain concentration the D_{32} is constant. This indicates that at concentrations above this point all coalescence is inhibited. Cho and Laskowski (2002) termed this frother concentration the critical coalescence concentration (CCC). The CCC varies between frothers and can therefore be used to compare their strengths (Figure 3.8). Stronger frothers reach their CCC at a lower concentration. Cho and Laskowski also showed that the type of flotation cell does not affect the unique CCC value for each frother by quoting the values from Randall et al. (1990), Tucker et al. (1994) and their own open-top and three-hole sparger cells for MIBC bubble size with increasing MIBC frother concentration. It was shown that the CCC point for MIBC in all tests appeared around 10 ppm despite different flotation cells and operating conditions. They also correlated DFI to CCC and showed that it is possible to predict the value of CCC from literature values for DFI. It was shown that strong frothers have a high DFI and a low CCC while weaker and more selective frothers have a high CCC and a low DFI.

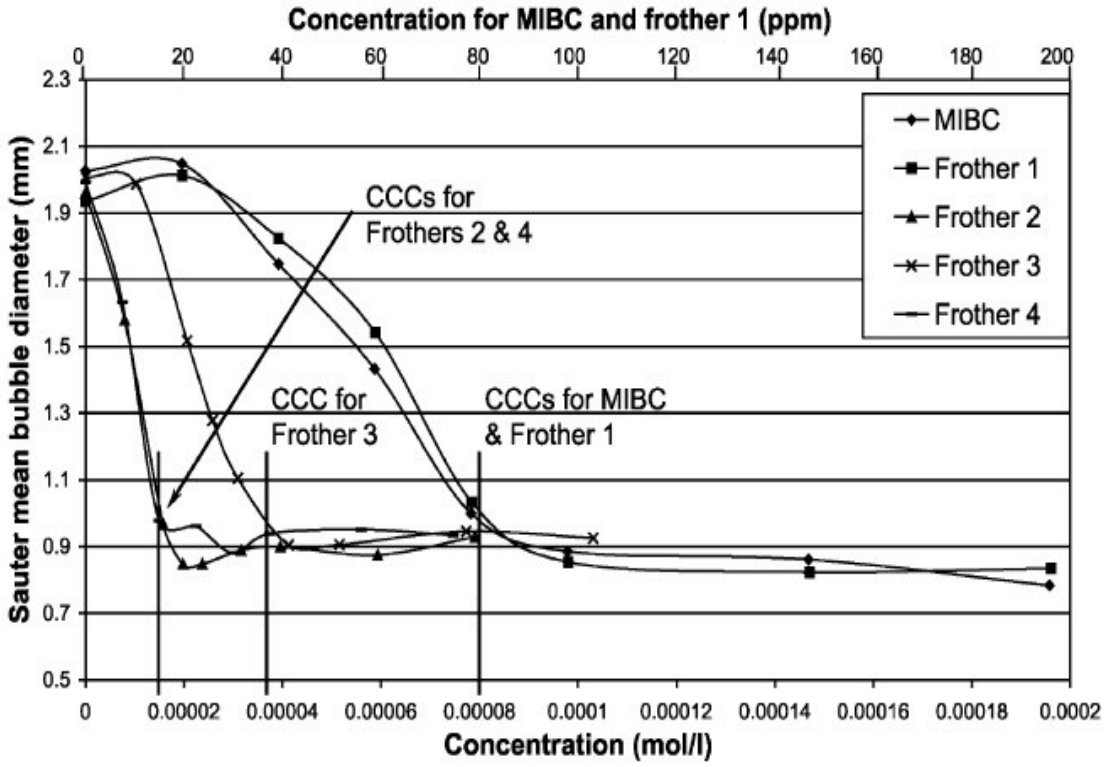

Figure 3.8 - D_{32} as a function of frother concentration in Leeds flotation cell (CCC curves) (Cho and Laskowski, 2002)

Nesset et al. (2007) tested the CCC concept on a number of commercial frothers in a 0.8 m^3 Metso mechanical cell and using a McGill bubble size analyzer (MBSA) (Hernandez-Aguilar et al., 2004) which is an upgraded version of Grau and Heiskanen's (2002) HUT visual bubble size analyser. The MBSA makes use of a sampling tube and a tilted viewing chamber on which a backlight and a high resolution camera are mounted to collect bubble images which are analysed off-line using image analysis software. They showed that the dependence of bubble size on frother concentration fit into an exponential decay trend, originally proposed by Comley et al. (2002), to interpret Sweet et al. (1997) bubble size data in Figure 2.1:

$$D_{32} = D_{limiting} + A \cdot exp(-b \cdot C) \tag{3.17}$$

where C is the frother concentration, $D_{limiting}$ the smallest bubble size, A is the range (D_{32} at zero frother concentration to $D_{limiting}$) and b the decay constant.

Due to the difficulty in establishing the actual value of CCC which is the endpoint of an exponential decay function, they introduced the CCCx concept as a measure of CCC by using the

3-parameter model in equation 3.17 to identify when x % of the range A is reached. Nesset et al. (2007) showed the point where 95% of the range is reached, or CCC95, closely approximates Laskowski's CCC values (Figure 3.8). Laskowski et al. (2003), Nesset et al. (2012) and Zhang et al. (2012) also investigated correlations between the chemical structures of the frothers and their CCC. Laskowski et al. showed that the correlation between the molecular weight of a frother and its CCC depends on the frother class, but that in general as it increased, CCC decreased. They also showed that as the number of propylene oxide groups in polyglycol frothers or the number of carbons in alcohols increased, the CCC decreased and the DFI increased. Laskowski (2004) also established a general diagram depicting the strength and selectivity of frothers based on their HLB and MW (molecular weight). Nesset et al. (2012) showed that the ratio of HLB to Mw can also be used to predict CCC95 however the correlation was scattered for polyglycols at higher ratios. Zhang et al. (2012) correlated only HLB to CCC95 based on the different frother classes. It was shown that as HLB increased, the CCC95 increased as well for all frother classes but under different correlations. The correlations were modelled relative to variables such as the number of carbons and propylene oxide groups.

3.3. Gas holdup characterization technique

Azgomi et al. (2007) proposed using gas holdup as a surrogate for bubble size and as a frother characterization technique, the advantage being that gas holdup is a very simple parameter to measure. Bubble size is known to affect gas holdup through the effect on bubble velocity i.e smaller bubbles rise slower and therefore increase gas holdup. An important observation was that at similar gas holdup, different frothers had different bubble size which implies a chemistry effect on bubble velocity. Nine different frothers were tested in a flotation column and established a correlation between gas holdup and frother type (Figure 3.9).

It was observed that for alcohols, gas holdup increases with increasing hydrocarbon chain length and for polyglycols the gas holdup increased with increasing propylene oxide groups. In effect, the results obtained are similar to other more complex characterization techniques. Nevertheless, gas holdup is very sensitive to a number of factors (gas rate, liquid properties, cell dimensions, temperature and pressure, and sparging method) and therefore can present a challenge for accurate characterization of frothers.

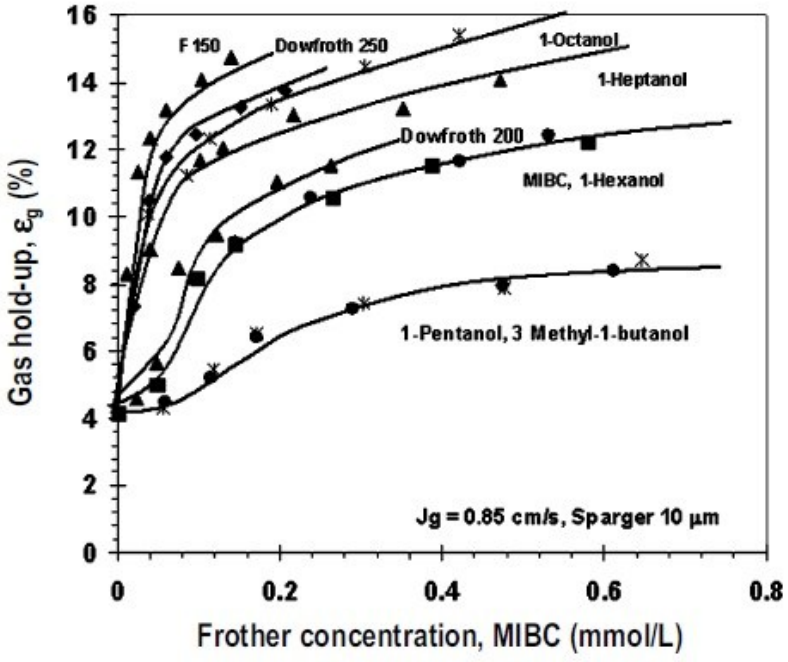

Figure 3.9 - Gas holdup as a function of frother concentration (Azgomi et al., 2007)

Moyo (2005) correlated gas holdup to water carrying rate of bubbles J_{wo}, which is the amount of water carried by the bubbles into the overflow both as a layer on the bubble surface and as a trailing wake. It was found that frothers can be grouped into four classes based on their water carrying capacity, as shown in Figure 3.10.

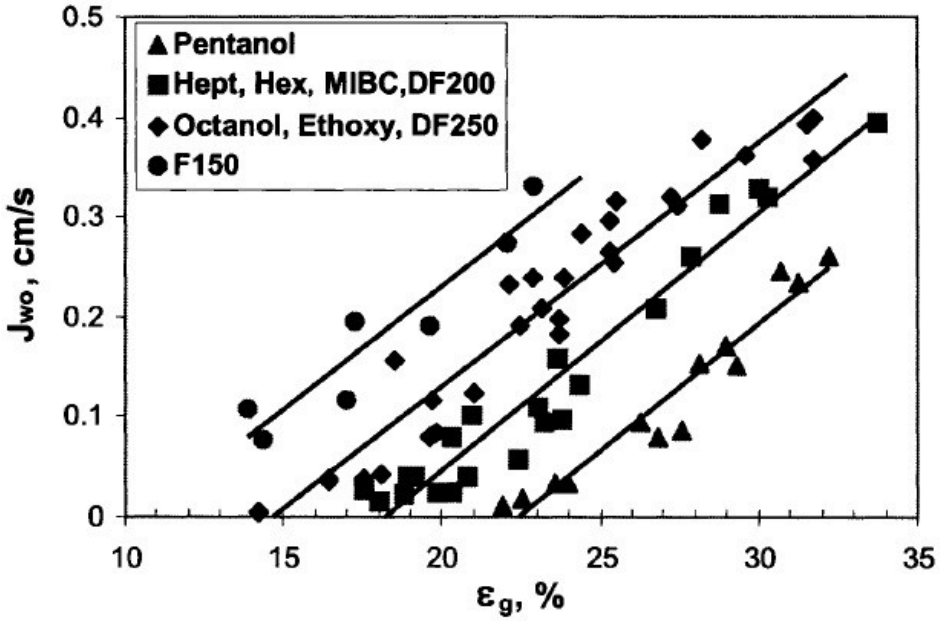

Figure 3.10 - Water carrying rate as a function of gas goldup (Moyo, 2005)

3.4. Conclusion: towards a dilution characterization technique

Many of these techniques are used today in conjunction with each other to complement their findings. The optimal method of comparing frothers remains subjective but many studies are continuously being done especially as new classes of frothers are being developed. It is the author's opinion that the best option to compare frothers at the current time would be using a combination of DFI, Mw, HLB and CCC. Mw and HLB can be obtained from literature or through calculation from given formulas whereas DFI and CCC can be done experimentally. The main limitation of the CCC is its inability to tackle and characterise systems of natural surfactants or salts found in industrial waters. In this research, a novel approach to determine a 'system' CCC by employing a dilution technique (CCC-D) is proposed. This requires that the dilution technique be consistent with the addition technique. Once established, the CCC-D curves for the natural surfactants can be developed and their concentration expressed as an equivalent frother concentration. This provides a measure of the natural surfactants' bubble size reduction capability by reference to a known frother and a way to compare process waters from different locations.

3.5. References

Azgomi, F., Gomez, C. O., Finch, J. A., 2007. Characterizing Frothers Using Gas Hold-Up. Canadian Metallurgical Quarterly, Vol. 46, pp. 237-242

Barbian N., Ventura-Medina E., Cilliers, J.J., 2003. Dynamic Froth Stability in Froth Flotation. Minerals Engineering, Vol. 16, pp. 1111-1116

Bikerman, J.J., 1938. The unit of foaminess. Trans. Faraday Society 34, pp. 634-638.

Cho, Y.S., Laskowski, J.S., 2002. Effect of flotation frothers on bubble size and foam stability. International Journal of Mineral Processing, Vol. 64, pp. 69– 80

Comley, B.A., Harris, P.J., Bradshaw, D.J., Harris, M.C., 2002. Frother Characterization using Dynamic Surface Tension Measurements. International Journal of Mineral Processing, Vol. 64, pp. 81-100

Espinosa-Gomez, R., Finch, J.A., Bernert, W., 1988. Coalescence and froth collapse in the presence of fatty acids. Colloids and Surfaces, Vol. 32, pp. 197-209

Finch, J.A., Nesset, J.E., Acuna, C., 2008. Role of frother on bubble production and behaviour in flotation, Part 3: Frother and bubble size reduction. Minerals Engineering, Vol. 21, pp. 949-957

Grau, R.A., Heiskanen, K., 2002. Visual technique for measuring bubble size in flotation machines. Minerals Engineering, Vol. 15, pp. 507–513

Hofmeier, U., Yaminsky, V.V., Christenson, H.K., 1995. Observations of solute effects on bubble formation. Journal of Colloid and Interface Science, Vol. 174. 199-210

Iglesias, E., Anderez, J., Forgiarini, A., Salager, J-L., 1995. A New Method to Estimate the Stability of Short-Life Foams. Collide and Surface 98A, pp. 167-174

Laskowski, J.S., Tlhone, T., Williams, P., Ding, K., 2003. Fundamental Properties of the Polyoxypropylene Alkyl Ether Flotation Frothers. International Journal of Mineral Processing, Vol. 72, pp. 289-299

Laskowski, J. S., 2004. Testing Flotation Frothers. In: Physiochemical Problems of Mineral Processing, Vol. 38, pp.13-22

Lunkenheimer, K., Wantke, K.D., 1981. Determination of the surface tension of surfactant solutions applying the method of Lecomte du Nouy (ring tensiometer). Colloid Polymer Science, Vol. 259, pp. 354-366

Malysa, K., Czubak-Pawlikowska, J., Pomianowski, A., 1978. Frothing properties of solutions and their influence on floatability. In: Proceedings of 7th International Congress of Surface Active Substances, Moscow, 3, pp. 513-520

Malysa, K., Lunkenheimer, K., Miller, R., Hartenstein, C., 1981. Surface elasticity and frothability of n-octanol and n-octanoic acid solutions. Colloids and Surfaces, Vol. 3, pp. 329-338

Malysa, K., Lunkenheimer, K., Miller, R., Hempt, C., 1985. Surface elasticity and dynamic stability of wet foams. Colloids & Surfaces, Vol. 16, pp.9-20

Malysa, E., Malysa, K., Czarnecki, J., 1987. A method of comparison of the frothing and collecting properties of frothers. Colloids and Surfaces 23 (1-2), pp. 29-39

Moyo, P., 2005. Characterization of Frothers by Water Carrying Rate. M.Eng. Thesis, McGill University, pp.36-44

Nesset, J.E., Finch, J.A., Gomez, C.O., 2007. Operating variables affecting the bubble size in forced-air mechanical flotation machines. In: Proceedings AusIMM 9th Mill Operators' Conference, Fremantle, Australia, pp. 66–75

Nesset, J.E., Zhang, W., Finch, J.A., 2012. A benchmarking tool for assessing flotation cell performance. In Proceedings of 44th Annual Meeting of the Canadian Mineral Processors (CIM), Ottawa, Canada, 17–19 January 2012, pp. 183–209

Randall, E.W., Goodall, C.M., Fairlamb, P.M., Dold, P.L., O'Connor, C.T., 1989. A method for measuring the sizes of bubbles in two- and three-phase systems. Journal of Physics, Section E, Scientific Instrumentation, Vol. 22, pp. 827–833

Randall, E.W., O'Connor, C.T., Goodall, C.M., Franzidis, J.P., 1990. Measurement of bubble sizes in air agitated systems. In: Proceedings of the 14th Congress of CMMI, Edinburgh, Scotland, pp.93-103

Sun, S-C., 1952. Frothing characteristics of Pine oils in flotation. Transactions of American Institute of Mining Engineers 256, pp. 65-71

Sweet, C., Van Hoogstraten, J., Harris, M., Laskowski, J.S., 1997. The Effect of Frothers on Bubble Size and Frothability of Aqueous Solutions, Proceedings of the second UBC-McGill Bi-annual international symposium of fundamentals of mineral processing, Edited by Finch, J.A., Rao S.R. and Holubec, L, Sudbury, Ontario, August 17-19, pp. 235-245

Sweet, C.G., Bradshaw, D.J., Cilliers, J.J.L, Wright, B.A., De Jager, G., Francis, J.J., 2000. The extraction of valuable minerals from mined ore. Smartfroth, Adams & Adams Patent Attorneys Pretoria A&A, REF: v13676, pp. 1-11

Tucker, J.P., Deglon, D.A., Franzidis, J.P., Harris, M.C., O'Connor, C.T., 1994. An evaluation of a direct method of bubble size distribution measurement in a laboratory batch flotation cell. Minerals Engineering, Vol. 7, 667–680

Zhang, W., Nesset, J., Rao, R., Finch, J.A, 2012. Characterizing Frothers through Critical Coalescence Concentration (CCC)95-Hydrophile-Lipophile Balance (HLB) Relationship. Open Access Minerals, Vol. 2, pp. 208-227

CHAPTER 4: APPARATUS AND EXPERIMENTAL METHODOLOGY

In order to establish the new dilution method to characterize industrial process waters and to investigate the oil sands samples, a lab-scale flotation column was used. The column was originally at McGill University equipped with the required instrumentation to monitor gas holdup and to measure bubble size distribution. The setup was used at McGill for the first part of the research (results in chapter 5) and then dismantled and shipped to Edmonton for the second part of the research (results in Chapter 6). This chapter describes the overall setup and the instruments used during experimentation.

Part 1 of the research involved establishing a 'system' CCC by employing a dilution method (CCC-D) and was completed at McGill University. This required that the dilution technique be proven to yield consistent results to the addition technique which was tested using the commercial frother DF-250. Once established, the CCC-D curves for the natural surfactants were developed and their concentration expressed as an equivalent DF-250 concentration. Gas holdup was also shown to be a fast substitute for bubble size opening the possibility of on-line applications (Chapter 5).

Having explored the dilution technique, ***Part 2*** of the research involved testing a number of samples from Shell Albian Sands but closer to source. In this case, the set-up was erected in a research facility in Edmonton (Coanda R&D) (Chapter 6).

4.1. Part 1: McGill Set-up

The setup used was an air/liquid system in a 7.6 cm diameter, 3 m high column (Figure 4.1). Pressurized air was supplied from McGill regulated to approximately 50 psi, flowing into a porous cylindrical steel sparger mounted vertically at the bottom of the column (5μm nominal porosity). The sparger dispersed the air into bubbles at a set gas (superficial) velocity (J_g) maintained throughout the experiments at approximately 0.7 cm/s at the sparger (taking into account hydrostatic head and temperature effects). The setup was operated in closed loop with

the overflow returning to the mixing tank and then pumped to the bottom of the column co-currently to the air flow. The feed was introduced into the column using a peristaltic pump (Cole Palmer Model 7520-25) and maintained at a flow rate of 3.4 L/min such that no significant froth layer is formed, and was maintained during all experiments. A froth layer is not desirable as it removes some of the surfactants from the water and can interfere with the upper pressure tapping point. Gas holdup was calculated from differential pressure ΔP (Bailey model PTSDDD1221B2100) tapped between 170 cm and 260 cm from the base as follows:

$$E_g = 100 * \frac{\Delta P}{L} \tag{4.1}$$

where ΔP is in cm of water and L is the distance between the tapping points, also in cm. In addition to the differential pressure sensor, absolute pressure P_{abs} (No-Shok pressure sensor) at the base of the column, temperature T (Thermopar K) and air flow (MKS. model 1162B-30000SV) instruments were connected to an interface and signal conditioner (opto 22), which in turn relayed and recorded the data on an Intellution iFix platform installed on a PC.

To characterize bubble size reduction as a function of frothers the CCC curves were plotted (Sauter mean bubble diameter D_{32} against frother concentration), where D_{32} is given by equation 2.2.

The D_{32} represents the mean size of bubble having the same total bubble volume to surface area ratio as the bubble size distribution. There are a number of ways to measure bubble size distribution in flotation systems (Tucker et al., 1994; Grau and Hesinaken, 2002; Rodrigues and Rubio, 2003). The instrument of choice was the MBSA (Figure 4.1). It is a widely accepted technology (Harbort and Schwarz, 2010) used in both laboratory and on-site studies, and compares favorably to other techniques (Hernandez-Aguilar et al., 2004). It consists of a 6 L, PVC viewing chamber with opposing sloped (15^o) windows made of reinforced glass connected to a sampling tube which is inserted into the column to collect bubbles. Facing the upper window is a high resolution camera (Canon 50D with macro lens) with backlighting to create bubble shadow images.

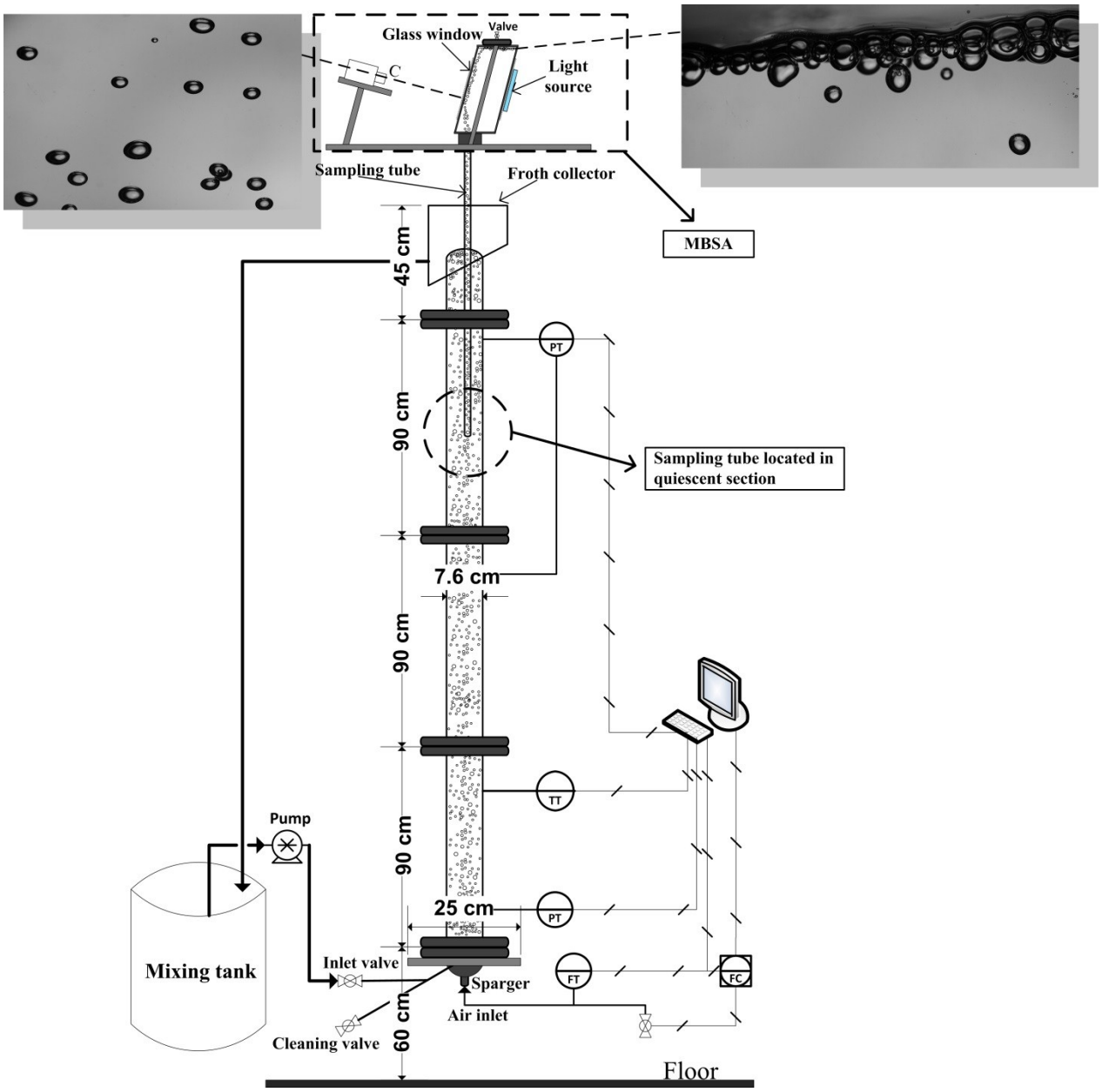

Figure 4.1 - Column set-up with McGill Bubble Size Analyzer, MBSA (drawn using Microsoft Visio™)

The procedure for bubble size determination starts by immersing the sampling tube closed with a rubber stopper, which is connected to a cable, to a depth midway between the gas holdup pressure tapping points. The sampling tube is attached to the viewing chamber and the MBSA assembly is filled with the solution being tested. With the viewing chamber nearly full, a ruler inside is used to focus the camera and a picture is taken to calculate the number of pixels/cm. The chamber lid is then put in place and the valve closed. Upon reaching steady state, judged by steady gas holdup signals, the stopper is removed by pulling the cable and bubbles rise through

the sampling tube into the viewing chamber. Since the liquid level in the chamber decreases with time this imposes a limit on the number of images collected.

Using manual settings (focus, shutter speed, aperture and ISO) and a remote controller, the camera is set to capture at least 100 successive images which are subsequently analysed off-line using Empix Northern Eclipse v8.0 coupled with in-house image analysis software. Sufficient images are collected per run to give at least 3,000 bubbles which are analyzed to calculate D_{32}.

The column was operated continuously; addition of frother (addition method) or dilution water was done with the system running with air flow turned off intermittently to allow adequate mixing as judged by steady gas holdup readings.

4.2. Part 2: Edmonton Set-up

The experimental set-up for Part 2 was assembled at Coanda's research facility in Edmonton using a specifically designed scaffolding structure since there was no mezzanine structure as in McGill to reach the top of the column (Figures 4.2, 4.3). The set-up and operating variables were kept identical to that in Part 1 with the exception of a new porous stainless steel sparger at the bottom of the column with 10μm nominal porosity. The set-up was operated in closed loop with the overflow returning to the mixing tank and pumped back to the bottom of the column co-current to the air flow. Gas holdup was calculated from differential pressure (ΔP) measured as in Part 1. Absolute pressure P_{abs} (No-Shok pressure sensor) at the base of the column was also connected to an interface. A new portable signal conditioner was built (electronic components included I/O modules, Dutec board, voltage specific transformer, etc.) and used to relay the readings to an Intellution iFix platform installed and configured on a laptop. Air flow was controlled using a calibrated flow meter. A higher resolution camera (Canon 60D with macro lens) was used with LED backlighting to create bubble shadow images.

Operating at the top of the scaffolding required wearing a harness. A pulley was also installed to transport the water to the top in order to fill the MBSA chamber. Pressure was supplied from a compressor (Dewalt model D55168, 200 psi, 15 gallon) and regulated to 40 psi. Waste water was dumped in a 1000 L container and properly disposed of with the help of Syncrude Canada Ltd.

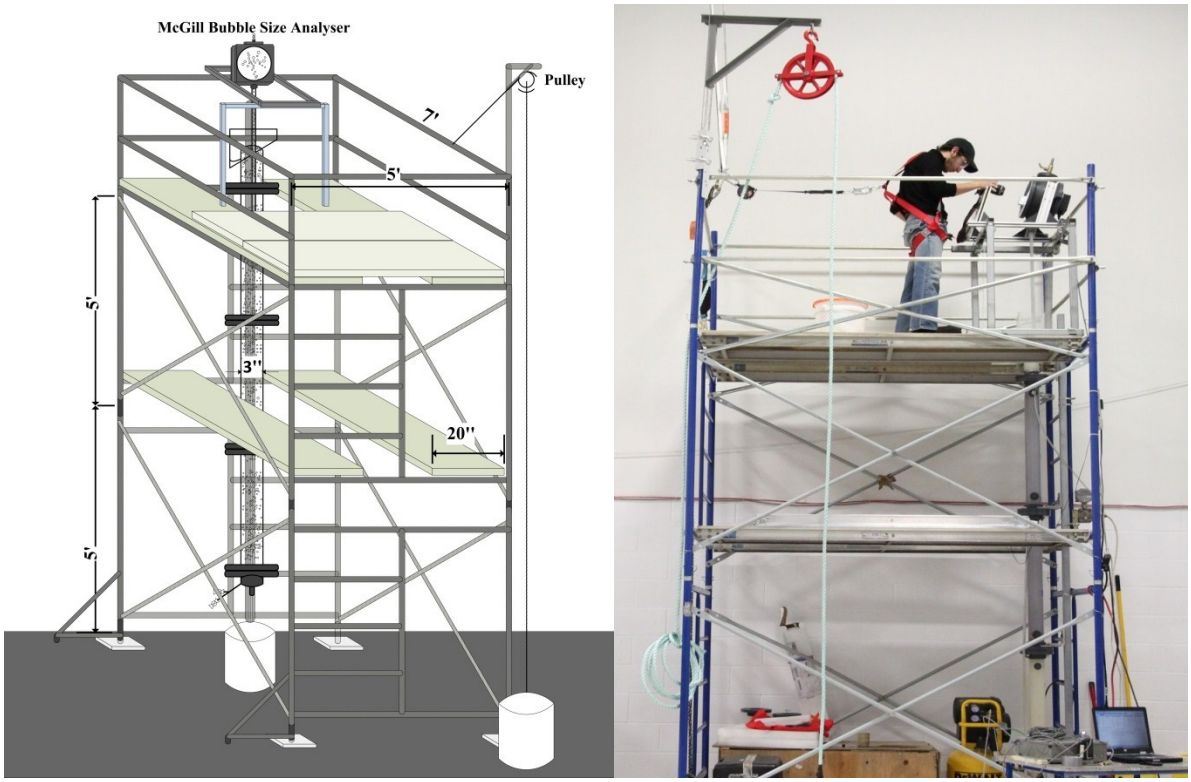

Figure 4.2 - Scaffolding design and Edmonton set-up

The process water samples were received from the MRM extraction facility at Shell Albian Sands in sealed 20 L pails and were collected from the thickener overflow (OF), in addition to a sample from the recycle water stream (RCW). After visiting Albian Sands and discussing with the engineers on-site, the thickener OF sampling point was chosen considering its proximity to the extraction process whilst having minimal bitumen content (which would have intruded on the column operation), and due to the relative ease in collecting many samples. The thickener OF samples were turbid and at times containing minor amounts of bitumen whereas the RCW sample was clear. The process waters were allowed to settle for at least a week prior to opening the seal such that a layer of clay and silt formed at the bottom of the pail and any bitumen aggregated at the top. This allowed the pumping of the process water with precision from the middling section of the pail such that a relatively clear water sample was obtained.

4.3. References

Harbort, G. J., Schwarz, S., 2010. Characterization Measurements in Industrial Flotation Cells, in Flotation Plant Optimization (Ed. C. Greet), AusIMM No. 16, pp. 95-106

Hernandez-Aguilar, J.R., Coleman, R.G., Gomez, C.O., Finch, J.A., 2004. A comparison between capillary and imaging techniques for sizing bubbles in flotation systems. Minerals Engineering Vol. 17, pp. 53–61

Grau, R.A., Heiskanen, K., 2002. Visual technique for measuring bubble size in flotation machines. Minerals Engineering, Vol. 15, pp. 507–513

Rodrigues, R.T., Rubio, J., 2003. New basis for measuring the size distribution of bubbles. Minerals Engineering, Vol. 16, pp. 757–765

Tucker, J.P., Deglon, D.A., Franzidis, J.P., Harris, M.C., O'Connor, C.T., 1994. An evaluation of a direct method of bubble size distribution measurement in a laboratory batch flotation cell. Minerals Engineering, Vol. 7, pp. 667–680

CHAPTER 5: DEVELOPING CRITICAL COALESCENCE CONCENTRATION CURVES FOR INDUSTRIAL PROCESS WATERS USING DILUTION

Abstract

Critical coalescence concentration (CCC) is commonly used to characterize frothers. The CCC is determined from a plot of Sauter mean bubble size (D_{32}) vs. frother concentration, referred to here as the 'addition' method. Industrial flotation systems can encounter a number of naturally occurring surfactants and salts that also influence bubble size. In effect there is a 'system' CCC. This paper introduces a dilution method to identify the system CCC. The study verifies the dilution technique using the commercial frother DF-250. It is shown that the system CCC can be expressed as an equivalent DF-250 concentration to provide context and a means of comparing water samples. The viability of using gas holdup to provide an estimate of process water D_{32} is also explored. To illustrate the procedure three samples of process water from the Albian Sands bitumen processing plant were examined. They proved to be similar and yielded a system CCC equivalent to about 20 ppm DF-250. It is concluded that the dilution and frother equivalent techniques can be used to help identify system hydrodynamic properties.

5.1. Introduction

In flotation the rate with which particles are recovered is driven by bubble size: the smaller the bubbles the more collisions with particles and the greater the bubble surface area for transport of the collected particles. In most mineral flotation systems, surfactants known as frothers are added to help produce bubbles of about 1 mm (Nesset et al., 2006). Frothers are hetero-polar compounds that adsorb at the air/water interface (Leja and Schulman, 1954) and are commonly held to act through coalescence prevention (Harris, 1976). The reduced bubble size can increase flotation rate more than 10-fold (Ahmed and Jameson, 1985).

One method to characterize this bubble size reduction function of frothers is to plot the Sauter mean bubble diameter (D_{32}) against frother concentration, where D_{32} is given by:

$$D_{32} = \Sigma_1^n \frac{D_i^3}{D_i^2} \tag{5.1}$$

where a D_i is bubble diameter. The D_{32} represents the mean size of bubble having the same total bubble volume to surface area ratio as the bubble size distribution. Given that flotation is driven by bubble surface area, the D_{32} is the mean size commonly used in flotation studies. Over the past 20 years methods to determine bubble size distribution in order to calculate D_{32} have been developed, for example the McGill Bubble Size Analyzer (MBSA) (Gomez and Finch, 2007).

The D_{32}-*Concentration* plot shows an initial rapid decrease in D_{32} as frother concentration is increased but levels off to become approximately constant above a certain concentration, referred to as the critical coalescence concentration (CCC) (Cho and Laskowski, 2002). The curves (for discussion purposes referred to as CCC curves) usually fit a first order exponential decay model:

$$D_{32} = D_{limiting} + A \cdot exp(-B \cdot ppm) \tag{5.2}$$

where A is the range (D_{32} at zero frother concentration to D_{32} at CCC), B the decay constant and $D_{limiting}$ the smallest bubble size, i.e., size at CCC (Finch et al., 2008). As a measure of CCC we use the CCC-95 determined from the fit to Eq (2) when 95 % of the range A is reached.

A parameter related to bubble size, gas holdup (E_g), is also used to characterize frothers (Azgomi et al., 2007). Gas holdup is the volume of air in a vessel relative to the volume of the air-water (or air-slurry) mix. Gas holdup is related to bubble size, increasing as bubble size reduces because small bubbles rise more slowly than large bubbles, at least for bubbles less than ca. 2-3 mm (Clift et al., 1978). This means gas holdup may substitute for bubble size, the advantage being that gas holdup, at least in two-phase air-water systems, is easier to measure than D_{32}. For discussion purposes bubble size and gas holdup are referred to as 'hydrodynamic' characteristics. These characterization techniques have helped improve frother selection and circuit distribution strategies (Cappuccitti and Nesset, 2009).

In some flotation systems, frothers are not added, the natural surfactant or high salt content deriving from the ore or water supply producing a bubble size comparable to that with frother. An example of high salt content substituting for frother is Xstrata's Raglan concentrator (Quinn et al., 2007); from measurement of gas holdup an example of natural surfactants having frother

functions appears to be in oil sands processing (Zhou et al., 2000). Direct measurement of bubble size in mechanical cells in the Albian Sands extraction facility shows the presence of small bubbles (<1mm) (Gomez, 2007). The example studied in this paper is the oil sands case.

The natural surfactants deriving from bitumen ore are a complex mix, predominantly believed to be aliphatic carboxylates having hydrocarbon chains of at least five carbons, typically C_{15} to C_{17} (Schramm, 2000). It is not feasible to isolate the individual surfactants responsible for bubble size reduction to determine the CCC by the addition method. We therefore propose to determine a 'system' CCC by employing a dilution method (CCC-D). This requires that the dilution technique be consistent with the addition technique which is tested using the commercial frother DF-250. Once established, the CCC-D curves for the natural surfactants can be developed and their concentration expressed as an equivalent DF-250 concentration. This not only provides a measure of the natural surfactants' bubble size reduction capability by reference to a known frother but also provides a way to compare process waters from different locations and over time. To facilitate the latter, gas holdup might prove a fast substitute for bubble size opening the possibility of on-line applications. The purpose of this paper, therefore, is to establish the dilution method of determining system CCC and expressing as frother DF-250 equivalent using oil sands process waters as a case study.

5.2. Apparatus and Methodology

The setup was an air/liquid system in a 7.6 cm diameter, 3 m high column (Figure 5.1). A porous cylindrical steel sparger mounted vertically at the bottom of the column (5µm nominal porosity) dispersed the air into bubbles at a set gas (superficial) velocity (J_g) maintained throughout the experiments at approximately 0.7 cm/s at the sparger. The setup was operated in closed loop with the overflow going to the mixing tank and returned to the bottom of the column co-currently to the air flow. The feed was introduced into the column using a peristaltic pump (Cole Palmer Model 7520-25) and maintained at a flow rate of 3.4 L/min such that no significant froth layer is formed, and was maintained during all experiments. A froth layer is not desirable as it removes some of the surfactants from the water and can interfere with the upper pressure tapping point.

Gas holdup was calculated from differential pressure ΔP (Bailey model PTSDDD1221B2100) tapped between 170 cm and 260 cm from the base as follows:

$$E_g = 100 * \frac{\Delta P}{L} \quad (5.3)$$

where ΔP is in cm of water and L is the distance between the tapping points, also in cm. In addition to the differential pressure sensor, absolute pressure P_{abs} (No-Shok pressure sensor) at the base of the column, temperature T (Thermopar K) and air flow (MKS. model 1162B-30000SV) instruments were connected to an interface and signal conditioner, which in turn relayed and recorded the data on an Intellution iFix platform installed on a PC.

There are a number of ways to measure bubble size distribution in flotation systems (Tucker et al., 1994; Grau and Heiskanen, 2002; Rodrigues and Rubio, 2003). The instrument of choice was the MBSA (Figure 1). It is a widely accepted technology (Harbort and Schwarz, 2010) used in both laboratory and on-site studies, and compares favorably to other techniques (Hernandez-Aguilar et al., 2004). It consists of a 6 L, PVC viewing chamber with opposing sloped (15^o) windows made of reinforced glass connected to a sampling tube which is inserted into the column to collect bubbles. Facing the upper window is a high resolution camera (Canon 50D with macro lens) with backlighting to create bubble shadow images.

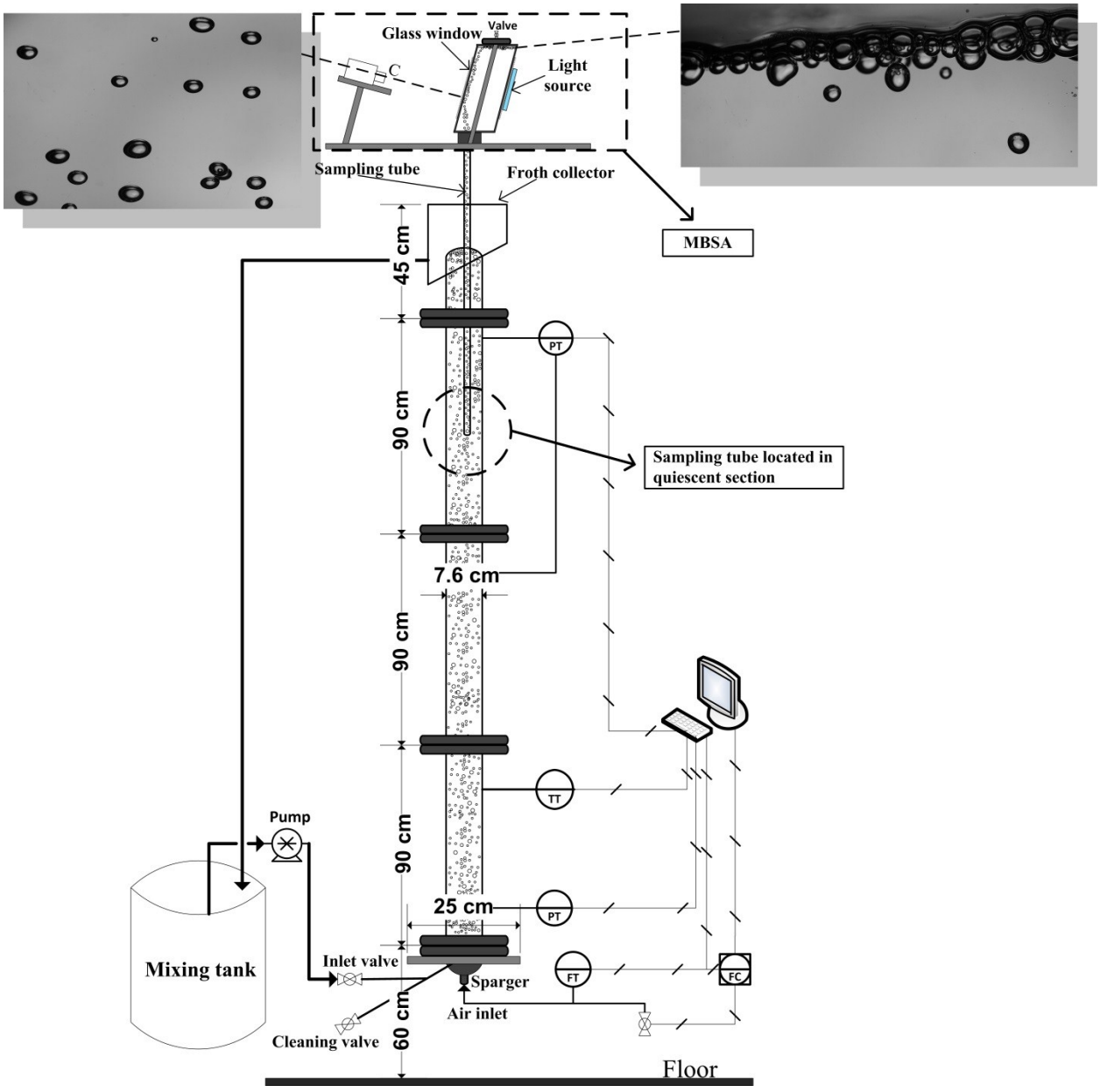

Figure 5.1 - Column set-up with McGill Bubble Size Analyzer, MBSA

The procedure for bubble size determination starts by immersing the sampling tube closed with a rubber stopper, which is connected to a cable, to a depth midway between the gas holdup pressure tapping points. The sampling tube is attached to the viewing chamber and the MBSA assembly is filled with the solution being tested. With the viewing chamber nearly full, a ruler inside is used to focus the camera and a picture is taken to calculate the number of pixels/cm. The chamber lid is then put in place and the valve closed. Upon reaching steady state, judged by steady gas holdup signals, the stopper is removed by pulling the cable and bubbles rise through

the sampling tube into the viewing chamber. Since the liquid level in the chamber decreases with time this imposes a limit on the number of images collected.

Using manual settings (focus, shutter speed, aperture and ISO) and a remote controller, the camera is set to capture at least 100 successive images which are subsequently analysed off-line using Empix Northern Eclipse v8.0 coupled with in-house image analysis software. Sufficient images are collected per run to give at least 3,000 bubbles which are analyzed to calculate D_{32}.

The column was operated continuously; addition of frother (addition method) or dilution water was done with the system running with air flow turned off intermittently to allow adequate mixing as judged by steady gas holdup readings.

The dilution experiments with DF-250 entailed starting with a concentration above the CCC and sequentially diluting back to 1 ppm. Montreal tap water was used (composition can be found online: Montreal 2011)[1]. The temperature ranged between 14 ºC - 18 ºC. The process water samples were supplied from the thickener overflow in Shell Albian Sands' bitumen extraction plant and were likewise diluted with tap water.

[1] http://ville.montreal.qc.ca/pls/portal/docs/PAGE/EAU_FR/MEDIA/DOCUMENTS/MONTREAL%20DRINKING%20WATER%20REPORT%20-%20%202011.PDF

5.3. Results

5.3.1. Addition vs. dilution

The data from the DF-250 addition (CCC) and dilution (CCC-D) tests are compared in Figure 5.2 and show excellent agreement with each other and fit to the decay model.

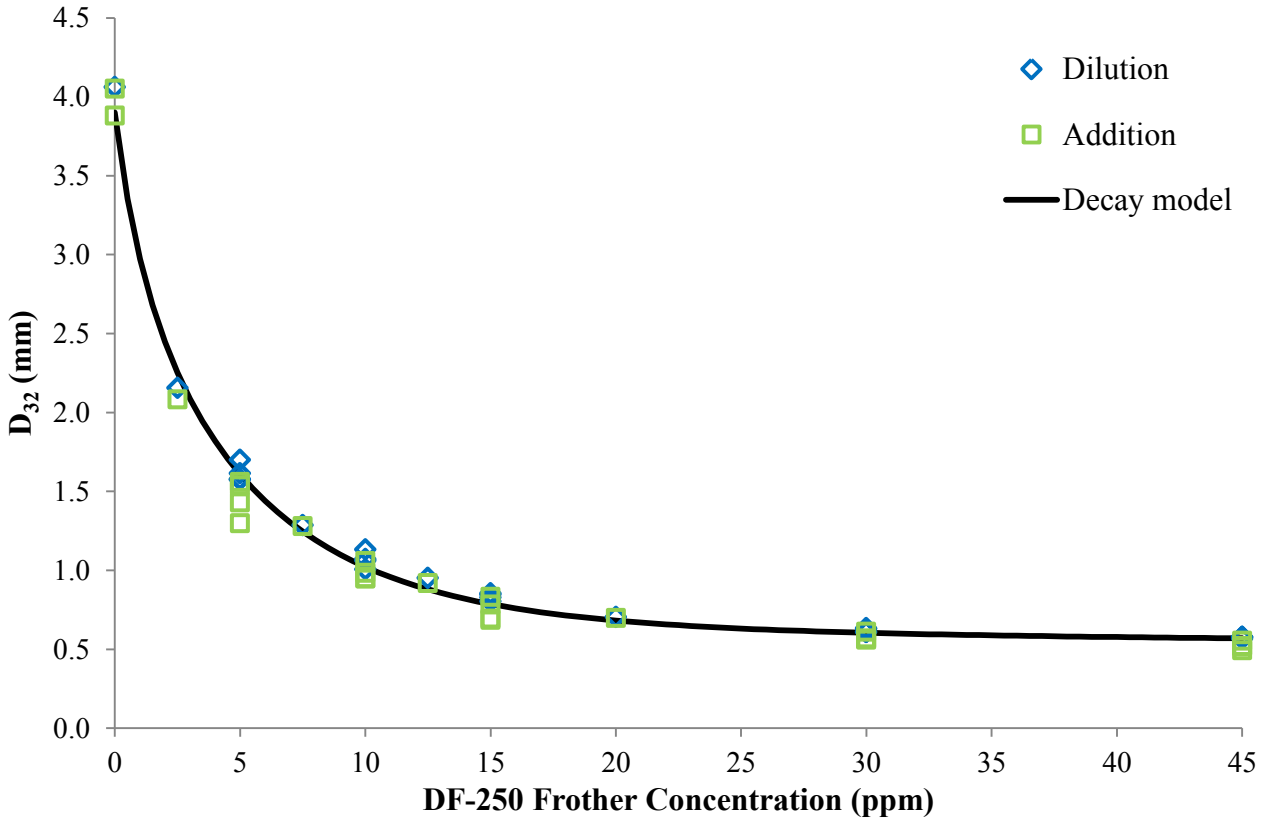

Figure 5.2 - D_{32} as a function of concentration for addition and dilution tests using DF-250

After tracking the main source of experimental error due to water displaced from the MBSA, the mean difference (dilution – addition) was brought to 2.05 ± 4.93 % at a 99 % confidence level; i.e., there is no difference between the two techniques.

5.3.2. *Dilution technique: process water samples*

Having verified the dilution technique and using the same operating parameters (liquid flow rate, gas velocity), the dilution (CCC-D) curves were established for the three process water samples (Figure 5.3). The concentration scale in these tests is the ratio of the remaining volume of original process water to the total volume of the diluted solution.

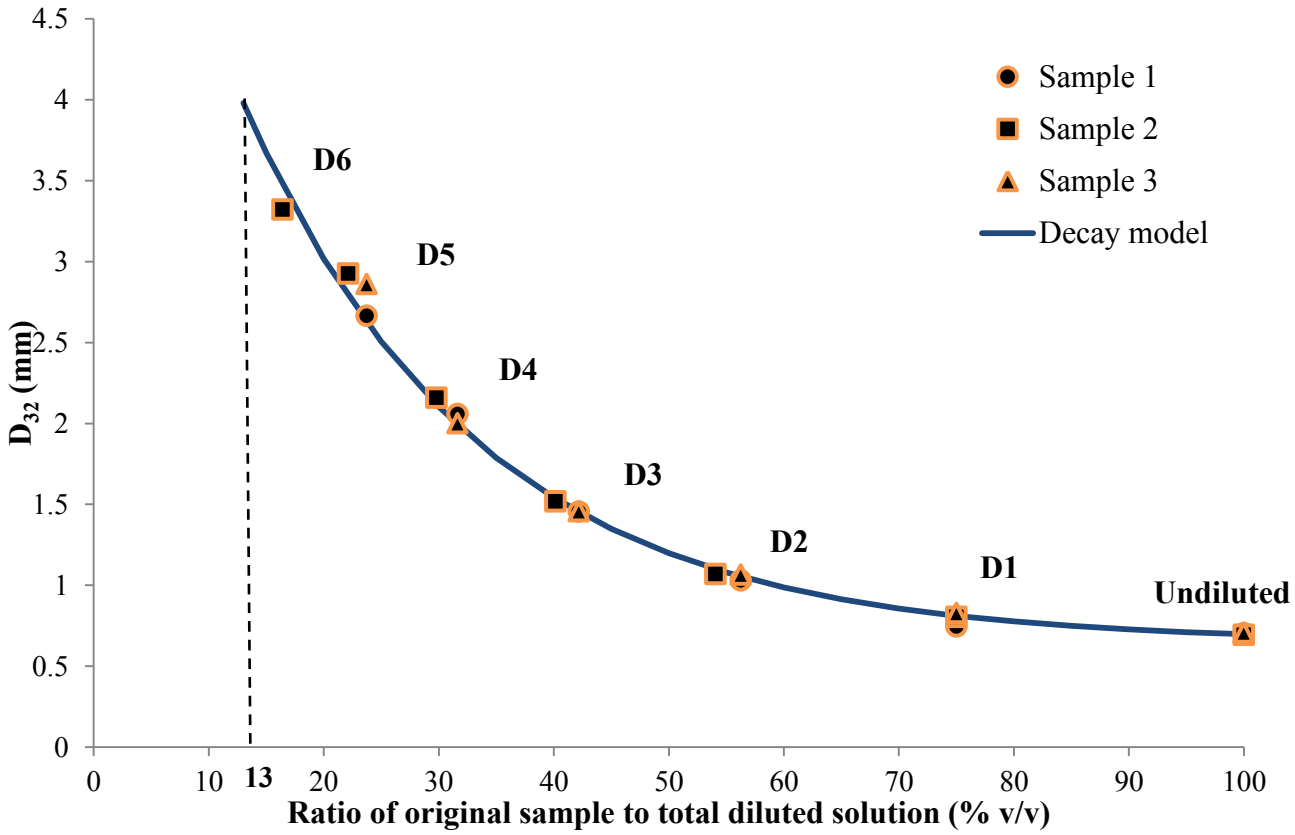

Figure 5.3 - D_{32} as a function of process water concentration by volume (CCC-D curve) for the three Albian Sands process water samples (Note: D1 etc refer to first dilution point etc.)

Figure 5.3 shows that the dilution curve exhibits the same trend found for DF-250. The three process water samples showed a consistent Sauter mean diameter with dilution. The trend suggests the undiluted samples are close to the 'system' CCC and achieve a D_{32} corresponding to Montreal tap water at about 13% of the initial concentration.

5.3.3. *DF-250 equivalent concentration for process water samples*

Combining the DF-250 trend from Figure 5.2 and the process water data from Figure 5.3, Figure 5.4 is developed from which we can determine a DF-250 equivalent concentration corresponding to process water dilution points. This equivalence is illustrated for three examples corresponding to undiluted, D3 and D5 process water dilutions where the DF-250 concentration is read off the upper x-axis at the same D_{32}. Referring to a DF-250 equivalent helps quantify the "frother potential" of the process waters. For the three samples the undiluted process water has a frother potential equivalent to about 20 ppm DF-250.

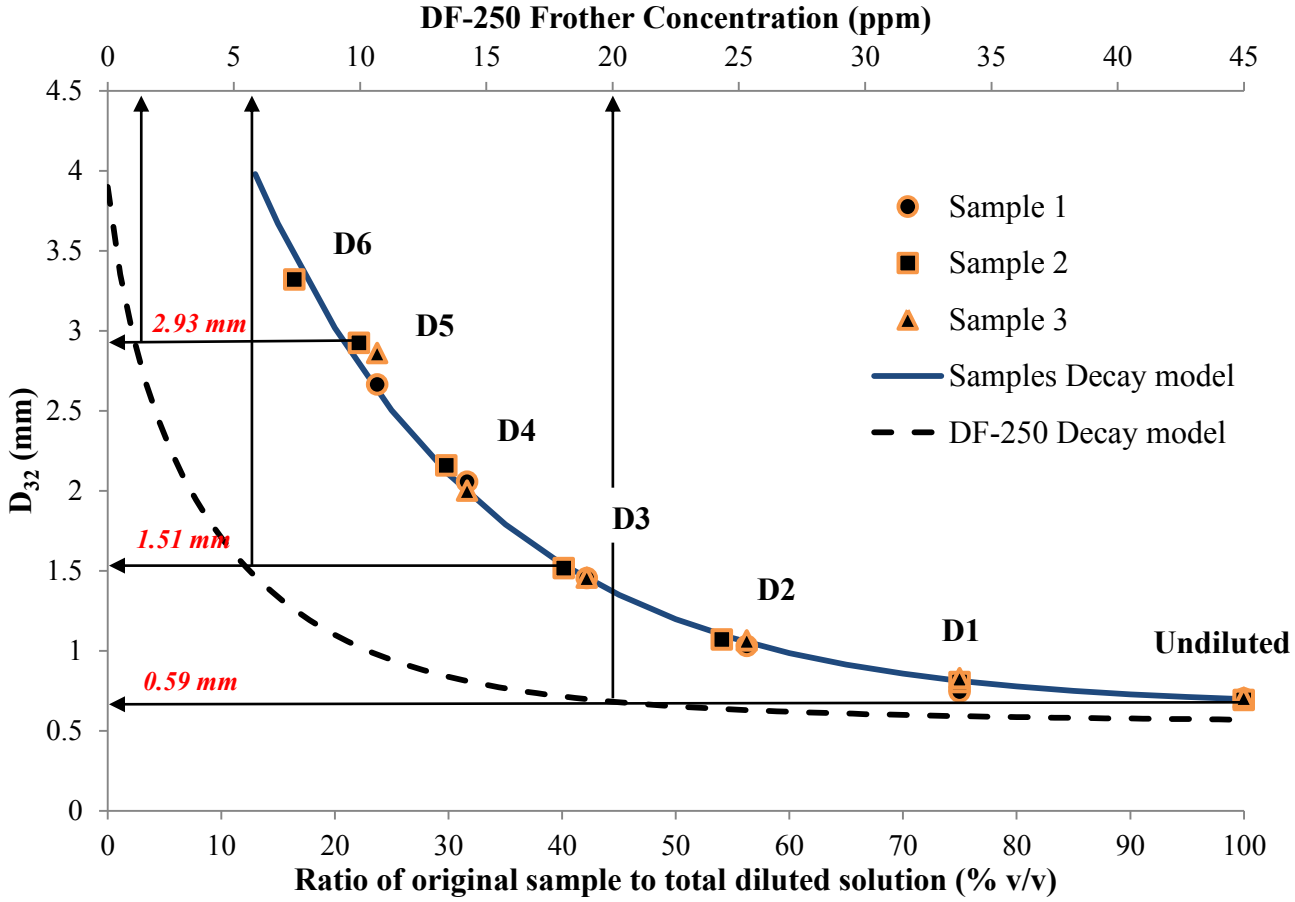

Figure 5.4 - D_{32} as a function of DF-250 concentration (upper x-axis) and process water dilution (lower x-axis)

The images in Figure 5.5 demonstrate the similarity in bubble size between process water and DF-250 for the three examples in Figure 5.4. Due to higher turbidity the process water sample images have a slightly darker background than the water/frother samples.

a) undiluted and 20 ppm DF-250

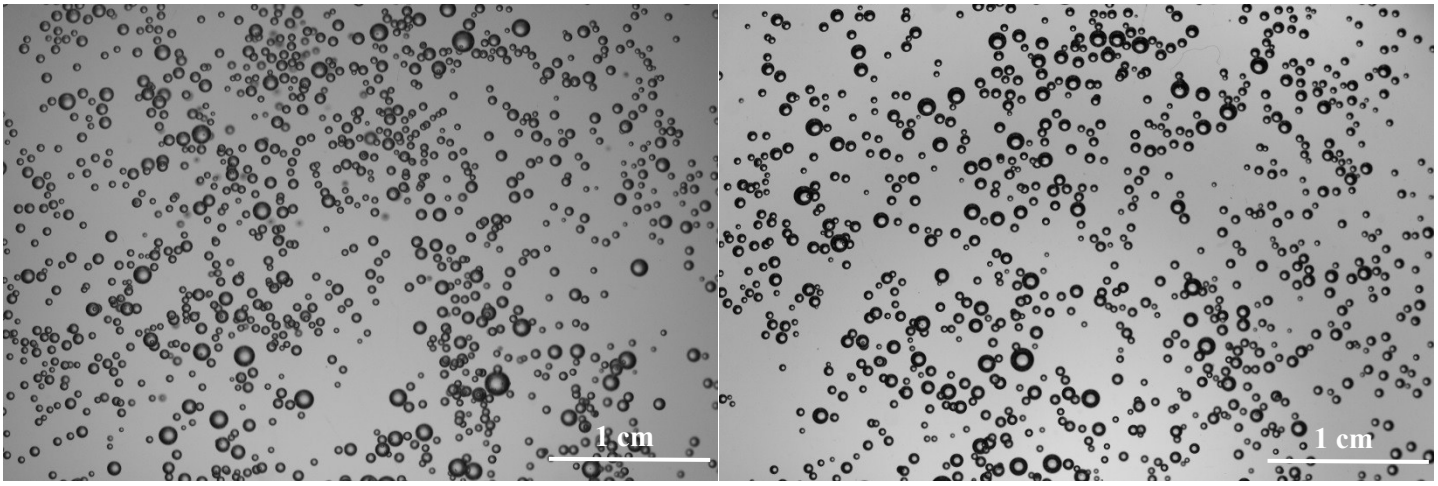

b) dilution D3 and 5 ppm DF-250

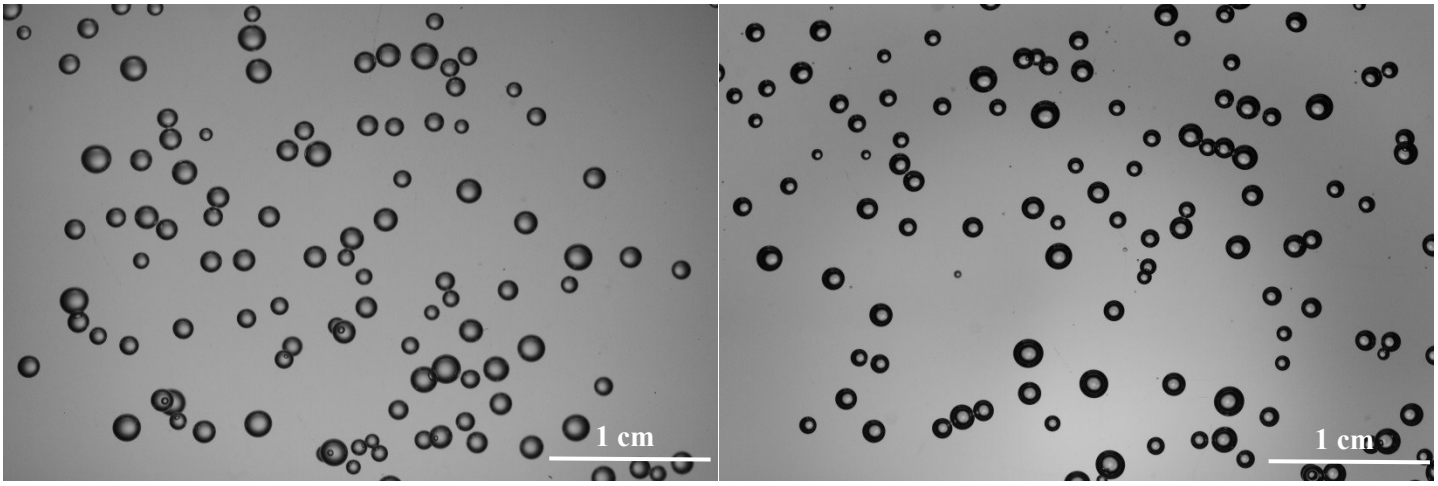

c) dilution D5 and 1 ppm DF-250

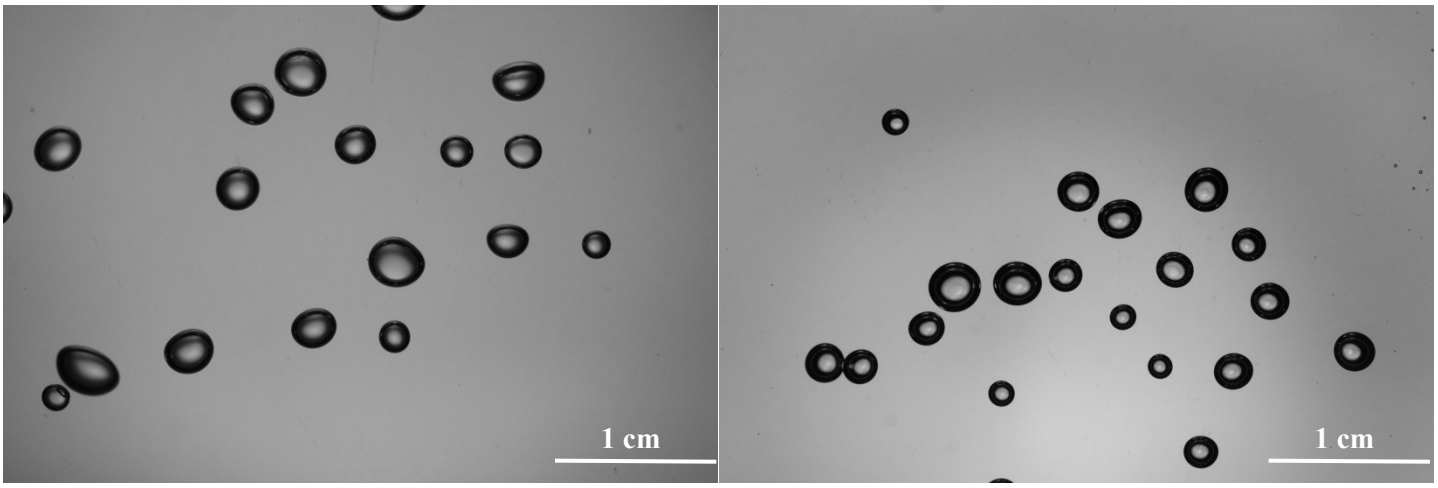

Figure 5.5 - Comparison of bubble size between process water 2 samples (left) and water/DF-250 samples (right): a) undiluted and 20 ppm DF-250; b) dilution D3 and 5 ppm DF-250; c) dilution D5 and 1 ppm DF-250

5.3.4. Substituting gas holdup for bubble size

Figure 5.6 shows D_{32} vs. E_g for DF-250 constructed from the addition and dilution data. As frother concentration increases, D_{32} decreases which signifies the generation of smaller, slower rising bubbles which increase gas holdup, hence the trend seen. The process water samples (not differentiated since they have essentially the same bubble size control ability) follow the same trend and fall within the 98% prediction limit of the model based on DF-250. The relationship in Figure 5.6 shows that D_{32} can be approximated from E_g, a procedure taking around 5 minutes compared to more than an hour using the MBSA (including image analysis).

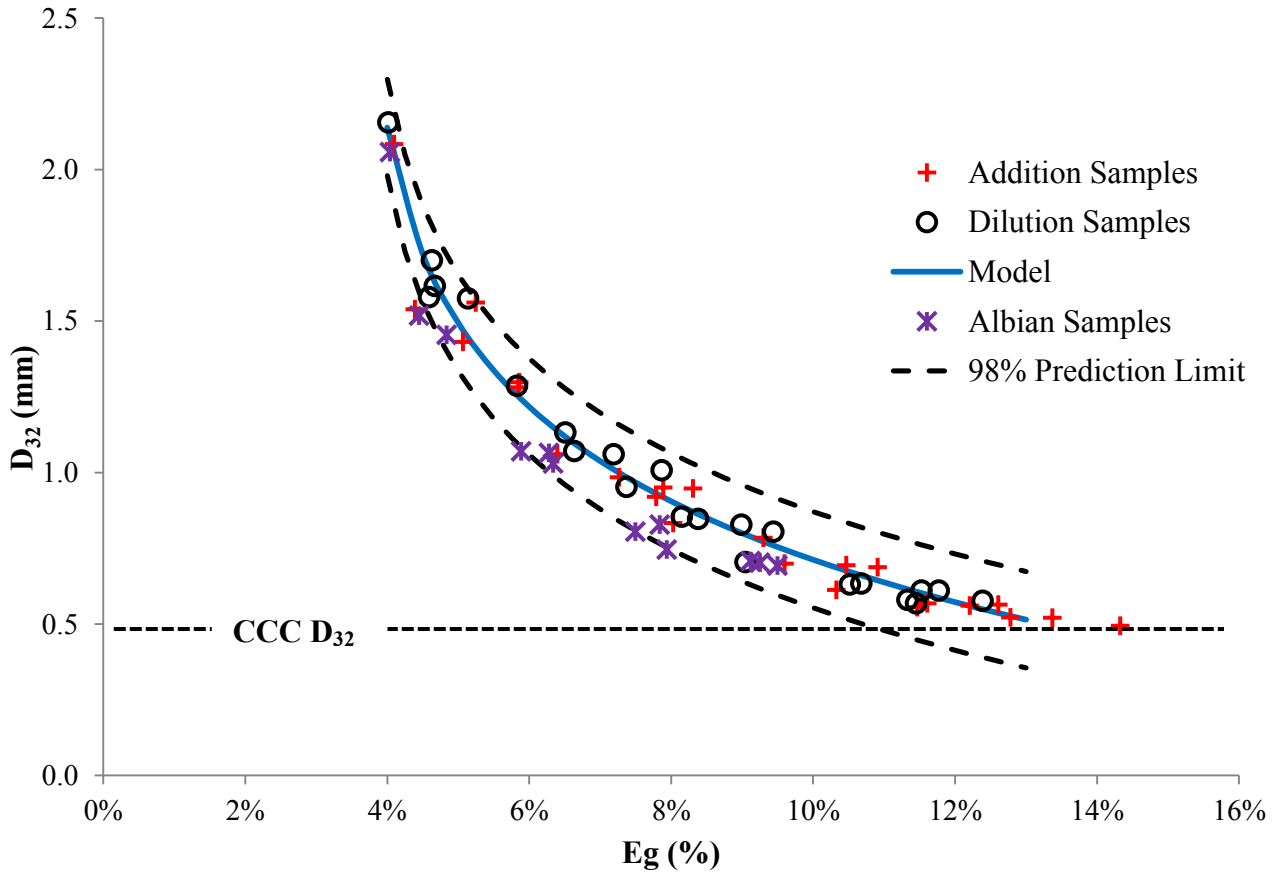

Figure 5.6 - D_{32} as a function of gas holdup: Correlation model based on DF-250 data

5.4. Discussion

It is recognized that when evaluating a flotation system it is important to allow for water chemistry effects (Klimpel and Hansen, 1987; Crozier and Klimpel, 1989; Klimpel and Isherwood, 1991; Comley et al., 2002). The dilution method introduced here provides a way to characterize the overall "frother potential" produced by the system chemistry present in industrial waters. The case study considered natural surfactants released in processing bitumen ore but should be equally applicable to other situations, such as high salt content. It was proven consistent with the addition method and high reproducibility was achieved by thorough control of dilutions and, in present case, allowance for water displaced from MBSA.

Figure 5.3 shows the undiluted samples produced a bubble size comparable to that observed in the mechanical cells at Albian Sands extraction facility (Gomez, 2007). The three samples showed a relatively consistent D_{32} which suggests similar composition and concentration of surfactants. The curve, still suggestive of a downward trend, implies that the undiluted samples are close to, but perhaps not at, the CCC point of the system. After dilution at about 13 %v/v sample concentration, the D_{32} reaches the maximum value measured using Montreal tap water. The samples were not fresh having been transported to and subsequently stored at McGill prior to testing. This may influence the results (but not the concept being tested). Testing fresh samples on-site is needed to determine how representative the findings are, work that is underway.

To transfer the dilution values to ones more familiar we introduced an equivalent DF-250 concentration. Once a CCC curve is developed for a known frother, any industrial process waters can be analyzed and assigned an equivalent frother concentration. Regardless of the choice of frother, the "frother potential" established using this method helps quantify the system's ability to produce the hydrodynamic conditions for flotation.

Compared to bubble size gas holdup is more readily measured in the two-phase system. It was modelled against D_{32} (Figure 5.6) which facilitated prediction of D_{32} without having to use the MBSA. Azgomi et al. (2007) discussed characterizing frothers based on their comparative gas holdup. It was found that different frothers could present different bubble size (D_{32}) at identical gas holdup values. This was traced to an effect of frother type on bubble rise velocity,

independent of its effect on bubble size (Tan et al., 2013). Thus the correlation in Figure 5.6 is dependent on the type of frother. Nevertheless, in the present case there is agreement between the gas holdup values for D_{32} obtained for both DF-250 and the process water samples suggesting at least a comparable effect on bubble rise velocity. In other instances a frother other than DF-250 may have to be used to achieve the correspondence with the process water samples.

The next stage is to transfer this CCC-D concept on site and test a range of fresh samples. A longer term ambition is to consider using gas holdup for on-line application to evaluate possible changes in process waters which may impact the hydrodynamic properties.

5.5. Conclusion

The notion of a system critical coalescence concentration is introduced and a dilution technique is developed to determine it. The dilution technique was verified using DF-250 and its use illustrated with water samples from the Albian Sands bitumen processing plant. The method allowed the process waters to be assigned an equivalent DF-250 concentration. The frother equivalence quantifies the potential of the process waters to control hydrodynamic properties such as bubble size and gas holdup.

5.6. Acknowledgments

Funding was through the Chair in Mineral Processing at McGill University, under the Collaborative Research and Development program of NSERC (Natural Sciences and Engineering Research Council of Canada) with industrial sponsorship from Shell Canada, Vale, Teck, Barrick Gold, Xstrata Process Support, COREM, SGS Lakefield Research and Flottec. Special thanks go to Shell Canada Ltd. (Mr. Gavin Freeman and Mr. Jason Schaan) for the process water samples, the site visits and their support.

5.7. References

Ahmed, N., Jameson, G.J., 1985. The effect of bubble size on the rate of flotation of fine particles. International Journal of Mineral Processing, Vol. 14, pp. 195–215

Azgomi, F., Gomez, C. O., Finch, J. A., 2007. Characterizing Frothers Using Gas Hold-Up. Canadian Metallurgical Quarterly, Vol. 46, pp. 237-242

Cappuccitti, F., Nesset, J. E., 2009. Frother and collector effects on flotation cell hydrodynamics and their implication on circuit performance. In Proceedings 7th UBC-McGill-UA International Symposium on Fundamentals of Mineral Processing (Eds. C. Gomez, J. Nesset, S. Rao), CIM, pp. 169-182

Cho, Y.S., Laskowski, J.S., 2002. Effect of Flotation Frothers on Bubble Size and Foam Stability. International Journal of Mineral Processing, Vol. 64, pp. 69-80

Clift, R., Grace, J.R., Weber, M.E., 1978. Bubbles, Drops and Particles. Academic Press, New York.

Comley, B.A., Harris, P.J., Bradshaw, D.J., Harris, M.C., 2002. Frother characterization using dynamic surface tension measurements. International Journal of Mineral Processing, Vol. 64, pp. 81-100

Crozier, R.D., Klimpel, R.R., 1989. Frothers: Plant practice. Gordon and Breach, New York, NY, pp. 257-280

Finch, J.A., Nesset, J.E., Acuna, C., 2008. Role of frother on bubble production and behaviour in flotation, Part 3: Frother and bubble size reduction. Minerals Engineering, Vol. 21, pp. 949-957

Gomez, C.O., 2007. Albian Sands: Benchmark Gas Dispersion Measurements in Flotation Cells. Report by COG Technologies submitted to Shell Canada Ltd

Gomez, C. O., Finch, J. A., 2007. Gas Dispersion Measurements in Flotation Cells. International Journal of Mineral Processing, Vol. 84, pp. 51-58. (Special issue honoring Professor Peter King)

Grau, R.A., Heiskanen, K., 2002. Visual technique for measuring bubble size in flotation machines. Minerals Engineering, Vol. 15, pp. 507-513

Harbort, G. J., Schwarz, S., 2010. Characterization Measurements in Industrial Flotation Cells, in Flotation Plant Optimization (Ed. C. Greet), AusIMM No. 16, pp. 95-106

Harris, C.C., 1976. Flotation Machines in Flotation. A.MGaudin Memorial Volume, Vol. 2, Chapter 27, pp. 753-815

Hernandez-Aguilar, J.R., Coleman, R.G., Gomez, C.O., Finch, J.A., 2004. A comparison between capillary and imaging techniques for sizing bubbles in flotation systems. Minerals Engineering, Vol. 17, pp. 53–61

Klimpel, R.R., Hansen, R.D., 1987. Frothers: Reagents in Mineral Technology. Marcel Dekker, New York, NY, pp. 663-681

Klimpel, R.R., Isherwood, R.D., 1991. Some industrial implications of changing frother chemical structure. International Journal of Mineral Processing, Vol. 33, pp.369-381

Leja, J., Schulman, J.H., 1954. Flotation Theory: Molecular Interactions Between Frothers and Collectors at Solid–Liquid–Air Interfaces. Trans. AIME 199, pp. 221–228

Masliyah, J.H., Zhou, Z., Xu, Z., Czarnecki, J., Hamza, H., 2004. Understanding Water-Based Bitumen Extraction from Athabasca Oil Sands. Canadian Journal of Chemical Engineering Vol. 82, pp. 628–654

Nesset, J. E., Hernandez-Aguilar, J. R., Acuna, C., Gomez, C. O., Finch, J. A., 2006. Some Gas Dispersion Characteristics of Mechanical Flotation Machines. Minerals Engineering, Vol. 19, pp. 807-815

Quinn, J.J., Kracht, W., Gomez, C.O., Gagnon, C., Finch, J.A., 2007. Comparing the effect of salts and frother (MIBC) on gas dispersion and froth properties. Minerals Engineering, Vol. 20, pp. 1296–1302

Rodrigues, R.T., Rubio, J., 2003. New basis for measuring the size distribution of bubbles. Minerals Engineering, Vol. 16, pp. 757–765

Schramm, L.L., 2000. Surfactants: Fundamentals and Applications in the Petroleum Industry. Cambridge University Press, pp. 377-378

Tan, Y.H., Rafiei, A.A., Elmahdy, E., Finch, J.A., 2013. Bubble Size, Gas Holdup and Bubble Velocity Profile of Some Alcohols and Commercial Frothers. International Journal of Mineral Processing, Vol. 119, pp. 1-5

Tucker, J.P., Deglon, D.A., Franzidis, J.P., Harris, M.C., O'Connor, C.T., 1994. An evaluation of a direct method of bubble size distribution measurement in a laboratory batch flotation cell. Minerals Engineering, Vol. 7, pp. 667–680

CHAPTER 6: DETERMINING FROTHER-LIKE PROPERTIES OF PROCESS WATER IN BITUMEN FLOTATION

Abstract

In oil sands flotation, bitumen is known to release natural surfactants into the process water following the addition of NaOH. These surfactants appear to replace the need for frother. Measuring bubble Sauter mean diameter (D_{32}) vs. dilution, it was possible to characterize the frother-like properties of process waters as an equivalent concentration of a known frother, DF-250 in this case. Process water samples from thickener overflow at the Shell Albian plant were examined. The study showed equivalent concentrations up to 60 ppm DF-250 and variations between samples. Reasons for the variability are discussed. A gas holdup vs. D_{32} correlation was established which reduced the experimental effort.

6.1. Introduction

The oil sands of Canada are among the largest reserves of hydrocarbons in the world, containing the equivalent of 1.7 trillion barrels of oil, of which 170 billion barrels are recoverable using current technology (ERCB, 2011). The oil sands are found as unconsolidated sandstone deposits consisting of very heavy crude (bitumen) and sand, separated by a thin film of water containing mineral rich clays (Clark, 1944; Takamura, 1982; Czarnecki et al., 2005). The largest deposits are found in the Athabasca region in Alberta, with the Wabiskaw-McMurray deposit containing the highest bitumen concentrations. All large open-pit mining operations such as Albian Sands (Shell), Syncrude, Suncor, Horizon (CNRL) and Kearl (Imperial Oil) are located in this area, with bitumen ore grade ranging between 9 - 13 wt. % and a total established mineable bitumen reserve of 27 billion barrels (ERCB, 2011; Masliyah et al., 2011).

The commercial method currently employed to extract bitumen from the oil sands is the Clark hot-water extraction process. In this process, the mined oil sands are conditioned with caustic soda (NaOH) and hot water (50 to 80 ^{0}C), aerated and transferred using pipeline hydrotransport to a large gravity separation tank (the primary separation cell, or PSC) (Clark, 1929; Clark and Pasternak, 1932; Masliyah et al., 1981; Schramm et al., 2000; Masliyah et al., 2011). Most of the bitumen is recovered in a rich froth formed in the PSC. A middlings stream drawn from the

central part of the PSC, and tailings drawn from near the bottom of the PSC are sent to conventional mechanical flotation cells to recover the remaining bitumen. The process has been shown to give high recoveries for bitumen-rich estuarine ores, although poorer performance on leaner marine ores (Schramm and Smith, 1985a).

A key characteristic of the Canadian oil sands is the thin water film surrounding the sand grains, which renders them easy to release from the bitumen using water-based methods such as the Clark hot-water process. The extraction process decreases the viscosity due to the increase in temperature and releases natural surfactants from the bitumen due to the addition of caustic and increase in pH (Leja and Bowman, 1968; Sanford, 1983). The combination facilitates ablation of bitumen-sand lumps and release (liberation) of bitumen from the sand using mechanical agitation (Takamura and Chow, 1985; Schramm and Smith, 1985a; Hupka and Miller, 1991). Depending on the ore grade and the amount of fine particles, different levels of NaOH are needed to release sufficient surfactants to reach what is termed the critical free surfactant concentration, the concentration which maximises bitumen recovery (Schramm and Smith, 1985b, 1990a, 1990b). Rich ores need less caustic to reach the critical surfactant concentration than lean ores.

The surfactants released following caustic addition are predominantly aliphatic carboxylates - $CH_3(CH_2)_{x>4}COONa$ – with carbon chains ranging from C_{15} to C_{17} (Schramm et al., 1987; Schramm et al., 2000). Tailings and recycled water are also shown to be rich in a mixture of carboxylic acids known as naphthenic acids and their water-soluble and surface active sodium salts (Mackinnon and Boerger, 1986; Holowenko et al., 2000). The concentration of naphthenic acids in the process waters was found to be in the range of 30-125 mg/L (Schramm et al., 2000; Holowenko et al., 2000) of which only about 2% are water soluble salts (Masliyah, 2004). Direct addition of surfactants in-lieu of NaOH was also explored and shown to deliver good recovery without the need for high pH levels (Sanford, 1981).

One factor that may enhance flotation is the impact of the released surfactants on reducing bubble size. In mineral flotation systems reduction in bubble size is commonly achieved with frother. Frothers reduce bubble size (diameter) from typically 4-5 mm in water only to 1 mm or less (Nesset et al., 2006) which can increase flotation kinetics by a factor of 10 or more (Ahmed and Jameson, 1985). Frothers adsorb at the air/water interface (Leja and Schulman, 1954) and are commonly held to aid reduction in bubble size through coalescence prevention (Harris,

1976). The surfactants released in bitumen processing may also adsorb at the air/water interface and act in similar manner to frothers, to reduce coalescence and promote bubble size reduction.

A method to characterize the bubble size reduction function of frothers is to plot the Sauter mean bubble diameter (D_{32}) against frother concentration (C). The D_{32} represents the mean size of a bubble having the same total bubble volume to surface area ratio as the bubble size distribution. Given that flotation is driven by bubble surface area, the D_{32} is the mean size often used in flotation studies. To determine bubble size distribution and calculate $D_{32,}$ various devices are now available (Tucker et al., 1994; Grau and Hesinaken, 2002; Rodrigues and Rubio, 2003) including the McGill Bubble Size Analyzer (MBSA) (Hernandez-Aguilar et al., 2004; Gomez and Finch, 2007).

The D_{32}-C plot shows an initial rapid decrease in D_{32} as frother concentration is increased but levels off to become approximately constant beyond a particular frother concentration, which could represent the concentration at which all bubble coalescence is prevented. Cho and Laskowski (2002) defined this concentration as the critical coalescence concentration (CCC) thus introducing a parameter to compare different frothers with respect to their effect on bubble size reduction. A recent publication has listed the CCC for a range of frothers (Zhang et al., 2012). Laskowski (2003) uses a graphical method to estimate CCC. We have elected to fit the D_{32}-C data to a three-parameter exponential decay model to determine the CCC-95, i.e., the concentration giving 95 % of the bubble size reduction compared to water alone. The CCC-95 was shown to closely approximate the CCC values determined graphically (Nesset et al., 2007; Finch et al., 2008; Zhang et al., 2012).

As an alternative to bubble size for characterizing frothers gas holdup (E_g) has been proposed (Azgomi et al., 2007). Gas holdup is the volume of gas relative to the volume of the gas-liquid (slurry) mix. As bubble size reduces, gas holdup increases since small bubbles rise more slowly than large bubbles (Clift et al., 1978). This means gas holdup may substitute for bubble size, the advantage being that gas holdup is easier to measure than D_{32}. Bubble size and gas holdup are referred to as 'hydrodynamic' characteristics that are analyzed using various gas dispersion instruments that have helped improve frother selection and distribution strategies (Cappuccitti and Nesset, 2009).

Few studies on hydrodynamics in bitumen flotation have been conducted. Small bubbles are claimed to lead to better bitumen-bubble attachment due to shorter induction time and are considered beneficial for bitumen flotation (Yoon and Luttrell, 1989; Gu et al., 2004). Zhou et al. (2000) studied the effect of process water chemistry on gas dispersion in bitumen flotation by measuring the gas holdup in a water column and inferring bubble size using drift-flux analysis. They showed that gas holdup increased (bubble size decreased) with an increase in NaOH concentration. They also highlighted the relationship between smaller bubble size and higher bitumen recovery. Direct measurement of bubble size in flotation cells treating bitumen reported small bubbles (ca. 1 mm) (Gomez, 2007), which reasonably could be attributed to the released surfactants. A way to characterize the impact of the released surfactants on the hydrodynamics is required.

It is not feasible to isolate the individual surfactants responsible for bubble size reduction to determine the CCC by the conventional method of adding known concentrations and measuring D_{32}, for discussion purposes referred to as the 'addition' method. Instead, treating the system as a whole, Nassif et al., (2013) proposed a 'dilution' method, measurement of D_{32} vs. dilution volume and, by comparison with the D_{32}-C for a known frother, translate the dilution values to frother equivalent concentrations. They also explored the use of gas holdup as a substitute for bubble size measurement. The frother concentration equivalence gives the 'frother potential' ('hydrodynamic potential') of process water in readily understood terms. The purpose of this paper is to use the dilution method to determine the hydrodynamic potential of process waters sampled from the Albian Sands plant.

6.2. Apparatus and Methodology

The experimental set-up, a 7.6 cm diameter, 3 m high column (Figure 6.1), was assembled at Coanda's research facility in Edmonton using specifically designed scaffolding. A cylindrical porous stainless steel sparger mounted vertically at the bottom of the column (10µm nominal porosity) dispersed air into bubbles at a set gas rate of 2.14 L/min or gas superficial velocity (J_g) of ca. 0.7 cm/s (at the sparger). The set-up was operated in closed loop with the overflow returning to the mixing tank and pumped back to the bottom of the column co-current to the air flow. The feed was introduced into the column using a peristaltic pump (Cole Palmer Model 7520-25) at a constant 3.4 L/min. The conditions ensured that no significant froth layer formed

during the experiments (A froth layer is not desirable as it removes some of the surfactants from the water and can interfere with the upper pressure tapping point).

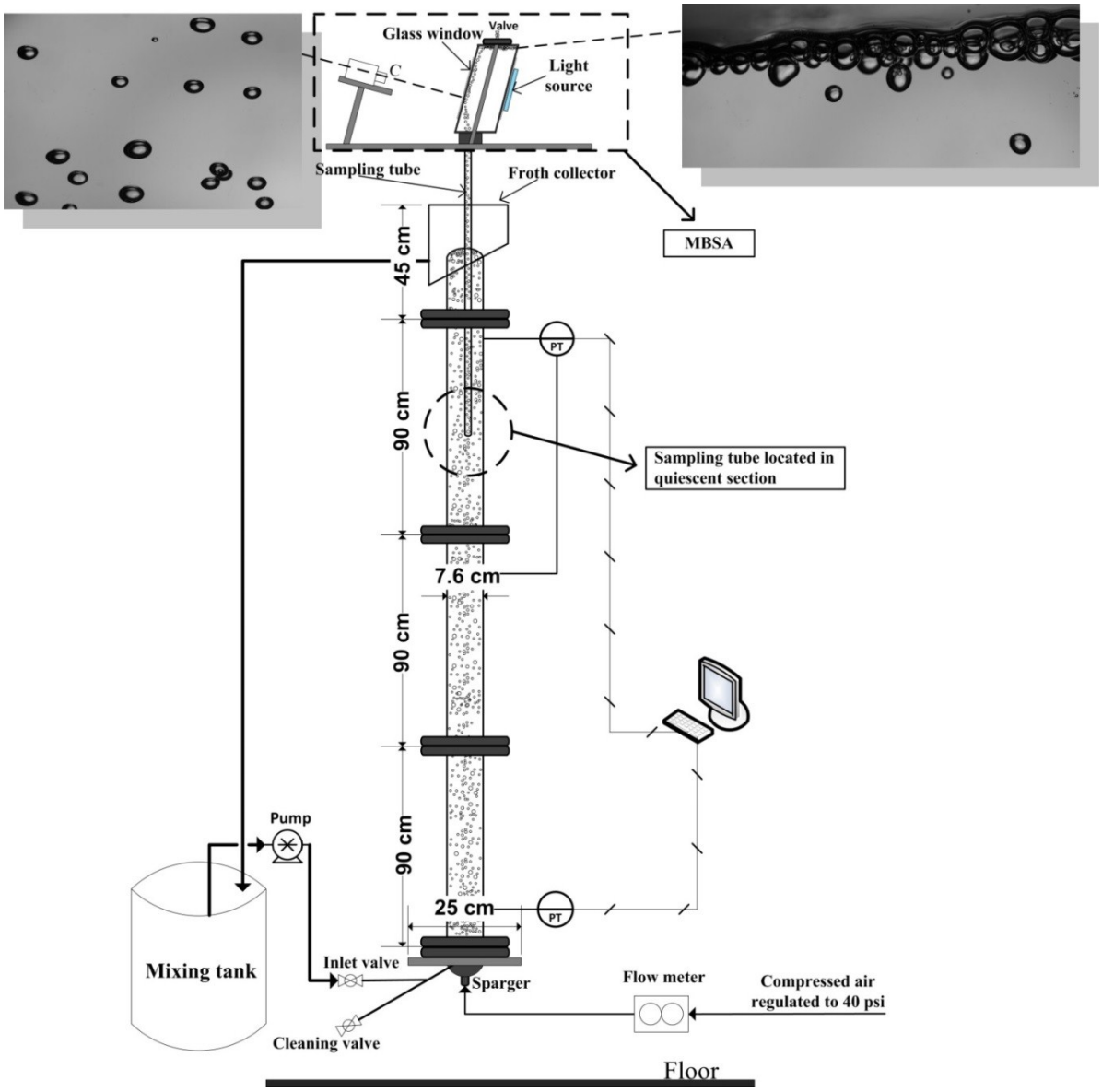

Figure 6.1 - Column set-up with McGill Bubble Size Analyser (MBSA)

Gas holdup was calculated from differential pressure (ΔP) measured using Bailey model PTSDDD1221B2100 tapped between 170 cm and 260 cm from the base as follows:

$$E_g = \frac{\Delta P}{L} * 100 \tag{6.1}$$

where ΔP in equation 6.1 is in cm of water and L is the distance between the tapping points. Absolute pressure P_{abs} (No-Shok pressure sensor) at the base of the column was also connected to an interface and portable signal conditioner, which in turn relayed and recorded the data on an Intellution iFix platform installed on a laptop. Air flow was controlled using a calibrated flow meter.

Bubble size distribution was measured using the MBSA comprising a 6 L, PVC viewing chamber with opposing sloped (15^o) windows made of reinforced glass connected to a sampling tube which is inserted into the column to collect bubbles. Facing the upper window is a high resolution camera (Canon 60D with macro lens) with backlighting to create bubble shadow images.

The procedure for bubble size determination is described in detail elsewhere (Nassif et al., 2013). As the known frother DF-250 was selected. To validate the dilution method, it was tested on DF-250. The process water samples were received from Muskeg River Mine (MRM) extraction facility at Shell Albian Sands in sealed 20 L pails. They were collected from the thickener overflow (OF), with one sample from the recycle water stream (RCW). The thickener OF sampling point was chosen considering its proximity to the extraction process whilst having minimal bitumen content. The waters were allowed to settle for at least a week prior to opening the seal such that any clay and silt settled at the bottom of the pail and any bitumen aggregated at the top. This allowed essentially clear water to be pumped out from the mid-section of the pail. Clear water facilitates use of the MBSA and avoids clogging the porous sparger. For dilution Edmonton tap water was used (composition found online: Epcor 2012)[2]. The dilution water was added with the air flow turned off intermittently to allow adequate mixing as judged by steady gas holdup readings. The water temperature ranged between 12 ºC - 14 ºC.

[2] http://www.epcor.com/water/reports-edmonton/Documents/wq-edmonton-quality-assurance-2012.pdf

6.3. Results

6.3.1. DF-250 CCC curves

DF-250 addition and dilution test results are seen in Figure 6.2 and show excellent agreement, similar to the previous experience (Nassif et al., 2013). Fitting to the decay model was by the least squares method (Microsoft Excel 2010 Solver). The critical coalescence concentration was determined based on the three-parameter model (CCC-95).

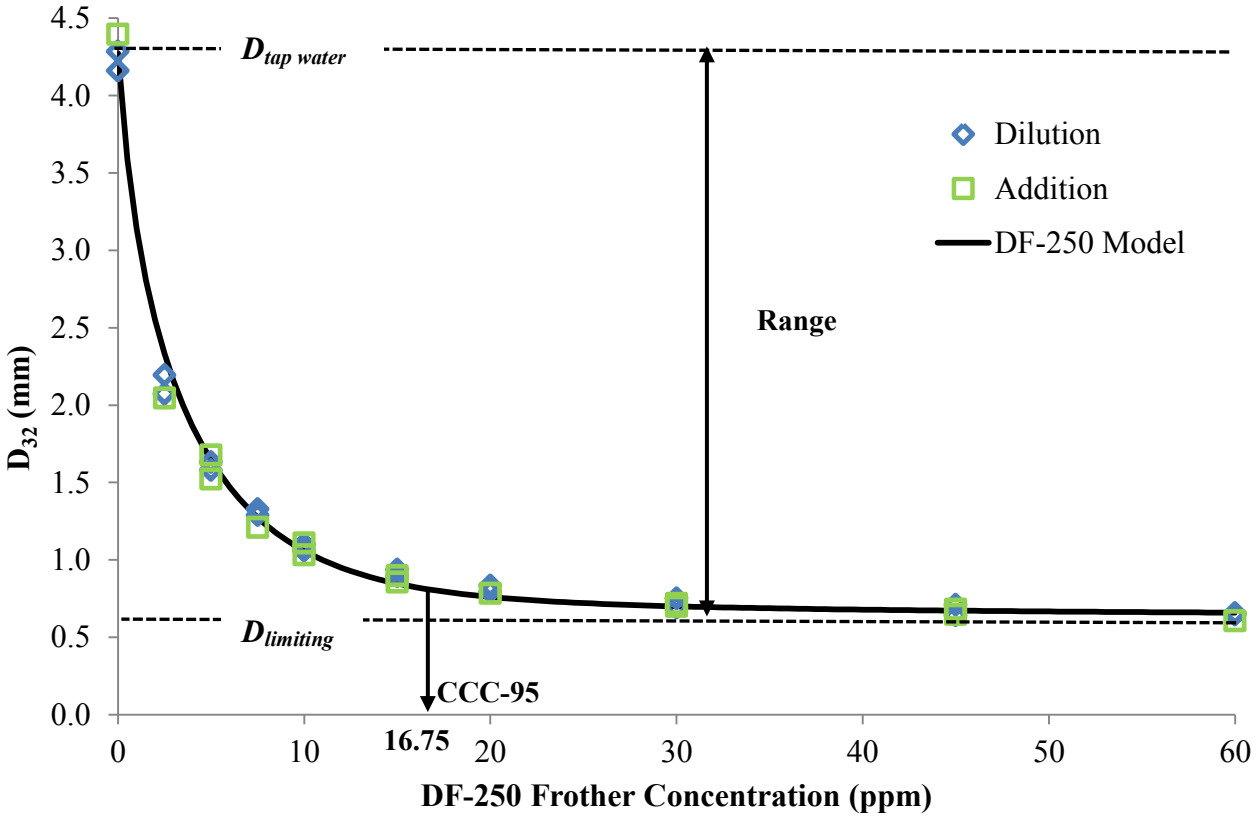

Figure 6.2 - D_{32} as a function of concentration for addition and dilution tests using DF-250

6.3.2. Process water dilution curves and frother equivalence

Using the dilution technique, whilst keeping the operating parameters consistent with the frother tests (liquid flow rate and gas velocity), the dilution curves were developed for the process water samples (Figure 6.3). The concentration scale in these tests is the ratio of the remaining volume of original process water to the total volume of the diluted solution. Samples that were collected on September 30th and October 1st were tested on the week of October 18th. The rest were conducted 3 weeks later also over a span of 2 weeks. The fitting to the decay models was conducted using the least squares method. The DF-250 concentration data were converted to

volume percent (%v/v) and included in Figure 6.3 in order to determine DF-250 equivalent concentrations.

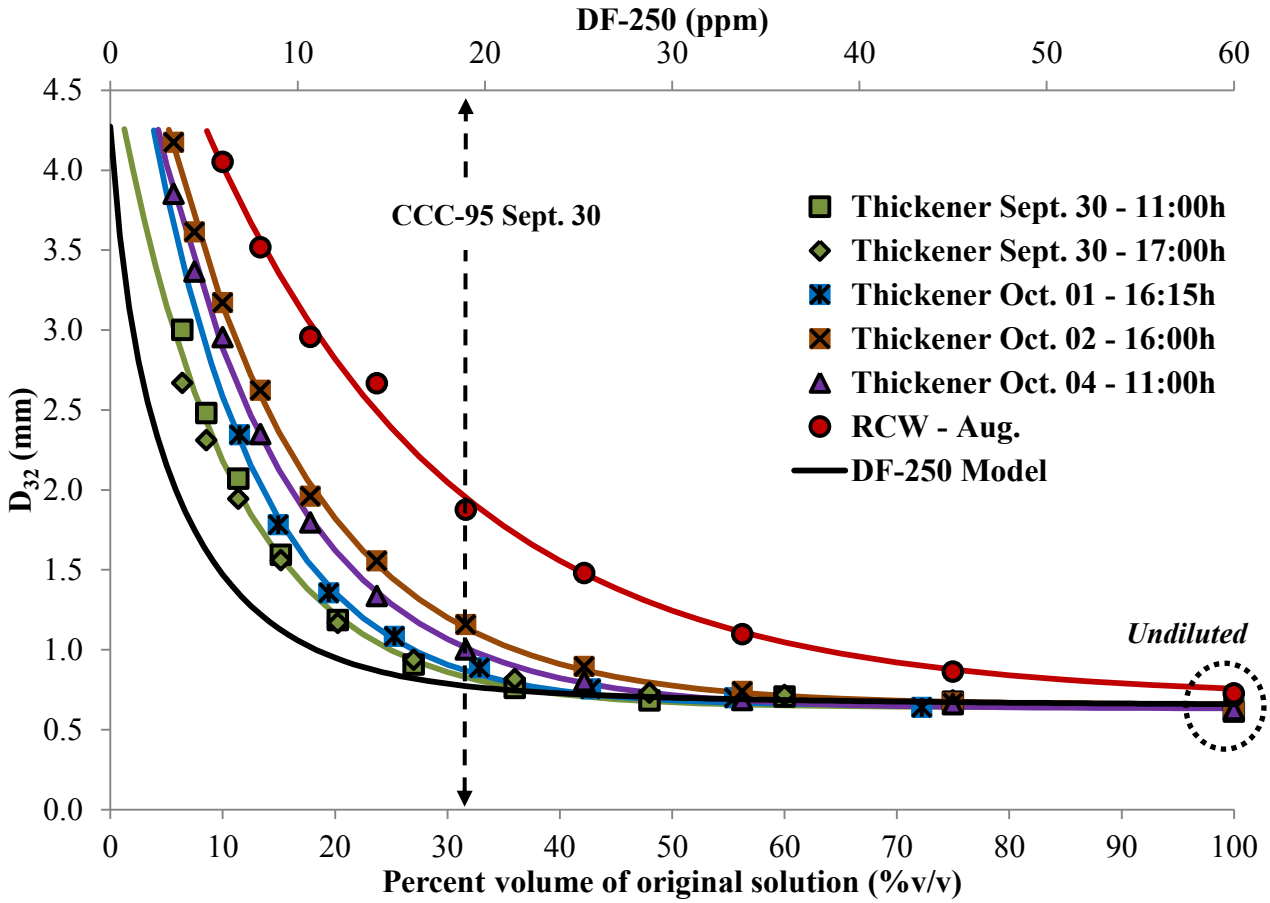

Figure 6.3 - D_{32} as a function of process water concentration by volume for the Albian Sands process water samples

Figure 6.3 shows that the dilution curves of sample waters exhibit a similar trend to that of DF-250. Using the procedure described in Nassif et al. (2013) where DF-250 equivalence is determined by equating the D_{32} values, the 5 thickener OF samples all have an undiluted equivalent concentration of ca. 60 ppm DF-250 and the RCW an equivalent concentration of ca. 24 ppm DF-250.

The images in Figure 6.4 demonstrate the similarity in bubble size between undiluted process water samples and DF-250. (The RCW sample is compared to 20 ppm DF-250 instead of 24 ppm as the closest available set of images). Note the slightly darker background in the thickener overflow sample image due to higher turbidity caused by suspended solids, believed to be clays.

a)

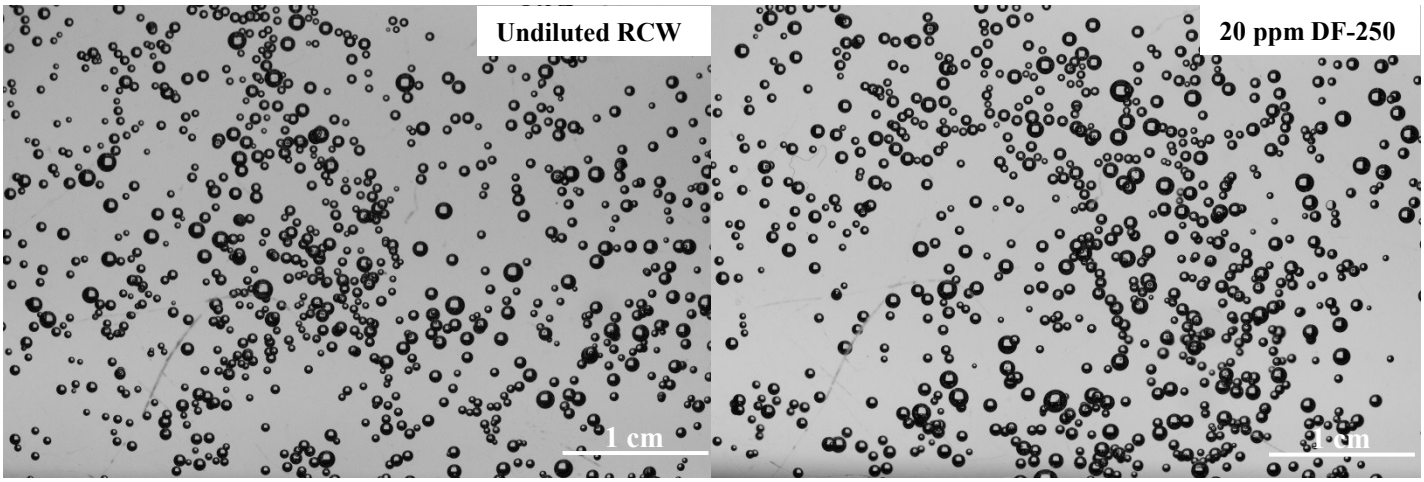

b)

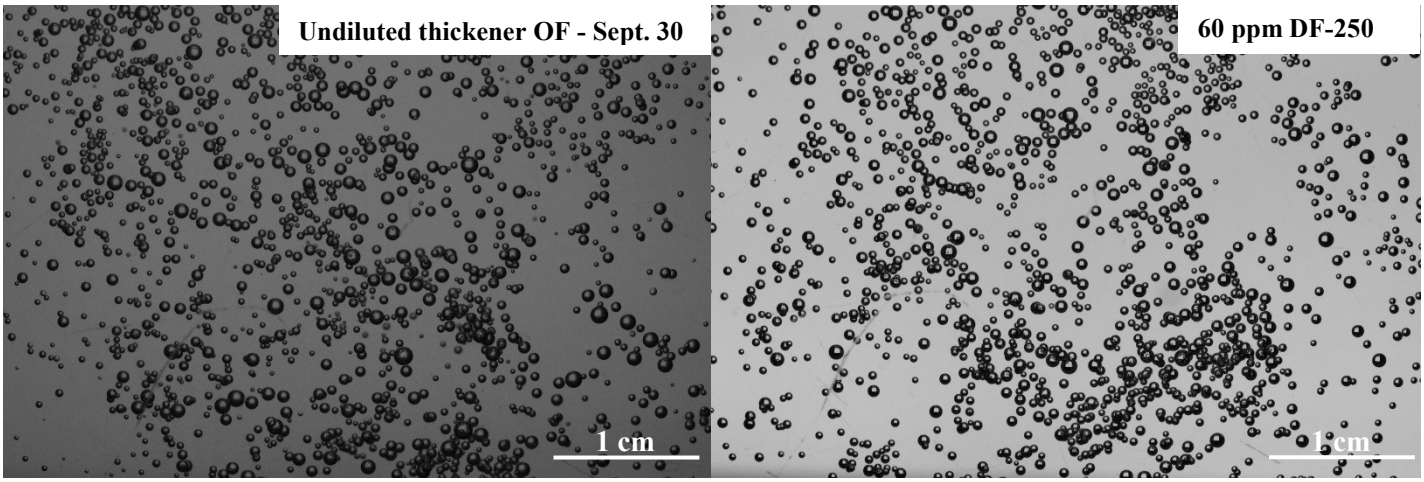

Figure 6.4 - Comparison of bubble size between process water samples (left) and water/DF-250 samples (right): a) undiluted RCW and 20 ppm DF-250; b) undiluted thickener sample Sept. 30 and 60 ppm DF-250

The process water samples show variability in the Sauter mean diameter (D_{32}) with dilution summarized by their CCC-95 %v/v values (Table 6.1). To convert the CCC-95 %v/v to DF-250 equivalent concentrations requires a modification of the procedure. In the original procedure, equivalence is determined by equating D_{32} values but at the CCC-95 the D_{32} is essentially the same and thus differences in the DF-250 equivalent concentration are lost. In the modification, we compare on the basis of equivalent dilutions; in other words we compare vertically. To illustrate, the estimated CCC-95 for thickener OF – Sept. 30, 32 %v/v, is equivalent to 19 ppm DF-250. Using the same procedure, table 6.1 is completed for the remaining samples.

Table 6.1 - Summary of results for CCC-95 quoted in %v/v and in DF-250 equivalence (ppm)

Sample	CCC-95 (%v/v)	CCC-95 (DF-250 equivalence, ppm)
Thickener Sept. 30	32	19
Thickener Oct. 01	34	20
Thickener Oct. 02	45	27
Thickener Oct. 04	41	25
RCW- Aug	75	45

6.3.3. Substituting gas holdup for bubble size

As the concentration decreases, D_{32} increases which signifies the generation of larger, faster rising bubbles which decrease gas holdup, hence the trend seen in Figure 5 which shows D_{32} as a function of gas holdup (E_g) (constructed from the process water data for all the samples). The model was developed based on a logarithmic relationship (equation 2):

$$D_{32} = -\tau * \ln(\frac{E_g - E_{g,min}}{E_{g,max} - E_{g,min}}) \quad (6.2)$$

where τ = diameter constant, $E_{g,min}$ = minimum percent gas holdup, $E_{g,max}$ = maximum percent gas holdup. Optimal values for the constant, minimum holdup and maximum holdup were determined using least squares method (Microsoft Excel 2010 Solver). The values were 0.618 mm, 3.68 % and 28.13 % respectively.

The DF-250 frother data were included and essentially show the same bubble size control ability as the process waters as they mostly fall within the 95% prediction limit of the model. (Data with Sauter mean diameter larger than 2.5 mm were excluded as they do not lie within the region of interest and also exhibit high variation because of the steepness of this part of the curve). Figure 5 shows that D_{32} can be approximated from E_g, a procedure taking less than 5 minutes compared to more than an hour using the MBSA (including image analysis).

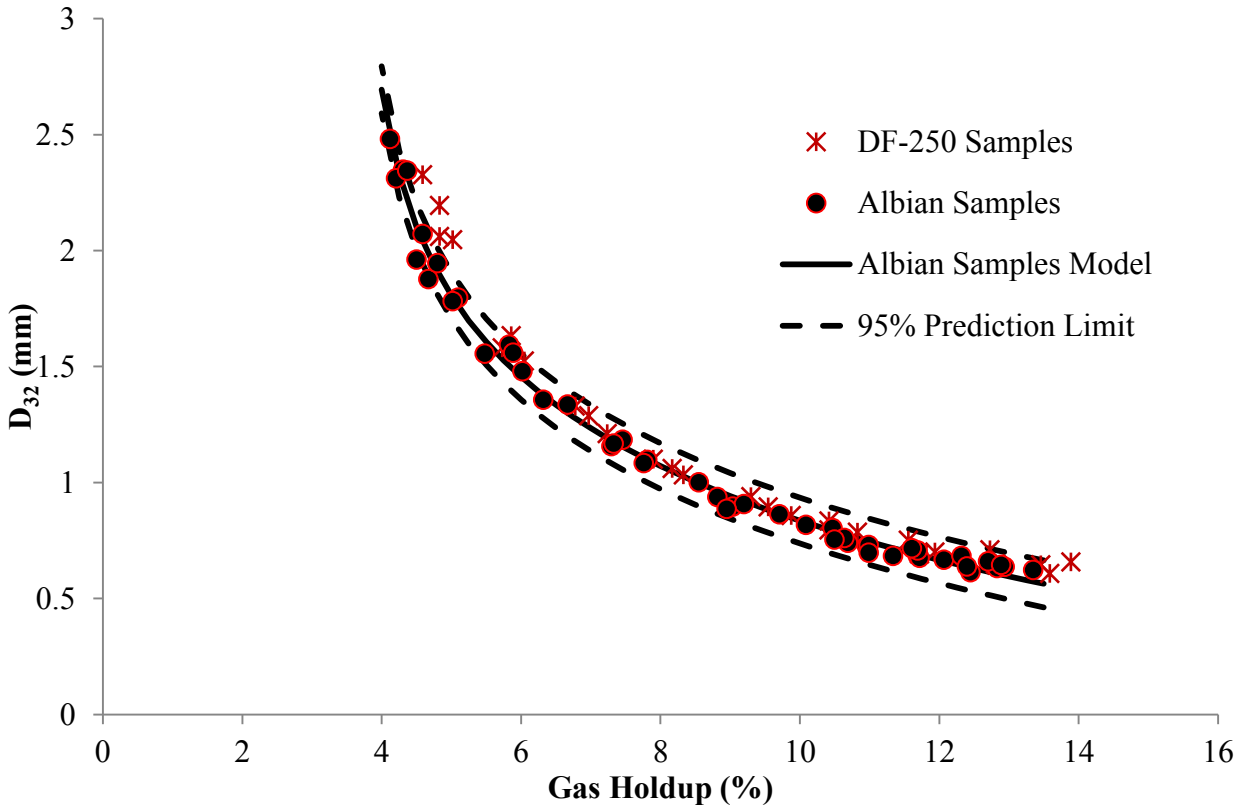

Figure 6.5 - D_{32} as a function of gas holdup: Correlation model based on Albian samples data

6.4. Discussion

The addition of NaOH and the natural surfactants released in processing bitumen ore, in addition to the ionic and clay components, lead to a complex and variable water chemistry that affects bitumen recovery (Schramm and Smith, 1987; Kasongo et al., 2000; Ding et al., 2006; Zhao et al., 2009). It is recognized that when evaluating flotation systems it is important to allow for water chemistry effects (Klimpel and Hansen, 1987; Crozier and Klimpel, 1989; Klimpel and Isherwood, 1991; Comley et al., 2002). The aim of the current work was to analyse the impact of Albian Sands water chemistry on the system hydrodynamics by measuring two gas dispersion parameters, bubble Sauter mean diameter and gas holdup. While other factors may have some role, the released surfactants likely contribute most of the hydrodynamic properties and thus it was logical to apply the bubble size and gas holdup techniques developed to characterize frothers.

Using the methodology introduced by Nassif et al. (2013) the system hydrodynamics were expressed in terms of DF-250 equivalent concentration. Estimates of the equivalent DF-250

concentration for the undiluted samples were made using the original technique which in the case of the thickener overflow gave ca. 60 ppm DF-250 equivalent. The dilution curves showed different CCC-95 values between the samples. To convert to equivalent DF-250, the procedure was modified. The differences might suggest different surfactant types or combinations, but because CCC-95 is quoted as %v/v rather than absolute concentration, there may be an effect of initial undiluted concentration. For example, the RCW CCC-95 in DF-250 equivalence is 45 ppm but this water may have the same surfactant composition as the thickener OF but is more dilute. Nevertheless, the surfactants appear to be weaker than DF-250 as their CCC-95 values are higher than that of DF-250 (ca.17 ppm).

Another point that appears to be related to the use of concentration as a dilution ratio is the fact that the curves do not converge to the same D_{32} with increasing dilution. The converging value D_{32} should be that of tap water.

Variations in surfactant composition and concentration are believed to be related to the bitumen content of the ore (and the amount of fines present) which affects the amount of free surfactant released upon treatment with NaOH. Variations in surfactant release could result in varying hydrodynamic conditions making flotation difficult to control. In the present case, certainly the undiluted thickener OF samples appear to have DF-250 equivalents capable of supporting the hydrodynamic conditions necessary for flotation.

A change in composition of bitumen process waters has been shown to result from the biodegradation of water-soluble naphthenic salts by naturally occurring bacteria (Herman et al., 1994; Holowenko et al., 2001). Biodegradation is encouraged when process water is isolated from bitumen over an extended period of time such as in the tailings pond, or in the case of this work, storage of the water samples. Another important degradation process is precipitation of these anionic surfactants at low pH and in the presence of calcium and/or magnesium ions (Masliyah et al., 2011). These degradation processes possibly contribute to the variation in the process waters especially between thickener samples and RCW.

In the previous paper (Nassif et al., 2013), process water samples from the thickener OF had been aged for months following transportation to and storage at McGill, and when tested showed undiluted 20 ppm DF-250 equivalence. This represents a 67 % decrease in frother potential

compared to the current thickener OF samples that is difficult to attribute solely to a change in bitumen ore quality. Ageing effects are believed to be the cause. One consequence is the need to test samples soon after collection. This is the reason the set-up was established at Edmonton to be nearer to the source. Ideally testing should be in the plant.

Compared to bubble size, gas holdup is more readily measured in the two-phase system. Gas holdup was modelled against D_{32} (Figure 6.5) which facilitated estimation of D_{32} which greatly speeded up the method. The data show the D_{32}-E_g trend for DF-250 agrees with that for the process samples, which further supports the use of DF-250 as the appropriate frother for determining the equivalence in this case.

The water samples supplied were ones readily available and low in bitumen. The thickener overflow samples represent conditions close to those in the flotation circuit but ideally we should include samples directly from the process units. One sample from the PSC middlings stream was taken and clarified water extracted after a period of settling. While not enough volume to test undiluted a 67% diluted sample gave a gas holdup of 12.6% with estimated D_{32} (from Figure 6.5) of 0.62 mm. Since this dilution-gas holdup data fitted the trend for the current samples (Figure 6.5) it suggests the original (undiluted) PSC water was at least comparable in frother potential to the undiluted thickener overflows. The use of gas holdup combined with knowledge of the dilution-gas holdup trend opens a quick way to check other process units for frother potential.

The next stage is to transfer the characterization techniques to site such that a range of fresh samples from various sampling points can be tested over time. One objective would be to establish variability in process water hydrodynamics and link with operating conditions, for example bitumen grade and fines content. There may be a case for addition of frother to smooth out variations in the hydrodynamics. Variability will likely increase as a concern as leaner ores are treated requiring more process aids, and as new methods are being developed to decrease the process temperature and to enhance tailings de-watering (Sanford, 1981; Schramm et al., 2002; Masliyah et al., 2011). Another ambition is to consider using gas holdup for on-line monitoring of process waters.

6.5. Conclusion

This paper describes a dilution method used to express the hydrodynamic potential of bitumen process waters by a frother equivalent concentration. In this example using samples from the Albian Sands plant DF-250 was the frother equivalent. The method uncovered the high DF-250 equivalence (ca. 60 ppm) of thickener overflow process waters and identified variability that may be related to characteristics of the released surfactants. The use of gas holdup in place of bubble size determination greatly speeded up the measurement.

6.6. Acknowledgements

Funding was through the Chair in Mineral Processing at McGill University, under the Collaborative Research and Development program of NSERC (Natural Sciences and Engineering Research Council of Canada) with industrial sponsorship from Shell Canada, Vale, Teck, Barrick Gold, Xstrata Process Support, COREM, SGS Lakefield Research and Flottec. Special thanks go to Shell Canada Ltd. (Mr. Gavin Freeman and Mr. Jason Schaan) for the process water samples and logistics support. Thanks go also to Coanda R&D for their help in getting set up and running in their Edmonton facility.

6.7. References

Ahmed, N., Jameson, G.J., 1985. The effect of bubble size on the rate of flotation of fine particles. International Journal of Mineral Processing. Vol. 14, pp. 195–215

Azgomi, F., Gomez, C.O., Finch, J.A., 2007. Characterizing Frothers Using Gas Hold-Up. Canadian Metallurgical Quarterly. Vol. 46, pp. 237-242

Cappuccitti, F., Nesset, J. E., 2009. Frother and collector effects on flotation cell hydrodynamics and their implication on circuit performance. In Proceedings 7th UBC-McGill-UA International Symposium on Fundamentals of Mineral Processing (Eds. C. Gomez, J. Nesset, S. Rao). CIM, pp. 169-182

Cho, Y.S., Laskowski, J.S., 2002. Effect of Flotation Frothers on Bubble Size and Foam Stability. International Journal of Mineral Processing. Vol. 64, pp. 69-80

Clark, K.A., 1929. Bituminous Sand Processing. Canadian Patent 289058, issued on April 4, 1929

Clark, K.A., Pasternak, D.S.,1932. Hot Water Separation of Bitumen from Alberta Bituminous Sand. Industrial and Engineering Chemistry, Vol. 24, pp. 1410-1416

Clark, K.A., 1944. Hot-Water Separation of Alberta Bituminous Sand. Transcript of Canadian institute of Mining and Metallurgy. Vol. 47, pp. 257-274

Clift, R., Grace, J.R., Weber, M.E., 1978. Bubbles, Drops and Particles. Academic Press, New York

Comley, B.A., Harris, P.J., Bradshaw, D.J., Harris, M.C., 2002. Frother characterization using dynamic surface tension measurements. International Journal of Mineral Processing. Vol. 64, pp. 81-100

Crozier, R.D., Klimpel, R.R., 1989. Frothers: Plant practice. Gordon and Breach, New York, NY. pp. 257- 280

Czarnecki, J., Radoev, B., Schramm, L.L., Slavchev, R., 2005. On the nature of Athabasca oil sands. Advances in Colloid Interface Science. Vol. 114-115, pp. 53-60

Ding, X., Repka, C., Xu, Z., Masliyah, J., 2006. Effect of illite clay and divalent cations on bitumen recovery. Canadian Journal of Chemical Engineering. Vol. 84, pp. 643-650

Energy Resources Conservation Board (ERCB), 2011. ST98: Alberta's Energy Reserves 2011 and Supply/Demand Outlook 2012-2021. Calgary

Finch, J.A., Nesset, J.E., Acuna, C., 2008. Role of frother on bubble production and behaviour in flotation, Part 3: Frother and bubble size reduction. Minerals Engineering. Vol. 21, pp. 949-957

Gomez, C.O., 2007. Albian Sands: Benchmark Gas Dispersion Measurements in Flotation Cells. Report by COG Technologies submitted to Shell Canada Ltd

Gomez, C.O., Finch, J.A., 2007. Gas Dispersion Measurements in Flotation Cells. International Journal of Mineral Processing. Vol. 84, pp. 51-58. (Special issue honoring Professor Peter King).

Gu, G., Sanders, R.S., Nandakumar, K., Xu, Z., Masliyah, J.H., 2004. A Novel Experimental Technique to Study Single Subble Bitumen Attachment in Flotation. International Journal of Mineral Processing. Vol. 74, pp. 15-29

Harris, C.C., 1976. Flotation Machines in Flotation. A.M. Gaudin Memorial Volume. Vol. 2, Chapter 27, pp. 753-815.

Herman, D.C., Fedorak, P.M., Mackinnon, M.D., Costerton, J.W., 1994; Biodegradation of naphthenic acids by microbial populations indigenous to oil sands tailings. Canadian Journal of Microbiology. Vol. 40, pp.467-477

Holowenko, F.M., Mackinnon, M.D., Fedorak, P.M., 2000. Methanogens and sulfate-reducing bacteria in oil sands fine tailings waste. Canadian Journal of Microbiology. Vol. 46, pp. 927-937

Holowenko, F.M., Mackinnon, M.D., Fedorak, P.M., 2001. Naphthenic Acids and Surrogate Naphthenic Acids in Methanogenic Microcosms. Water Research. Vol. 35, pp. 2595-2606

Hupka, J., Miller, J.D., 1991. Electrophoretic characterization and processing of Asphalt Ride and Sunnyside tar sand. International Journal of Mineral Processing. Vol. 31, pp. 217-231

Kasongo, T., Zhou, Z., Xu, Z., Masliyah, J.H., 2000. Effect of clays and calcium ions on bitumen extraction from Athabasca oil sands using flotation. Canadian Journal of Chemical Engineering. Vol. 78, pp. 674-681

Klimpel, R.R., Hansen, R.D., 1987. Frothers: Reagents in Mineral Technology. Marcel Dekker, New York, NY, pp. 663-681

Klimpel, R.R., Isherwood, R.D., 1991. Some industrial implications of changing frother chemical structure. International Journal of Mineral Processing. Vol. 33, pp.369-381

Leja, J., Schulman, J.H., 1954. Flotation Theory: Molecular Interactions Between Frothers and Collectors at Solid–Liquid–Air Interfaces. Trans. AIME 199, pp. 221–228

Leja, J., Bowman, C.W., 1968. Application of Thermodynamics to the Athabasca Tar Sands. Canadian Journal of Chemical Engineering. Vol. 49, pp. 479-481

Mackinnon, M., Boerger, H., 1986. Description of Two Treatment Methods for Detoxifying Oil Sands Tailings Pond Water. Water Pollution Research Journal of Canada. Vol. 21, pp. 496-512

Masliyah, J.H., Kwong, T., Seyer, F.A, 1981. Theoretical and experimental studies of gravity separation vessel. Industrial and Engineering chemistry process design and development. Vol. 20, pp. 154-160

Masliyah, J.H., Zhou, Z., Xu, Z., Czarnecki, J., Hamza, H., 2004. Understanding Water-Based Bitumen Extraction from Athabasca Oil Sands. Canadian Journal of Chemical Engineering, Vol. 82, pp. 628–654

Masliyah, J.H., Czarnecki, J., Xu, Z., 2011. Handbook on Theory and Practice of Bitumen Recovery from Athabasca Oil Sands - Volume 1: Theoretical Basis. Kingsley Knowledge Publishing, pp. 115-116

Nassif, M., Finch, J.A., Waters, K.E., 2013. Developing critical coalescence concentration curves for industrial process waters using dilution. Minerals Engineering. Submitted April 2013

Nesset, J. E., Hernandez-Aguilar, J. R., Acuna, C., Gomez, C. O., Finch, J. A., 2006. Some Gas Dispersion Characteristics of Mechanical Flotation Machines. Minerals Engineering. Vol. 19, pp. 807-815

Nesset, J.E., Finch, J.A., Gomez, C.O., 2007. Operating variables affecting the bubble size in forced-air mechanical flotation machines. In: Proceedings AusIMM 9th Mill Operators' Conference, Fremantle, Australia, pp. 66–75

Quinn, J.J., Kracht, W., Gomez, C.O., Gagnon, C., Finch, J.A., 2007. Comparing the effect of salts and frother (MIBC) on gas dispersion and froth properties. Minerals Engineering. Vol. 20, pp. 1296–1302

Sanford, E., 1981. Process Aids for the Conditioning Step in Hot-Water Extraction Process for Tar Sand. Canadian Patent 1100074, issued on April 28, 1981

Sanford, E.C., 1983. Processibility of Athabasca oil sand: Interrelationship between oil sand fine solids, process aids, mechanical energy and oil sand age after mining. The Canadian Journal of Chemical Engineering. Vol. 61, pp. 554-567

Schramm, L.L., Smith, R.G., 1985a. The Influence of Natural Surfactants on Interfacial Charges in the Hot-Water Process for Recovering Bitumen from the Athabasca Oil Sands. Colloids and Surfaces. Vol. 14, pp. 67-85

Schramm, L.L., Smith, R.G., 1985b. Control of Process Aid Used in Hot Water Process for Extraction of Bitumen from Tar Sand. Canadian Patent 1,188,644

Schramm, L.L., Smith, R.G., 1987. Two Classes of Hot Anionic Surfactants and their Significance in Water Processing of Oil Sands. The Canadian Journal of Chemical Engineering. Vol. 65, pp. 799-811

Schramm, L.L., Smith, R.G., 1990a. Monitoring Electrophoretic Mobility of Bitumen in Hot Water Extraction Process Plant Water to Maximize Primary Froth Recovery. Canadian Patent 1265463, issued on February 6, 1990

Schramm, L.L., Smith, R.G., 1990b. Monitoring Surfactant Content to Control Hot Water Process for Tar Sand. Canadian Patent 1270220, issued on June 12, 1990

Schramm, L.L., 2000. Surfactants: Fundamentals and Applications in the Petroleum Industry. Cambridge University Press, pp. 377-378.

Schramm, L.L., Stasiuk, E.N., Yarranton, H., Maini, B.B., Shelfantook, B., 2002.Temperature Effects in the Conditioning and Flotation of Bitumen From Oil Sands in Terms of Oil Recovery and Physical Properties. In: Proceedings of the Canadian International Petroleum Conference, Calgary, Alberta.

Tang C., Heindel T.J., 2004. Time-Dependent Gas Holdup Variation in an Air-Water Bubble Column. Chemical Engineering Science. Vol. 59, pp. 623-632

Takamura, 1982. Microscopic structure of Athabasca Oil Sand. Canadian Journal of Chemical Engineering. Vol. 60, pp. 538-545

Takamura, K., Chow, R.S., 1985. The Electric Properties of the Bitumen/Water Interface, Part II: Application of the ionisable Surface-Group Model. Colloids and Surfaces. Vol.15, pp. 35-48

Tan, Y.H., Rafiei, A.A., Elmahdy, E., Finch, J.A., 2013. Bubble Size, Gas Holdup and Bubble Velocity Profile of Some Alcohols and Commercial Frothers. International Journal of Mineral Processing. Vol. 119, pp. 1-5

Tucker, J.P., Deglon, D.A., Franzidis, J.P., Harris, M.C., O'Connor, C.T., 1994. An evaluation of a direct method of bubble size distribution measurement in a laboratory batch flotation cell. Minerals Engineering Vol. 7, pp. 667–680

Yoon, R.H., Luttrell, G.H., 1989. The Effect of Bubble Size on Fine Particle Flotation. Mineral Processing and Extractive Metallurgical Review. Vol. 5, pp. 101-122

Zhang, W., Nesset, J., Rao, R., Finch, J.A, 2012. Characterizing Frothers through Critical Coalescence Concentration (CCC)95-Hydrophile-Lipophile Balance (HLB) Relationship. Open Access Minerals, Vol. 2, pp. 208-227

Zhao, H., Dang-Vu, T., Long, J., Xu, Z., Masliyah, J., 2009. Role of bicarbonate ions in oil sands extraction systems with a poor processing ore. Journal of Dispersion Science and Technology. Vol. 30, pp. 809-822

Zhou, Z., Xu, Z., Masliyah, J., 2000. Effect of Natural Surfactants released from Athabasca Oil Sands on Air Holdup in a Water Column. The Canadian Journal of Chemical Engineering. Vol. 78, pp. 617-624

CHAPTER 7: CONCLUSIONS AND RECOMMENDATIONS

7.1. Conclusions

The objectives completed and discoveries made in this Master's research project can be summarized as follows:

- New dilution technique has been established and shown to be a viable method to characterize industrial process water gas dispersion parameters. A system critical coalescence concentration and a frother equivalence concept were introduced

- Demonstrated the oil sands process water to be very rich in frother-like surfactants, with a frother equivalence reaching 60 ppm DF-250. This in turn indicates that bitumen flotation is currently subject to good hydrodynamics due to the rich natural surfactants systems present in the process water

- Explored the use of gas holdup to D_{32} correlation instead of the MBSA for continuously measuring bubble size distributions in on-site trials. D_{32} was successfully obtained for a PSC middlings sample using uniquely gas holdup

Overall there seems to be variability in the surfactant systems present in the oil sands process waters. There also seems to be an ageing effect eroding the frother-like characteristics of the process water. Further application of these characterization techniques and studies on the ability of process water to generate hydrodynamic conditions required for bitumen flotation are needed to address questions regarding the origins of the observed variations.

7.2. Future Work

The next stage of the research entails using these characterization techniques for a range of fresh samples from various sampling points and tested over time in an effort to determine the sources of variability. In addition to the change in bitumen grade and its perceived effect on the amount of natural surfactants present in process water, a seemingly crucial point of interest is the ageing process and its detrimental effect on the process water's frother potential.

The following recommendations are made for future research on oil sands process water hydrodynamics:

- Sample and test thickener OF and PSC middings samples from the same operating day over an extended period of time
- Determine D_{32} for undiluted samples and leave to age for a number of months while testing intermittently and storing in cool environment
- Develop compact unit to test frother-potential
- Study temperature effects

It is important to consider using gas holdup on-line in bitumen flotation to more easily evaluate possible changes in process waters that may be having an impact on flotation performance. Developing a compact unit, made of only one segment of the column used in this research and with conductivity rings instead of differential pressure, can be tested and calibrated on-site. This in turn would allow quick analyses of process water frother-potential and shed information on how the overall surfactant system is behaving relative to changes in ore and water quality.

APPENDIX A: COLUMN INTERFACE

The following personalized interface on Intellution iFix was created for the column:

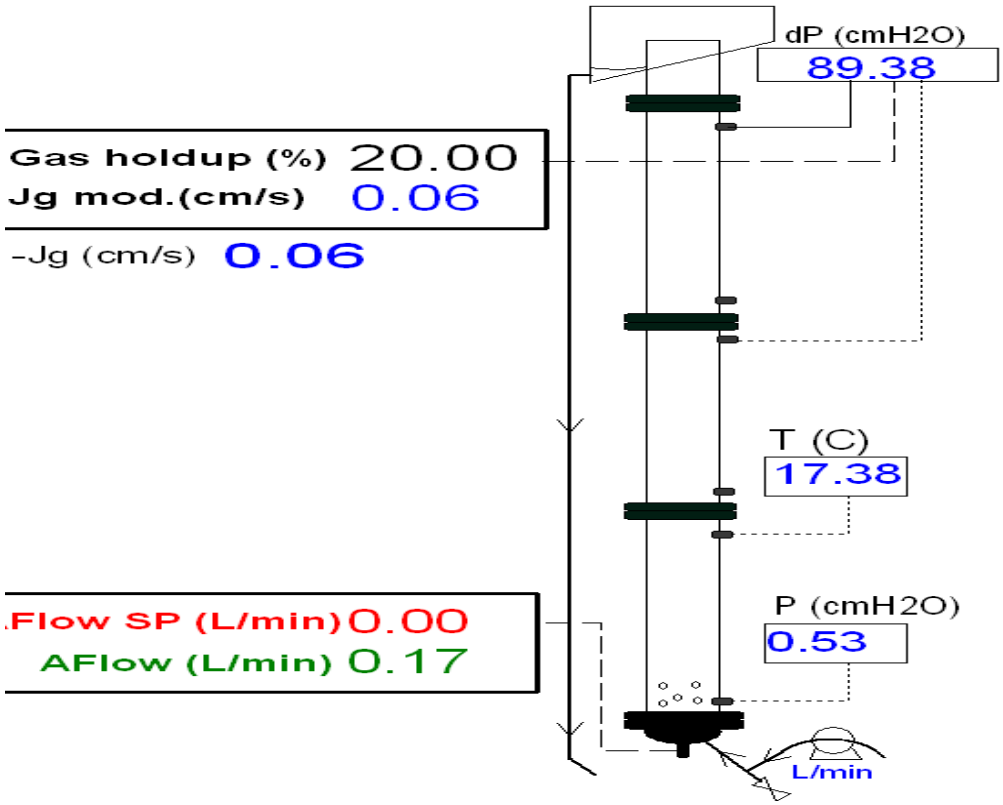

Figure A.1 - iFix interface for column controllers and sensors

where Flow SP is the air flow setpoint, AFlow is the measured air flow rate, P is the absolute pressure at the base of the column, T is temperature and dP is the differential pressure in cm H_2O used to measure gas holdup according to equation B.3. The tapping points for the differential pressure are 90 cm apart (L in equation B.3 is 90). J_g mod is the superficial gas velocity modified to account for hydrostatic head and local temperature according to the ideal gas law as follows:

$$J_g = \frac{Q_g}{A_{cross}} \tag{A.1}$$

$$J_{g\,mod} = \frac{(J_g * P_{atm})}{(P_{atm} + P_{abs})} * \frac{(273+T)}{273} \tag{A.2}$$

Based on the diagram below, the gas holdup derivation from differential pressure is as follows:

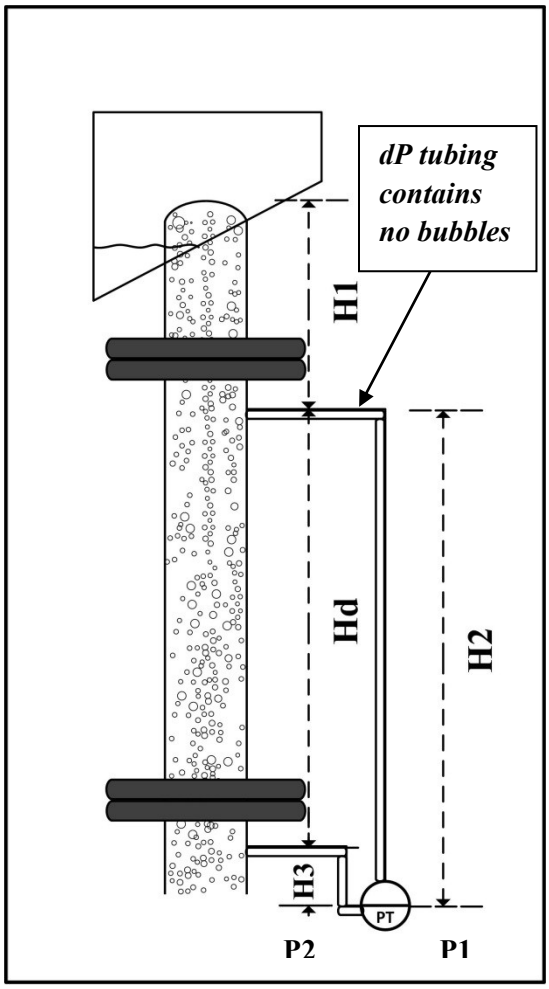

Figure A.2 - Differential pressure measurement

$$P_1 = \rho_{H_2O} g H_2 + \rho_b g H_1 + P_{atm} \; and \; P_2 = \rho_{H_2O} g H_3 + \rho_b g (H_d + H_1) + P_{atm} \quad (A.3)$$

Where **P1** and **P2** are upper and lower pressure tapping points respectively and ρ_b is bulk liquid density (Figure A.2). Knowing that:

$$H_2 = H_3 + H_d and \; \rho_b = \rho_{pulp}(1 - E_g) \quad (A.4)$$

$$\Delta P = P_1 - P_2 = \rho_{H_2O} g H_2 - \rho_{H_2O} g H_3 - \rho_b g H_d \quad (A.5)$$

$$\Delta P = \rho_{H_2O} g H_d - \rho_b g H_d = (\rho_{H_2O} - \rho_b) g H_d \quad (A.6)$$

$$and \; \rho_{H_2O} - \rho_b = \rho_{H_2O} E_g \quad (A.7)$$

$$\Delta P = \rho_{H_2O} E_g \times g H_d \quad (A.8)$$

$$E_g = \frac{\Delta P}{\rho_{H_2O} g H_d} = \frac{\rho_{H_2O} g H_{measured}}{\rho_{H_2O} g H_d} = \frac{H_{measured}}{H_d} \quad (A.9)$$

Since dP is being measured in cm of H_2O the final equation of gas holdup is defined as:

$$Percent\ E_g = 100 * \frac{dP}{L} \tag{A.10}$$

The sensors were continuously recording and saving the measurements at a frequency of a fraction of a second, which are then extracted using Excel. An example of sample results for DF-250 gas holdup and superficial gas velocity collected on excel yield the following graph:

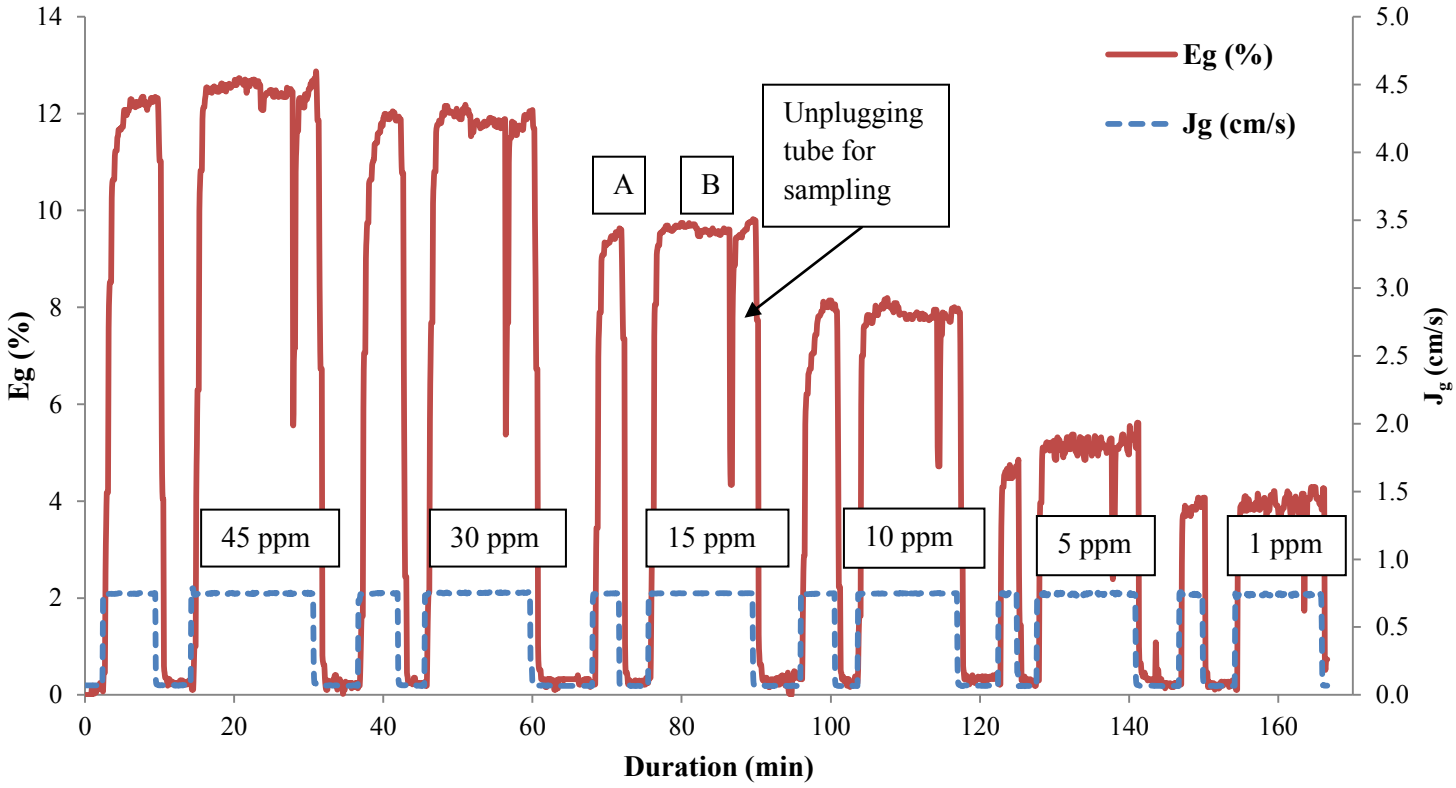

Figure A.3 - Gas holdup during column operation

A : Pre-mixing of the solution and waiting for pseudo-steady state followed by sparger shut-off and residence time equivalent of additional mixing time prior to extracting solution for viewer

B : Sparger turned back on and viewer filled up with solution. Once steady state is reached detected by steady gas holdup, the sample tube is unplugged which shows the sudden drop in differential pressure

Bubble size measurement was done using the McGill bubble size analyser at every concentration point. The technique utilizes an in-house macro to analyse a series of images and, with the help of variables such as shape factor, threshold level and minimum pixels/cm, allows us to eliminate unwanted objects from the calculation of sauter mean diameter. For reference check Hernandez-Aguilar et al., 2004.

APPENDIX B: EXPERIMENTAL DATA

B.1 D_{32} vs. Concentration Data

Conc.: Concentration (in ppm for DF-250, %v/v for process water)
D_{32}: Sauter mean diameter (mm)
E_g: Gas holdup measured in column (%)

Table B.1 - Raw Results Part 1: McGill - DF-250 Replicates

DF-250 Data		
Conc. (ppm)	**Addition D_{32}**	**Dilution D_{32}**
45	0.556	0.580
45	0.521	0.568
45	0.495	0.576
45	0.521	0.578
30	0.612	0.630
30	0.561	0.633
30	0.564	0.610
30	0.568	0.611
20	0.699	0.705
15	0.833	0.847
15	0.694	0.854
15	0.687	0.805
15	0.784	0.828
12.5	0.920	0.953
10	1.060	1.132
10	0.951	1.071
10	0.948	1.008
10	0.984	1.061
7.5	1.281	1.286
5	1.538	1.700
5	1.298	1.579
5	1.561	1.575
5	1.431	1.616
2.5	2.084	2.156
0	3.881	4.062
0	4.051	

Table B.2 - Raw Results Part 1: McGill - Process Water Samples

Process Water Data					
Pail 1		**Pail 2**		**Pail 3**	
Conc.	**D_{32}**	**Conc.**	**D_{32}**	**Conc.**	**D_{32}**
100	0.702	100	0.693	100	0.707
75	0.745	75	0.804	75	0.828
56.25	1.030	54.06	1.070	56.25	1.065
42.19	1.455	40.14	1.517	42.19	1.456
31.64	2.057	29.80	2.159	31.64	2.001
23.73	2.665	22.13	2.925	23.73	2.860
		16.43	3.321		

Table B.3 - Raw Results Part 2: Edmonton - DF-250 Replicates

DF-250 Data		
Conc. (ppm)	**Dilution D_{32}**	**Addition D_{32}**
60	0.657	
60	0.645	0.607
45	0.710	0.680
45	0.643	0.649
30	0.751	0.718
30	0.692	0.699
20	0.833	
20	0.794	0.785
15	0.938	0.898
15	0.895	0.858
10	1.100	1.109
10	1.060	1.033
7.5	1.328	
7.5	1.288	1.211
5	1.580	1.677
5	1.633	1.523
2.5	2.073	
2.5	2.194	2.046
0	4.160	
0	4.285	4.396

Table B.4 - Raw Results Part 2: Edmonton - Process Water Samples

Process Water Data											
Recycle Water (RCW)		**Thickener OF Sept.30 11:00h**		**Thickener OF Sept.30 17:00h**		**Thickener OF Oct. 01 16:15h**		**Thickener OF Oct. 02**		**Thickener OF Oct. 04**	
Conc.	**D_{32}**	**Conc.**	**D_{32}**	**Conc.**	**D_{32}**	**Conc.**	**D_{32}**	**Conc.**	**D_{32}**	**Conc.**	**D_{32}**
100	0.726	100	0.614	100	0.636	100	0.645	100	0.631	100	0.623
75	0.862	75	0.675	75	0.683	72.24	0.638	75	0.667	75	0.660
56.25	1.097	60.00	0.707	60.00	0.717	55.57	0.698	56.25	0.739	56.25	0.685
42.19	1.479	48.00	0.684	48.00	0.730	42.75	0.754	42.19	0.895	42.19	0.804
31.64	1.877	36.00	0.761	36.00	0.816	32.88	0.887	31.64	1.157	31.64	1.001
23.73	2.668	27.00	0.907	27.00	0.937	25.29	1.083	23.73	1.556	23.73	1.336
17.80	2.958	20.25	1.184	20.25	1.168	19.46	1.356	17.80	1.961	17.80	1.797
13.35	3.518	15.19	1.594	15.19	1.560	14.97	1.782	13.35	2.623	13.35	2.349
10.01	4.053	11.39	2.071	11.39	1.945	11.51	2.344	10.01	3.171	10.01	2.954
		8.54	2.481	8.54	2.311			7.51	3.613	7.51	3.367
		6.41	3.002	6.41	2.670			5.63	4.174	5.63	3.853

B.2 Gas Holdup to D_{32} Data

Table B.5 - Raw Gas Holdup Results

McGill			
DF-250 Data		Process Water Data	
Eg (%)	D_{32} (mm)	Eg (%)	D_{32} (mm)
14.33	0.495	9.5	0.693
13.37	0.521	9.25	0.702
12.78	0.521	9.12	0.707
12.61	0.564	7.94	0.745
12.39	0.576	7.84	0.828
12.21	0.561	7.5	0.804
11.77	0.610	6.34	1.030
11.61	0.568	6.28	1.065
11.53	0.611	5.89	1.070
11.47	0.556	4.84	1.455
11.45	0.568	4.45	1.517
11.33	0.580	4.04	2.057
10.91	0.687		
10.68	0.633		
10.52	0.630		
10.47	0.694		
10.33	0.612		
9.60	0.699		
9.44	0.805		
9.30	0.784		
9.05	0.705		
8.99	0.828		
8.38	0.847		
8.31	0.948		
8.15	0.854		
8.03	0.833		
7.89	0.951		
7.87	1.008		
7.79	0.920		
7.37	0.953		
7.27	0.984		
7.19	1.061		
6.64	1.071		
6.51	1.132		
6.40	1.060		
5.86	1.298		
5.85	1.281		
5.83	1.286		
5.25	1.561		
5.14	1.575		
5.07	1.431		
4.67	1.616		
4.63	1.700		
4.59	1.579		
4.39	1.538		
4.10	2.084		
4.02	2.156		

Edmonton			
Process Water Data		DF-250 Data	
Eg (%)	D_{32} (mm)	Eg (%)	D_{32} (mm)
13.35	0.623	13.89	0.657
12.94	0.636	13.59	0.607
12.89	0.645	13.46	0.645
12.83	0.631	12.83	0.643
12.7	0.660	12.81	0.649
12.45	0.614	12.73	0.710
12.4	0.638	11.94	0.699
12.32	0.683	11.72	0.692
12.07	0.667	11.56	0.751
11.72	0.675	10.83	0.785
11.69	0.685	10.42	0.833
11.69	0.707	10.42	0.794
11.61	0.717	9.88	0.858
11.34	0.684	9.55	0.895
10.99	0.730	9.3	0.938
10.99	0.698	8.33	1.033
10.96	0.726	8.17	1.060
10.69	0.739	7.9	1.100
10.64	0.761	7.24	1.211
10.5	0.754	6.97	1.288
10.47	0.804	6.78	1.328
10.09	0.816	6.05	1.523
9.71	0.862	5.86	1.633
9.2	0.907	5.73	1.580
9.04	0.895	5.02	2.046
8.95	0.887	4.83	2.060
8.82	0.937	4.83	2.194
8.55	1.001	4.59	2.326
7.81	1.097		
7.76	1.083		
7.46	1.184		
7.33	1.168		
7.3	1.157		
6.67	1.336		
6.32	1.356		
6.02	1.479		
5.89	1.560		
5.83	1.594		
5.48	1.556		
5.1	1.797		
5.02	1.782		
4.8	1.945		
4.67	1.877		
4.59	2.071		
4.5	1.961		
4.37	2.344		
4.31	2.349		
4.21	2.311		
4.12	2.481		

APPENDIX C: SAMPLE CALCULATIONS

Gas Holdup Model and Prediction Limit

Prediction intervals are used for estimation of range of future observations using the data at hand. Having determined the logarithmic model suitable for gas holdup, a prediction interval is developed as follows for a single observation:

$$Upper\ bound = y_{predicted} + t_{\alpha/2,n-2}\sqrt{\sigma^2[1+\frac{1}{n}+\frac{(x-\bar{x})^2}{S_{xx}}]} \quad (C.1)$$

$$Lower\ bound = y_{predicted} - t_{\alpha/2,n-2}\sqrt{\sigma^2[1+\frac{1}{n}+\frac{(x-\bar{x})^2}{S_{xx}}]} \quad (C.2)$$

$$S_{xx} = \sum_1^n (x_i - \bar{x})^2 \quad (C.3)$$

where α is the significance level, x_i are the recorded observations and σ^2 is their variance. The equation used to model the correlation between gas holdup E_g and D_{32} is:

$$D_{32} = -\tau * \ln(\frac{E_g - E_{g,min}}{E_{g,max} - E_{g,min}})$$

where τ= constant, $E_{g,min}$= minimum gas holdup, $E_{g,max}$= maximum gas holdup. Optimal values for the *constant*, *minimum* holdup and *maximum* holdup were determined using least squares method with the help of Microsoft Excel 2010. The values were *0.515, 3.6* and *29.12* respectively for part 1, and *0.618, 3.68* and *28.13* respectively for part 2.

Taking a sample point (x) E_g=7% at 95% confidence level (α=0.05) from the gas holdup data for Part 2, we get:

$$\bar{x} = 8.8 \quad (C.4)$$

$$S_{xx} = \sum_1^n (x_i - \bar{x})^2 = 0.11 \quad (C.5)$$

$$Upper: y_{predicted} + t_{\alpha/2,n-2}\sqrt{\sigma^2[1+\frac{1}{n}+\frac{(x-\bar{x})^2}{S_{xx}}]} = 1.23 + 2.01\sqrt{0.0024[1+\frac{1}{49}+\frac{(7-8.8)^2}{0.11}]} = 1.33 \quad (C.6)$$

$$Lower: y_{predicted} - t_{\alpha/2,n-2}\sqrt{\sigma^2[1+\frac{1}{n}+\frac{(x-\bar{x})^2}{S_{xx}}]} = 1.23 - 2.01\sqrt{0.0024[1+\frac{1}{49}+\frac{(7-8.8)^2}{0.11}]} = 1.14 \quad (C.7)$$

Repeating the previous calculation for the range of values for gas holdup, we get the following:

Table C.1 - Gas Holdup Model: Edmonton Results

Process Water data		Process Water Model		Prediction Limit	
Eg	D_{32}	Eg	D_{32}	Lower D_{32}	Upper D_{32}
13.35	0.623	13.5	0.564	0.463	0.665
12.94	0.636	13.25	0.580	0.479	0.680
12.89	0.645	13	0.596	0.495	0.696
12.83	0.631	12.75	0.613	0.512	0.713
12.7	0.660	12.5	0.630	0.530	0.730
12.45	0.614	12.25	0.648	0.548	0.748
12.4	0.638	12	0.666	0.566	0.766
12.32	0.683	11.75	0.685	0.585	0.785
12.07	0.667	11.5	0.704	0.605	0.804
11.72	0.675	11.25	0.724	0.625	0.824
11.69	0.685	11	0.745	0.646	0.844
11.69	0.707	10.75	0.767	0.668	0.866
11.61	0.717	10.5	0.789	0.690	0.888
11.34	0.684	10.25	0.812	0.713	0.911
10.99	0.730	10	0.836	0.737	0.935
10.99	0.698	9.75	0.861	0.762	0.960
10.96	0.726	9.5	0.887	0.788	0.986
10.69	0.739	9.25	0.914	0.816	1.013
10.64	0.761	9	0.943	0.844	1.041
10.5	0.754	8.75	0.972	0.874	1.071
10.47	0.804	8.5	1.004	0.905	1.102
10.09	0.816	8.25	1.037	0.938	1.135
9.71	0.862	8	1.071	0.973	1.170
9.2	0.907	7.75	1.108	1.010	1.207
9.04	0.895	7.5	1.148	1.049	1.246
8.95	0.887	7.25	1.189	1.090	1.288
8.82	0.937	7	1.234	1.135	1.333
8.55	1.001	6.75	1.283	1.184	1.382
7.81	1.097	6.5	1.335	1.236	1.435
7.76	1.083	6.25	1.393	1.294	1.492
7.46	1.184	6	1.456	1.357	1.556
7.33	1.168	5.75	1.527	1.427	1.627
7.3	1.157	5.5	1.607	1.507	1.707
6.67	1.336	5.25	1.699	1.599	1.799
6.32	1.356	5	1.806	1.706	1.906
6.02	1.479	4.75	1.937	1.836	2.037
5.89	1.560	4.5	2.103	2.002	2.203
5.83	1.594	4.25	2.330	2.229	2.431
5.48	1.556	4	2.693	2.592	2.795
5.1	1.797				
5.02	1.782				
4.8	1.945				
4.67	1.877				
4.59	2.071				
4.5	1.961				
4.37	2.344				
4.31	2.349				
4.21	2.311				
4.12	2.481				